

THE UNIVERSITY OF CHICAGO

ELUCIDATING THE BIOLOGY OF TUMOR-ASSOCIATED REGULATORY T CELLS

A DISSERTATION SUBMITTED TO
THE FACULTY OF THE DIVISION OF THE BIOLOGICAL SCIENCES
AND THE PRITZKER SCHOOL OF MEDICINE
IN CANDIDACY FOR THE DEGREE OF
DOCTOR OF PHILOSOPHY

COMMITTEE ON CANCER BIOLOGY

BY

DANIEL SOLOMON LEVENTHAL

CHICAGO, ILLINOIS

MARCH 2016

This work is first and foremost dedicated to the advancement of science and human knowledge. It is also a work of devotion and passion that would not have been possible without my earliest scientific influencers, Ethel "Auntie" Koch and Dr. Kenneth Teter, as well as my most recent teacher, mentor and lifetime drinking buddy Dr. Peter Savage. Finally, to my friends, family, fellow Savages and most importantly my amazing wife Jackie Leventhal, you all have given me endless love and support and have empowered me to achieve more than I would have ever imagined. For Science!

TABLE OF CONTENTS

LIST OF FIGURES.....	VIII
ACKNOWLEDGEMENTS.....	XI
ABBREVIATIONS.....	XV
ABSTRACT	XVI
BACKGROUND AND SIGNIFICANCE.....	1
An immunological dilemma: how to protect against pathogens without attacking ourselves.....	1
T cells can recognize tumor derived antigens and target mutated cancer cells	3
The antitumor immune response.....	5
Immunological tolerance mechanisms limiting antitumor immune responses	6
Identification of a subpopulation of CD4 ⁺ suppressor T cells (Tregs).....	8
Treg differentiation in the thymus and periphery	9
Tregs are enriched in many human tumors and often correlate with poor patient survival	11
Elucidating tumor-associated Treg function	12
Developmental origins and antigenic specificities of tumor-associated Tregs.....	14
Antigen presentation in the development and homeostasis of Tregs	17
Summary.....	18
MATERIALS AND METHODS.....	20
Mice.....	20
Generation of TCR transgenic mice	21
TCR CDR3 length distribution analysis	22
TCR sequencing and analysis.....	23

<i>454 Deep Sequencing of Vα2(TRA114)+ TCRα chains and Vβ3(TRBV26)+ TCRβ chains.....</i>	23
<i>iRepertoire complete TCRα chain analysis</i>	24
<i>Analysis of TCR repertoire similarity</i>	25
Antibodies, flow cytometry and fluorescence-activated cell sorting.....	26
Generation of mixed bone marrow chimeric mice	26
T cell transfer experiments	27
Thymocyte, splenocyte, lymphocyte and prostate dendritic cell isolations	27
MJ23tg T cell stimulation experiments	27
<i>In Vitro</i> Treg suppression assays	28
Thymocyte transfer and intrathymic injections	28
<i>In Vitro</i> MJ23tg thymocyte stimulation assay	29
Castration.....	30
Statistical analysis	30
RESULTS: AIRE-DEPENDENT THYMIC DEVELOPMENT OF TUMOR-ASSOCIATED REGULATORY T CELLS	31
Summary.....	31
Introduction	31
Results	32
<i>T cell receptor sequencing of Tregs from TRAMP prostate tumors identifies a conical and recurrently enriched TCR</i>	<i>32</i>
<i>The TCRs of Treg and Tconv tumor infiltrating cells are distinct and non-overlapping</i>	<i>39</i>
<i>Tumor-associated MJ23 Tregs are reactive to a prostate-associated self antigen..</i>	<i>41</i>

<i>MJ23 Tregs develop in the thymus and enrich in the prostate draining lymph nodes of male mice</i>	47
<i>MJ23 Treg development is Aire-dependent</i>	58
Conclusions.....	66
RESULTS: DENDRITIC CELLS COORDINATE THE DEVELOPMENT AND HOMEOSTASIS OF ORGAN-SPECIFIC REGULATORY T CELLS	67
Summary	67
Introduction	67
Results	71
<i>Thymic development of MJ23 Treg cells requires antigen presentation and CD80 and/or CD86 expression by bone marrow-derived cells</i>	72
<i>Antigen presentation by DCs is required for the thymic development of MJ23 Treg cells</i>	76
<i>Plasmacytoid DCs and CD8α⁺ cDCs are dispensable for the thymic development of MJ23 Treg cells</i>	84
<i>The thymic Treg cell repertoire is not impacted by Batf3 deficiency</i>	89
<i>The enrichment of MJ23 Treg cells in the pLNs is abrogated by loss of antigen in castrated mice</i>	93
<i>DCs are required for the optimal enrichment of MJ23 Treg cells in the pLNs</i>	97
<i>CCR7-dependent migratory DCs orchestrate MJ23 Treg cell enrichment in the pLNs</i>	101
Conclusions.....	107
DISCUSSIONS, FUTURE DIRECTIONS AND CONCLUSIONS	108
Overview	108
<i>TCR repertoires of tumor-associated Foxp3⁺ Tregs and CD4⁺ Tconv cells exhibit minimal overlap</i>	108

<i>The prostate tumor-associated Treg specificity MJ23 is reactive to a prostate-specific antigen and is thymic derived.....</i>	109
<i>MJ23 Treg development is dependent on the transcription factor Aire</i>	110
<i>Aire-dependent Treg development requires antigen presentation by thymic DCs.</i>	110
<i>CD8α^+ cDCs do not play a specialized role in thymic Treg development.....</i>	111
<i>MJ23 enrichment and activation in the pLNs is dependent on prostate-derived antigen and lost in Ccr7$^{-}$ mice lacking mDCs.....</i>	112
<i>Summary.....</i>	114
Developmental origins of tumor-associated Tregs and why targeting pTreg conversion may fail to provide clinical benefit.....	114
<i>Evidence for the conversion of tumor-reactive CD4$^+$ Tconv cells into pTregs.....</i>	115
<i>Endogenous prostate-tumor-associated Tregs are primarily thymic derived.....</i>	116
<i>Expanding our understanding for the developmental origins of endogenous Treg specificities in autochthonous murine models of cancer.....</i>	117
Antigenic specificities of tumor-associated Tregs.....	118
<i>Treg developmental origin and antigenic specificity are highly interrelated.....</i>	118
<i>Tumor infiltrating Tregs and Tconv cells likely recognize distinct sets of antigens</i>	119
<i>MJ23 Tregs are reactive to a prostate-specific, tumor-independent antigen.....</i>	120
<i>Identification of the MJ23 antigen could provide valuable tools for future inquiry..</i>	121
<i>Identifying the antigenic specificities of other tumor-associated Treg clonotypes in mice and humans.....</i>	122
The contribution of Aire to organ specific immune tolerance.....	123
<i>Mirroring peripheral self through the presentation of TRA's in the thymus.....</i>	123
<i>The impact of Aire on T cell development in the thymus.....</i>	124
<i>Aire-dependent development of naturally derived Treg specificities</i>	125

<i>Is there a role for Aire-dependent, organ-specific Tregs in modulating tumor progression and antitumor immunity?</i>	127
<i>A surprising conclusion: Tregs go “rogue” in the absence of Aire</i>	127
<i>Fezf2: a new player in the presentation of “peripheral self” in the thymus.....</i>	130
Antigen presentation and Treg development in the thymus	131
<i>Various APC subsets play distinct roles in the generation of a complete Treg repertoire.....</i>	132
<i>Presentation of Aire-dependent antigens in the thymus.....</i>	132
<i>Specialized or redundant: conflicting results for the role of CD8α^+ cDCs in thymic Treg development</i>	134
<i>The rationale for a specialized role for Sirpα^+ cDCs in thymic Treg development.</i>	137
Self antigen presentation in the function and homeostasis of Tregs	138
<i>Prostate-organ-specific Tregs require continuous antigen presentation for their activation and proper anatomical distribution</i>	139
Identifying the APC interaction partners that orchestrate organ-specific Treg homeostasis and function.....	140
CD11c-expressing DCs play a critical role in the homeostasis of MJ23 and some polyclonal Tregs in the pLNs	141
Organ-specific Tregs and their APC interaction partners	141
<i>Identifying the APC interaction partners that orchestrate organ-specific Treg homeostasis and function.....</i>	143
<i>Evaluating the contributions of distinct mDC subsets towards organ-specific Treg homeostasis and immune tolerance.....</i>	145
Conclusions.....	146
REFERENCES.....	148

LIST OF FIGURES

Figure 1: Enrichment of Tregs in TRAMP prostate tumors.....	34
Figure 2: Identification of a canonical TCR β chain recurrently expressed by Tregs infiltrating TRAMP prostate tumors.....	35
Figure 3: CD4 ⁺ Foxp3 ⁺ Tregs expressing a canonical TCR are recurrently enriched in TRAMP prostate tumors.....	36
Figure 4: In many TRAMP ^{+/-} Foxp3 ^{gfp} TCR β tg mice, the canonical V α 2-LYYNQGKLI chain is encoded by a single nucleotide sequence.	38
Figure 5: Five most common V α 2+ TCR α chains expressed by prostatic CD4 ⁺ Foxp3 ⁺ T cells from TRAMP ^{+/-} Foxp3 ^{gfp} TCR β tg mice.	40
Figure 6: MJ23 T cells recognize a prostate-associated self antigen.	42
Figure 7: Analysis of CD4 ⁺ Foxp3 ⁺ T cells in MJ23tg Rag1 ^{-/-} mice.....	44
Figure 8: Suppressive function of Tregs from MJ23tg Rag1 ^{-/-} males.....	45
Figure 9: Phenotypic analysis of MJ23tg Tregs.....	46
Figure 10: Thymic development of MJ23 Tregs.	50
Figure 11: Additional characterization of MJ23tg bone marrow chimeric mice.....	52
Figure 12: The OT-II TCR does not facilitate Treg development in the thymus of mixed bone marrow chimeric mice.	54
Figure 13: Polyclonal Tregs from TRAMP prostates express intermediate amounts of neuropilin-1.	55

Figure 14: Factors limiting the recovery of donor-derived MJ23tg T cells in chimeric mice.....	56
Figure 15: Negligible extrathymic development of MJ23tg Tregs.....	57
Figure 16: Aire-dependent thymic development of antigen-specific Tregs.....	60
Figure 17: Further characterization of MJ23tg T cells in Aire ^{-/-} and Aire ^{+/+} chimeric hosts.....	62
Figure 18: Thymic development of Tregs expressing the “RT83” TCR is Aire-dependent.	64
Figure 19: MJ23 Treg cell development is dependent on antigen presentation by bone marrow-derived cells.	74
Figure 20: Efficiency of MJ23 Treg development and polyclonal Treg numbers are impacted by loss of MHC-II and B7-1/B7-2 on bone marrow-derived cells.	75
Figure 21: Antigen presentation by dendritic cells is required for the thymic development of MJ23 Treg cells.....	78
Figure 22: Antigen presentation by dendritic cells is required for the thymic development of MJ23 Tregs.	79
Figure 23: B cells, plasmacytoid DCs, and CD8 α^+ cDCs are dispensable for the thymic development of MJ23 Tregs.....	81
Figure 24: Plasmacytoid DCs and CD8 α^+ cDCs are dispensable for the development of MJ23Tg Treg cells.....	86
Figure 25: Plasmacytoid DCs and CD8 α^+ cDCs are dispensable for the thymic development of a second Aire-dependent Treg specificity.....	87

Figure 26: Loss of Batf3-dependent CD8 α^+ cDCs has negligible impact on the thymic Treg cell repertoire. 91

Figure 27: Both thymic CD8 α^+ and Sirpa $^+$ cDCs can promote activation and Foxp3 induction by MJ23tg thymocytes in vitro. 92

Figure 28: Castration abrogates the enrichment and activation of MJ23 Treg cells in the prostate-draining lymph nodes. 95

Figure 29: Dendritic cells coordinate MJ23Tg Treg cell enrichment in the prostate-draining lymph nodes. 98

Figure 30: Dendritic cells coordinate MJ23tg Treg enrichment and impact polyclonal Treg frequencies in the prostate-draining lymph nodes. 99

Figure 31: CCR7-dependent migratory DCs are required for the activation and enrichment of MJ23 Treg cells in the prostate-draining lymph nodes. 103

Figure 32: CD103 $^+$ and CD11b $^+$ migratory DCs express CCR7 and are absent in the prostate draining pLNs of CCR7 $^{-/-}$ mice. 105

Figure 33: Batf3-deficiency has a minimal impact on the Aire-dependent Treg repertoire. 136

ACKNOWLEDGEMENTS

I would like to begin by acknowledging Dr. Peter Savage for his steadfast dedication to this project and to my training as a scientist. As with any scientific endeavor, the path was not always clear and we faced countless challenges along the way. Without Pete's unyielding patience, his inspiring mastery of the field and his contagious inquisitive nature, none of this work would have been possible. Additionally, Pete constructed an outstanding group of scientists who all contributed significantly to this work and my training. Benjamin Fischer and Saki Nishi were the first members of the Savage lab. They created and established many of our mouse models, and pioneered many of our protocols. As our lab manager Saki also ruled our lab with an iron fist, keeping the lab organized and fully stocked, all while supporting and assisting with many of our day-to-day experiments. Dr. Sven Malchow has been a mentor, collaborator, friend and brother. Sven has made significant contributions to a large percentage of the work shown here, by establishing models, carrying out experiments, analyzing data and authoring manuscripts. Lynn Shen and I were the first graduate students in the lab, and as such, Lynn was a large part of making it through graduate coursework, preliminary exams and qualifying exams. Lynn pioneered many of the early antigen presenting cell and tumor modeling approaches that are used in this work and in the lab today. Julian Berger, our resident undergraduate researcher, made significant intellectual contributions to this work and collaborated on a variety of experiments. He also helped to pioneer the use of immunofluorescence in the Savage Lab, contributing to numerous analyses not shown here. Julian's innate inquisitive nature and persistence

to question everything contributed to a variety of aspects of this work. I see great things in Julian's future as a scientist and in any other endeavors he may pursue. The second generation of graduate students in the Savage Lab, Dana Gilmore, Victoria Lee and Jaime Chao, have all individually contributed to various aspects of this work and its publication. More importantly they helped to create an inspiring and intellectually stimulating environment to conduct research in. They represent the next phase of research in the Savage Lab, and I know that the future of this research group will only prove to be more exciting than its humble beginnings. Last but not least, our most recent lab manager and technician Mary Schoenbach. Over the past year Mary has made significant contributions to this work by assisting with experiments and ensuring that the necessary reagents were well stocked. She has been an exceptional addition to the Savage Lab.

Much appreciation goes to our neighbors to the north, the Kline Lab. They contributed to this work and my training much in the same way that a brother or sister does. They always shared reagents, knowledge and expertise with us throughout the years. As newly formed labs, we grew and explored new science together, and they will always hold a place in my personal "Superawesomergroup". Throughout my graduate training and this work, Dr. Justin Kline has contributed as a second mentor, collaborator and friend. Douglas Kline (no relation) made significant contributions intellectually to this work, and provided critical resources and reagents which allowed the studies to reach a depth of understanding that would not have otherwise been possible. Dr. Xuifen Chen also provided reagents and assistance, as well as a smiling face after long and

challenging days in the lab. Finally Dominick Fosco was an absolute pleasure to work with and always ensured that every day at work was fun and interesting.

I would also like to thank our collaborators who individually played critical roles throughout the course of this work. Dr. Nicholas Socci, Head of Engineering and Bioinformatics at Memorial Sloan Kettering, carried out all the bioinformatics associated with analyzing T cell receptor repertoires. Dr. Gladell Paner, Associate Professor of Pathology at the University of Chicago, provided expertise and assistance with analyzing and staging of mouse prostate tissue sections. Dr. Donald Vander Griend, Assistant Professor in the Ben May Department for Cancer Research at the University of Chicago, and several members of his lab, Hannah Brechka and Dr. Jacob Kach, performed surgeries for all castration experiments. Dr. Haochu Huang, Associate Professor in the Department of Medicine at the University of Chicago, and several members of his lab, Dr. Jason Perera and Dr. Zhong Zheng, provided expertise and several mouse models which were essential for the completion of this work. Finally, the Committees on Immunology and Cancer Biology at the University of Chicago provided valuable feedback, resources, expertise and support, all of which were critical for the success of my training and this work. The University of Chicago is a truly unique place to carry out research with an overwhelming abundance of knowledge and passion for science that is second to none.

I would like to sincerely thank my committee members, Dr. Thomas Gajewski, Dr. Bana Jabri, Dr. Yang-Xin Fu and Dr. Justin Kline, for their support, feedback and contributions to my training as a scientist. They have all pushed me to excel beyond my own expectations and always treated me not as a student, but as a colleague.

A variety of core facilities and their members also made this research possible. Linda Degenstein and the Transgenics/ES Cell Technology Mouse Core Facility generated and maintained the T cell receptor transgenic mouse lines utilized in this study. The Flow Cytometry Core, run by Dr. Ann Sperling, Ryan Duggan and Mike Olson, provided expertise and maintained the instrumentation required for all experiments involving flow cytometry and fluorescence-activated cell sorting. Dr. Anita Chong and Dr. Dengping Yin with the Microsurgery Core assisted with experiments and my training involving intra-thymic injections. Finally, the amazing group that runs the KCBD Mouse Facility, in particular Renee Hoffman, Love Owens and Carrie Hoffman, maintained our mouse colony and ensured we had all the resources we required to perform all our *in vivo* experiments.

Acknowledgement also needs to be made to the Committee on Cancer Biology, Dr. Geoff Greene and Dr. Kay Macleod for taking a chance and accepting me into their PhD program. They have also provided me with mentorship and supported my training as a scientist and my interest in the interface between Cancer Biology and Immunology.

Finally, support for myself and my work also came from a variety of funding sources. Funding for me and my training came from an NIH sponsored Cancer Biology training grant, an HHMI sponsored Med-into-grad Program and an NIH/NCI sponsored F31 predoctoral fellowship (CA183357). This work was also funded by the following sources: R01 (R01CA160371), R01 (R01AI110507), a Cancer Research Institute Investigator Award, and the University of Chicago Comprehensive Cancer Center (UCCCC).

ABBREVIATIONS

antigen presenting cells (APCs); autoimmune regulator (Aire); bone marrow chimeras (BMCs); brachial lymph nodes (bLN); cell trace-violet (CTV); classical dendritic cells (cDCs); complementarity determining region (CDR3); conserved non-coding DNA sequence (CNS); danger-associated molecular patterns (DAMPs); dendritic cells (DCs); diphtheria toxin (DT); diphtheria toxin receptor (DTR); experimentally induced autoimmune encephalomyelitis (EAE); Forkhead box P3 (Foxp3); Foxp3⁺ regulatory T cells (Tregs); immune dysregulation, polyendocrinopathy, enteropathy, X-lined (IPEX); macrophages (MΦ); major histocompatibility complex class I (MHC-I); major histocompatibility complex class II (MHC-II); medullary thymic epithelial cells (mTECs); mesenteric lymph nodes (mLNs); methylcholanthrene (MCA); migratory dendritic cells (mDCs); Morisita-Horn (MH); neuropilin-1 (Nrp-1); pathogen-associated molecular patterns (PAMPs); periaortic lymph nodes (pLNs); peripherally-induced Treg (pTreg); plasmacytoid dendritic cells (pDCs); prostate (PR); spleen (SP or Spl); T cell receptor (TCR); T conventional (Tconv); thymic-derived Treg (tTreg); thymic epithelial cells (TECs); thymus (TH); tissue-restricted antigens (TRAs); toll like receptors (TLRs); transgenic (tg or Tg); transgenic adenocarcinoma of the mouse prostate (TRAMP); Treg-specific demethylated region (TSDR); wildtype (WT)

ABSTRACT

Due to the well-characterized role of Foxp3⁺ regulatory T cells (Tregs) in the regulation of immune responses to both self and foreign antigens, there has been significant interest in the clinical modulation of Tregs for the treatment of autoimmunity and cancer. Through T cell receptor (TCR) sequencing studies we demonstrate that the TCR repertoires of Tregs and CD4⁺ T conventional (Tconv) cells infiltrating genetically-driven murine prostate tumors are non-overlapping and we identified highly recurrent Treg clonotypes for further investigation. For one of the most highly recurrent prostate-tumor-associated Treg clonotypes, MJ23, we find that these cells are reactive to a prostate-associated antigen and they develop into Tregs in the thymus in an Aire-dependent manner. In the thymus, MJ23 Tregs require antigen presentation by CD11c⁺ dendritic cells (DCs) and develop in the absence of plasmacytoid and Batf3-dependent CD8 α ⁺ DCs. Furthermore, sequencing studies demonstrate that the thymic Treg repertoire is not impacted by the loss CD8 α ⁺ DCs. MJ23 Tregs enrich and become activated in the prostate-draining lymph nodes (pLNs) of prostate tumor-bearing and tumor-free male mice. We demonstrate that MJ23 Treg enrichment and activation in the pLNs occurs in an antigen-dependent manner and is lost in *Ccr7*^{-/-} mice lacking migratory DCs (mDCs). Altogether, these results suggest that prostate tumors co-opt organ-specific, Aire-dependent, thymic-derived Tregs and that antigen presentation by CCR7-dependent mDCs orchestrates the localization and activation of these cells in the pLNs. These findings provide critical insights towards the mechanisms that modulate Treg development and homeostasis, and provide new avenues for future inquiry.

BACKGROUND AND SIGNIFICANCE

An immunological dilemma: how to protect against pathogens without attacking ourselves

To effectively target and clear pathogens, such as bacteria and viruses, while preserving host tissues and maintaining homeostasis at steady state, the immune system must maintain a highly dynamic balance between proinflammatory “on-signals” and inhibitory “off-signals”. While several theoretical models have been described to explain how this balance was ultimately achieved throughout the evolution of our immune system, such as “Self versus Non-self”(1) and “Danger Theory”(2), these explanations remain highly debated topics. However, throughout the decades researchers have elucidated a multitude of mechanisms utilized by the immune system to recognize pathogens directly and combat them, all while limiting reactivity to self and minimizing collateral damage to surrounding tissues.

A variety of receptors have been identified that are encoded by fixed germline sequences in the genome that recognize fixed structural patterns conserved across a variety of pathogens (often referred to as pathogen-associated molecular patterns (PAMPs)). Stimulation of these receptors, such as the toll like receptors (TLRs), results in rapid immune responses and constitutes the immune system’s first line of defense often orchestrated by innate immune cell subsets such as neutrophils, macrophages and dendritic cells. In contrast, adaptive immune cell subsets, such as T and B cells, utilize highly variable receptors which are the product of a stochastic rearrangement of receptor alleles and insertion/deletions within the germline sequences of those alleles that results in an enormous diversity of specificities.

In the context of $\alpha\beta$ T cells, the T cell Receptor (TCR) is a heterodimer consisting of an α -chain and a β -chain which is capable of recognizing antigens in the form of oligomeric peptides presented in the context of major histocompatibility molecules (MHC). In humans, the germline sequences encoding the TCR α -chain include a series of V genes (with 70-80 genes) and J gene (with 61 individual genes) and a single C gene. During T cell development a V gene will be stochastically rearranged to pair with a J gene. Additionally, at the V-J junction, a region referred to as the complementarity determining region (CDR3), often one to several nucleotides will be randomly added or deleted, resulting in significant diversity even among TCRs sharing the same V and J genes. A similar process also ensues for the recombination of the V (with 52 genes), D (with 2 genes), J (with 13 genes) and C (with 2 genes) genes of the TCR β -chain. Finally, the sequence of the TCR serves as a unique fingerprint to that T cell and ultimately dictates the antigenic ligand it can bind to. While this process results in T cells and TCRs which theoretically can recognize almost any foreign stimulus, it also results in a large number of receptors which recognize peptides expressed by endogenous, self tissues.

To avoid attacking host tissues, a process central to autoimmune diseases, many self- or auto-reactive T cells are purged from the immune repertoire during development in the thymus in a process known as negative selection (3). Forkhead box P3 (Foxp3)⁺ CD4⁺ regulatory T cells (Tregs) are one of exceptions to this rule, as these cells are diverted into the Treg lineage in the thymus based on their reactivity to self antigens. Tregs function to suppress immune responses and maintain immune homeostasis, taking on the role of a peace keeper or police officer of the immune system.

T cells can recognize tumor derived antigens and target mutated cancer cells

Broadly, T cells can be broken down into CD8⁺ and CD4⁺ T cell subsets, with CD8⁺ T cells recognizing antigens presented on MHC class I (MHC-I) molecules and CD4⁺ T cells recognizing antigens presented on MHC class II (MHC-II) molecules. In general, peptides loaded onto MHC-I come from within the cytoplasm of the cell, while peptides found on MHC-II are typically taken up from surrounding cells or the microenvironment. In addition, exogenous antigens can be acquired by antigen presenting cells (APCs) and present via MHC-I in a process known as cross-priming or cross-presentation (4, 5). In either context, the presentation of peptides via MHC molecules enables T cells, via their TCR, to scan the external and internal proteomes of cells in search of their cognate antigen and potential threats to the host organism. This ability to detect internal changes in the proteome is not only useful for detecting viral or bacterial threats, but has also been shown to play an important role in the detection of mutant self proteins resulting from the mutational processes underlying tumorigenesis.

The earliest insights implicating a role for the immune system in cancer came from clinical observations made by Dr. William B. Coley in the 1890s, where he reported anecdotal evidence suggesting an association between active infection and cancer regression (6). In an effort to utilize infection as a means of treating cancer, Dr. Coley evaluated the efficacy of a novel treatment strategy for patients with inoperable tumors that involved intravenous injection of bacterial cultures or products, later referred to as Coley's toxin, and in some cases this treatment resulted in significant reduction in tumor mass. While these results suggested that the immune system may play a role in

modulating cancer, it was not till the 1950s and 1960s that seminal work utilizing chemically-induced sarcomas in mice demonstrated that T cells can directly recognize tumor cells in the same way that they can recognize cells infected by viruses and bacteria (7-9). In such experiments, mice immunized with irradiated sarcoma cells derived from syngeneic mice exhibited protection from subsequent challenge with the same cell line. This protection was found to be tumor-specific because immunization with a different sarcoma cell line did not confer resistance to tumor challenge. These early observations set the foundation for the concept that tumor cells can express unique antigens that can be recognized by the adaptive immune system (T and B cells). Later studies expanded upon our understanding and appreciation of the complex interactions between cancer and the immune system, not only in the context of treating the disease but also during tumor development.

As a result of decades of research, it is now widely accepted that the immune system acts as a double edged sword in how it impacts cancer cell growth and survival, acting either in a pro-tumorigenic or antitumorigenic fashion depending on the context of the interaction (10). The acquisition of tumor promoting inflammation and the avoidance of immune destruction are now being explored experimentally and exploited clinically as major mechanisms required for the development of a variety of cancers, adding them to the list of critical biological processes referred to as the “hallmarks of cancer” (11). In the past five years alone the field has seen significant clinical successes with the introduction of antibodies blocking immune “check-point” molecules, such as CTLA-4 (12) and PD-1 (13), that are hypothesized to promote T cell mediated antitumor immune responses and subsequently tumor rejection.

The antitumor immune response

Currently antitumor immune responses are conceptualized in a very T cell centric way. This process is outlined in a recent review from Daniel Chen and Ira Mellman (14) and is briefly discussed here. At the earliest stages of tumorigenesis cancer cells acquire spontaneous mutations throughout their genomes. These mutations can consist of point mutations, chromosomal translocations, and amplifications and deletions of distinct regions of the genome. While some mutations may occur in regulatory regions of genes, resulting in the aberrant gene activation or silencing, others can occur within the exons that encode the amino acid sequences of proteins. Sometimes the latter results in nonsynonymous mutations that change nucleotide codon sequences and thus alter the amino acid sequences of the proteins they encode. These mutations can have the potential to affect protein structure and function, and in some circumstances results in the generation of a new peptide sequence that can be recognized as “foreign” by the immune system. These newly arising peptide sequences are referred to as tumor “neo-antigens” or tumor-specific antigens. Additionally, due to the genetic or epigenetic changes occurring throughout cancer development, other non-mutated proteins can be over-expressed or aberrantly expressed, enabling immune recognition by T cells. These are often referred to or categorized as tumor-associated antigens.

As tumor cells die via failure to escape programmed cell death (apoptosis) or due to lack of oxygen or other nutrients (necrosis), it is thought that they release various danger-associated molecular patterns (DAMPs) along with tumor antigens that are then taken up by various APC subsets (such as macrophages (MΦ) and dendritic cells (DCs)). DAMPs released by tumor cells can then lead to activation of various innate

immune cell receptors and to a variety of downstream effector responses. Activated M Φ and DCs traffic to nearby tumor-draining lymph nodes where they present tumor derived antigens and co-stimulatory signals to T cells. If T cells with the capacity to recognize tumor-derived antigens exist in the T cell repertoire, antigen presentation can lead to the activation of these cells. Activated T cells then exit the lymph nodes, enter into the circulation and traffic to the tumor. Finally, upon encountering their cognate antigen in the tumor environment, T cells can exhibit a variety of effector functions, including the release of proinflammatory cytokines and the direct triggering of death or lysis of tumor cell targets.

Of course the multi-step process outlined above is a conceptual scenario outlining a productive antitumor T cell response. However, the fact that cancer frequently arises in subjects with a fully functional immune system indicates that in many cases, tumors evade destruction by the adaptive immune system. In this regard, several immunological mechanisms have been implicated in preventing antitumor immune responses at every step of the process outlined above.

Immunological tolerance mechanisms limiting antitumor immune responses

Since solid tumors originate from the oncogenic transformation of normal cells in the context of non-cancerous tissues, it is thought that the immune mechanisms that orchestrate recessive and dominant tolerance to self-antigens may ultimately restrict antitumor adaptive-immune responses.

'Recessive' tolerance mechanisms, such as the thymic deletion of T-cell precursors exhibiting excessive levels of reactivity to self antigens (referred to as central tolerance) (15) and the functional inactivation of autoreactive T cells post thymic development (referred to as a form of peripheral tolerance) (16), likely represent major barriers limiting antitumor immunity. Since these fundamental tolerance mechanisms ultimately shape the TCR repertoire by purging or inactivating cells that are overtly reactive to self antigens, and since tumor neo-antigens often vary from their non-mutated counter parts by a single amino acid, these mechanisms may limit the quantity and quality of TCRs capable of specifically recognizing tumor-derived antigens. Still, recessive tolerance is thought to be an imperfect process, and thus several additional mechanisms serve as "fail-safes" that ensure self-tolerance is maintained.

'Dominant' tolerance mechanisms are enforced by suppressor cell populations, such as Foxp3⁺ Tregs, which act *in trans* to suppress autoreactive T cells and to maintain systemic immune homeostasis (17). T cell co-inhibitory receptors, such as CTLA-4 and PD-1, also impact adaptive immune responses by delivering inhibitory signals or by blocking the co-stimulatory signals that function in concert with TCR signaling to properly prime and activate effector T cells (18).

Finally, Foxp3⁺ regulatory T cells (Tregs) can be thought to represent an interface between all three of these broad categories of tolerance. Treg cell development is often a result of central tolerance, committing to the Treg lineage due to reactivity to self ligands in the thymus (19). Treg cells also dominantly enforce peripheral tolerance via a variety of mechanisms (17), such as the stripping of co-

stimulatory molecules (B7-1/B7-2) off of antigen presenting cells via CTLA-4 on their cell surface.

Identification of a subpopulation of CD4⁺ suppressor T cells (Tregs)

CD4⁺CD25⁺ Treg cells were first described in seminal work by Shimon Sakaguchi in the mid-1990s, which described that approximately 10% of CD4⁺ cells expressed CD25 and demonstrated that autoimmune disease was induced upon adoptive transfer of CD25-depleted cells from pooled spleen and lymph nodes into athymic host mice (20). In addition, autoimmunity was prevented by the simultaneous provision of purified CD4⁺CD25⁺ T cells. These findings, and other data presented in this study, suggested that a minority population of CD4⁺ T cells that express high levels of CD25 were important for maintaining immune homeostasis and self-tolerance. Gene mapping and DNA sequencing analyses of Scurfy mutant mice (21) later identify a deleterious frame shift in the *Foxp3* gene as the causative mutation inducing the fatal early onset of autoimmunity observed in these mice (22). In the same year, mutations in the *FOXP3* gene were also linked to immune dysregulation, polyendocrinopathy, enteropathy, X-lined (IPEX) syndrome in humans (23). Finally, in seminal work in mice tying these concepts together, *Foxp3* was found to be exclusively expressed in CD4⁺CD25⁺ suppressor cells, required for the development of these cells in a cell-intrinsic manner, and was found to be sufficient to confer suppressor function following ectopic expression in CD4⁺CD25^{neg} T cells (24). It was also demonstrated that a subpopulation of CD4⁺CD25⁺ Tregs exhibit an activated phenotype, upregulating markers indicative of antigen encounter, such as CD44 and CD69, as well as rapidly

dividing at steady state (25). While these data indirectly suggested that Tregs are autoreactive, a subsequent study provided direct functional evidence for self-reactivity by demonstrating that expression of TCRs derived from CD4⁺CD25⁺ T cells results in the homeostatic expansion of T cells upon adoptive transfer, while expression of TCRs from CD4⁺CD25^{neg} T cells did not (26). Collectively, these findings identified Foxp3⁺ Treg cells as a distinct CD4⁺ T cell subset that are required for the maintenance of self-tolerance and immune homeostasis in mice and humans, and in many cases may be reactive to self antigens. Since the identification of Foxp3 as a Treg specific marker in mice, a large body of evidence has demonstrated that Treg mediated suppression plays a significant role in the modulation of a variety of immunological processes, including autoimmunity, infection, tolerance to commensal bacteria, allergy, metabolic inflammation and cancer (17).

Treg differentiation in the thymus and periphery

Differentiation into the Treg lineage can occur via one of two mechanisms, either during thymic development resulting in a cell referred to as a thymic-derived Treg (tTreg), or upon antigen encounter in the periphery resulting in a cell referred to as a “peripherally-induced” Treg (pTreg) (27).

Thymic selection of Tregs is thought to occur in two distinct steps (28). First, self-reactive CD4 single positive or CD4⁺CD8⁺ double positive thymocytes receive TCR instructive signals that results in the upregulation of the high affinity IL-2 receptor alpha chain, CD25. Following upregulation of CD25, Treg precursors no longer require TCR stimulation and instead are dependent on cytokine-dependent signals, conferred by IL-2

or IL-15 (29). Upon upregulation of Foxp3, thymic Treg precursors actively demethylate the Treg-specific demethylated region (TSDR) of the *Foxp3* promoter, keeping the *Foxp3* locus open and ensuring stable expression and commitment to the Treg lineage (30). Three conserved non-coding DNA sequence (CNS) elements can be found in the TSDR, with *CNS2* contributing to the stability of tTregs by ensuring *Foxp3* expression in the progeny of actively dividing Tregs (31).

In contrast, pTregs develop from CD4⁺Foxp3^{neg} T conventional cell precursors at extrathymic sites throughout the body in a process that is augmented by exposure to TGF- β and retinoic acid (32). The *CNS1* region of the *Foxp3* promoter plays a distinct role in the induction of Tregs in gut-associated lymphoid tissues and other mucosal site (31). It is unclear whether pTregs are reactive to a similar set of self antigens as tTregs, or whether they recognize a distinct set of self and environmental antigens. However, functional evidence from *CNS1*^{-/-} mice suggest a non-redundant role for pTregs in the regulation of Th2 inflammation against commensal bacteria (33) and at the maternal-fetal interface (34). TCR sequencing demonstrated that colonic Tregs express recurrent TCR specificities not found in other secondary lymphoid organs, and that many of these TCRs are reactive to colonic or bacterial extracts (35). Furthermore, the same study showed that the expression of colonic Treg-derived TCRs does not facilitate Treg development in the thymus, but instead drives the accumulation of pTregs in the colon, consistent with an extrathymic origin for these Tregs. Since antigens derived from a developing fetus or commensal bacteria are unlikely to be present in the thymus to enable development of tTregs reactive to such antigens, collectively these data would suggest that pTregs serve distinct immunomodulatory roles by expanding the diversity

of the overall Treg repertoire, allowing the immune system to generate Treg cells reactive to environmental antigens as needed.

The idea that the developmental origin of a Treg may provide meaningful insights about a cell's antigenic specificity, and vice versa, may be particularly useful for investigating the development and antigenic specificities of tumor-associated Tregs. For instance, if Treg cells within the tumor infiltrate were of thymic origin, this would imply that these tTregs are most likely reactive to antigens presented in the thymus. Reciprocally, if tumor-associated Tregs were reactive to unique neo-antigens that are only presented in the tumor environment, it may suggest an extrathymic origin in the tumor setting.

Tregs are enriched in many human tumors and often correlate with poor patient survival

Numerous epidemiological studies in humans have identified correlations between high densities of Tregs within tumors and clinical outcome (36), suggesting that Treg infiltration may have a direct impact on tumor progression. For most solid tumor types, including ovarian (37), breast (38), prostate (39, 40) and hepatocellular cancers (36), high frequencies of Treg infiltrates have been found to correlate with a poor prognosis. Furthermore, a decreased ratio of infiltrating CD8⁺ T cells compared to Tregs was found to be an even stronger predictor of poor patient survival in several of these studies. While these findings may suggest that Tregs directly impact the progression of disease or response to therapy for these particular tumor types, the correlative nature of these studies make them difficult to interpret. For example, it is

possible that Treg infiltration correlates with infiltration of another immune cell type or a particular oncogenic event or stage of disease progression, any of which could represent the primary driver of differences between patient outcomes, with Treg infiltration representing a purely correlative phenomenon. Additionally, in stark contrast to other tumor types, a high density of Treg infiltrates in colorectal cancer correlates with improved outcomes for patients (41). Given the correlative nature of these human studies, coupled with the differential association of Treg density with clinical outcome for different cancer types, it is critical to demonstrate a direct causal relationship and to elucidate the mechanistic basis of Treg function in tumor lesions using tractable mouse models of autochthonous cancer.

Elucidating tumor-associated Treg function

What is the functional impact of Treg infiltration on tumor development and progression? What are the mechanisms by which Tregs could directly, or indirectly, impact tumor growth? These are highly debated questions which have yet to be fully addressed. Due to their role in modulating T cell immunity against self and foreign antigens, one possibility is that Treg cells impact tumorigenesis by dampening T cell mediated antitumor immune responses. This could occur via direct suppression of CD4⁺Foxp3^{neg} Tconv and CD8⁺ T cells, suppressing either priming or effector function, or by modulating the APC subsets which prime T cell mediated antitumor immune responses.

Early studies utilizing anti-CD25 cell-depleting antibodies (42) and later studies utilizing *Foxp3*^{DTR} mice (43, 44) both demonstrate that Treg depletion can boost both

endogenous and vaccine-induced antitumor immune responses. However, the severe autoimmunity and additional secondary adverse effects of sustained Treg ablation have limited the ultimate utility of such manipulations for the kinds of longitudinal studies required to evaluate the impact of Tregs on tumor progression throughout tumorigenesis. Thus, studies utilizing transient depletion of Tregs have also been employed.

Transient depletion of Tregs in *Foxp3^{DTR}* mice demonstrated that such treatments impact the initiation and growth of several transplantable tumor cells lines and mouse sarcomas induced by treatment with chemical carcinogen methylcholanthrene (MCA) (45). Additionally, transient Treg depletion was also shown to impact the primary and metastatic tumor progression of an orthotopic, polyoma middle-T antigen-driven model of mouse mammary carcinogenesis, and significantly improved the efficacy of radiotherapy treatment for this model (46). Additionally, since both studies demonstrated that the suppression of tumor growth following transient Treg ablation occurs in an effector T cell-dependent manner, these findings suggest that Tregs may promote tumor progression by inhibiting T cell mediated antitumor immune responses. These conclusions were further supported by a recent study utilizing a genetically-engineered, autochthonous mouse model of lung adenocarcinoma which found that Tregs localized to tertiary lymphoid structures found in the tumor environment locally suppressed DC activation and subsequently antitumor effector T cell priming and proliferation (47). While the incorporation of genetically-driven mouse models of cancer in such studies is a critical step towards more faithfully recapitulating the disease dynamics of human cancers, these studies fail to evaluate the impact Tregs have on

early stages of tumor development. For example, it is important to note that the dampening of inflammation may also functionally inhibit several aspects of tumor development and metastasis, as the presence of specific immune cell subsets (48, 49), the release of certain cytokines (49) and various aspects of inflammation-induced tissue remodeling can play critical roles in the initiation and progression of a variety of tumor types (10, 50).

Regarding a specific role for Tregs in the modulation of APCs and inhibition of T cell priming, a variety of *in vitro* studies have demonstrated that Tregs can directly modulate APC phenotype in a cell-contact dependent manner via the presentation of membrane bound TGF- β (51, 52), stripping of the co-stimulatory molecules B7-1/B7-2 via CTLA-4 (53, 54), direct killing of APCs via perforin and granzyme (55), or by upregulating the local concentration of extracellular adenosine (56). However as described above, without a means of separating the contribution of Tregs suppression of systemic autoimmunity from their direct impact on antitumor immune responses, it will be difficult to provide functional evidence for these findings *in vivo*.

Developmental origins and antigenic specificities of tumor-associated Tregs

The antigenic specificity of tumor-associated Tregs is likely to drive several aspects of their biology, including development, activation, function and co-localization with various cellular interaction partners within the tumor environment. As discussed above, the developmental origins of tumor-associated Tregs and the nature of the antigens recognized by these cells are highly interrelated concepts. Thymic derived

tTregs are primarily thought to recognize self antigens, although little is known about the exact identify or nature of said antigens. Since Treg development in the thymus occurs in a TCR instructive manner that is dependent on the presence of cognate antigen (28), then it implies that tTregs specificities are most likely limited to antigens presented in the thymus during T cell development. Peripherally induced pTregs, however, develop from conventional T cells precursors extrathymically in a process that is thought to also be TCR instructive (35) and augmented by exposure to TGF- β and retinoic acid (32). In theory, pTregs could be specific for self, foreign or tumor derived antigens, having undergone induced Foxp3 expression upon exposure to these antigens in the proper immunological context.

Whether pTregs recognize a similar array of self antigens as tTregs is unclear. There are currently no perfect markers to delineate Foxp3⁺ thymic derived tTregs versus peripherally induced pTregs. Initial reports suggested that the transcription factor Helios is a marker of tTregs (57), however subsequent studies revealed that Helios can also be induced by experimentally generated pTregs (58, 59) and may more likely be a marker of activated Tregs with increased suppressive capacity (59, 60). Other reports suggested that induced Tregs of extrathymic origin express low levels of the marker neuropilin-1 (Nrp-1) (61, 62). These conclusions are primarily based on two findings. First, in the thymus Foxp3⁺ T cells express high levels of Nrp-1, while in the intestinal lamina propria (a site predicted to harbor increased frequencies of pTregs reactive to commensal microbiota) a large proportion of Treg cells are Nrp-1^{low} (62). Second, utilizing TCRtg T cells reactive against ectopically expressed model antigens, it was demonstrated that experimentally and peripherally induced TCRtg pTregs were

primarily Nrp-1^{low} (61, 62). However, in the same set of studies it was also demonstrated that in highly inflammatory environments (such as the spinal cords of mice with experimentally induced autoimmune encephalomyelitis (EAE) or from the lungs of mice with chronic asthma), TCRtg pTregs upregulate Nrp-1 (62). Thus, similar to Helios, Nrp-1 expression on Tregs may be more of a marker of Treg activation than a definitive marker of developmental origin.

Experimental evidence in favor of the peripheral conversion of Tconv cells as a mechanism of tumor immune evasion utilized *in vitro* cultures systems (63, 64) or the ectopic expression of model antigens combined with the adoptive transfer of high affinity TCRtg Tconv cells (65, 66). However, these experiments likely fail to accurately recapitulate the *in vivo* context in which endogenous T cell specificities, that have faced a gauntlet of recessive and dominant tolerance mechanisms, encounter naturally derived tumor-associated antigens. Direct functional evidence demonstrating the peripheral conversion of endogenous T cell specificities reactive to tumor associated antigens is lacking, and the relative contribution of tTreg versus pTregs towards the tumor-infiltrating Treg repertoire remains unclear. Thus, due to a lack of clear markers to delineate tTreg from pTreg, the best means to determine the developmental origins of endogenous tumor-associated Tregs may be to functionally evaluate the capacity of individual tumor-associated Treg TCR specificities to enable Treg lineage selection within the thymus or periphery.

Antigen presentation in the development and homeostasis of Tregs

As described above, antigen presentation plays a critical role in Treg development and differentiation. Additionally, TCR-mediated antigen recognition has been shown to be important for the homeostasis and function of Tregs. In this regard, studies involving the conditional ablation of the TCR on Foxp3-expressing cells demonstrated that loss of the TCR on Tregs led to a disruption in Treg function and the subsequent induction of systemic autoimmunity (67, 68). Despite the critical impact TCR engagement has on both the development and function of Tregs, little is known about the cell types that interact with and present antigen for recognition by Tregs at steady state; with even less known about the impact and identity of APCs in the tumor environment.

During the thymic development of tTregs, self antigen presentation by both medullary thymic epithelial cells (mTECs) and DCs are required to establish a replete Treg pool (69-71). However, since multiple MHC-II⁺ DC subsets can be found in the thymus, including plasmacytoid DCs, CD8 α ⁺ classical DCs (cDCs) and Sirp α ⁺ cDCs (15, 72), it will be important to determine if each subset plays redundant or individualized roles in facilitating the development of tTregs. In regards to the peripheral development of pTregs, previous studies utilizing the experimental targeting of antigen to migratory DCs (mDCs) via anti-DEC-205 or anti-Langerin antibodies led to the induction of antigen-specific, Foxp3^{neg} Tconv cells into Foxp3⁺ pTregs within the skin-draining lymph nodes (73). Since mDCs exhibit significant heterogeneity and can also be broken down into several unique subsets (74), it will also be important to determine if individual subsets serve redundant or specialized roles in the peripheral conversion of pTregs. Finally, in either developmental context, it will be important to delineate the

contributions of the various APC subsets towards the development of tumor-associated Treg specificities.

TCR-mediated signaling continues to play a significant role in Treg function after development (67, 68), and thus it will also be critical to identify the APCs that coordinate Treg function by orchestrating the presentation of Treg antigens within various lymphoid and non-lymphoid tissue, at both steady-state and in the context of disease. Under homeostatic conditions within the spleen, previous studies have demonstrated that the depletion of DCs, via diphtheria-toxin-mediated ablation in *CD11c^{DTR}* mice (75) or administration of anti-ICOSL antibodies (76), resulted in a loss of Treg frequency or loss of CD44^{high}CD62L^{low} Tregs, respectively. Additionally, an expansion of Tregs was also observed upon the expansion of Flt3L-dependent DCs in the spleen (75, 76). While these studies suggest that the homeostasis of some splenic Tregs is orchestrated by CD11c⁺ DCs, it is unknown whether a distinct DC subset supports Treg homeostasis at this site. Since the lymph nodes contain various APC populations not found in the spleen (77), it is also unclear whether the same dependency on CD11c⁺ cells would be operative, and if so, what the contribution of individual DC subsets at those sites would be. Finally, since such experiments were carried out at steady state, it will be important to elucidate the contribution of the various APCs in the context of disease, such as autoimmunity or cancer.

Summary

Foxp3⁺ Tregs play critical roles in the regulation of immune responses against self and foreign antigens. While Tregs are necessary for the maintenance of immune

tolerance throughout life, they are also co-opted by tumors, likely in order to suppress antitumor immune responses and promote tumorigenesis. Several fundamental aspects of tumor-associated Treg biology remain unclear, including the nature of antigens recognized by these cells and the mechanisms by which they develop. Based on these gaps in knowledge, we set out to characterize the endogenous T cell immune response to a genetically-driven and autologous murine-prostate-cancer model by performing TCR deep sequencing studies. Utilizing TCRtg mice expressing tumor-associated Treg TCRs identified in sequencing studies, we then sought to functionally evaluate various aspects of the biology of these cells, including identifying their developmental origins, mechanisms of development, antigenic specificities and antigen presenting cell interaction partners. In this way, we hoped to elucidate key aspects of tumor-associated Treg biology which may enable new approaches for selectively targeting these cells for the treatment of cancer and potentially autoimmunity.

MATERIALS AND METHODS (78, 79) ⁱ

Mice

All mice were bred and maintained in accordance with the animal care and use regulations of the University of Chicago and housed in a specific-pathogen free facility. All mice were on the C57BL/6J (B6) background. The following mouse strains were purchased from the Jackson Laboratory and maintained in our facility: C57BL/6J (B6) mice, *CD45^{1/1}* B6.SJL-*Ptprc^a Pepc^b*/BoyJ mice, TRAMP C57BL/6-Tg(TRAMP)8247ng/J mice, *Aire^{-/-}* B6.129S2-*Aire^{tm1.1Doi}*/J mice, *Foxp3^{GFP}* B6.Cg-*Foxp3^{tm2Tch}*/J mice, *Rag1^{-/-}* B6.129S7-*Rag1^{tm1Mom}*/J mice, *CD11c^{DTR}* B6.FVB-Tg(*Itgax-DTR/EGFP*) 57Lan/J mice, *BDCA2^{DTR}* C57BL/6-Tg(*CLEC4C-HBEGF*)956Cln/J mice, *MHC-II^{-/-}* B6.129S2-*H2^{dIAb1-Ea}*/J mice, *CD80^{-/-}/CD86^{-/-}* B6.129S4-*Cd80^{tm1Shr}Cd86^{tm2Shr}*/J mice, *Ccr7^{-/-}* B6.129P2(C)-*Ccr7^{tm1Rfor}*/J mice, CD11c-Cre B6.Cg-Tg(*Itgax-cre*)1-1Reiz/J mice, *MHC-II^{fllox/fllox}* B6.129X1-*H2-Ab^{1tm1Koni}*/J mice, *Batf3^{-/-}* B6.129S(C)-*Batf3^{tm1Kmm}*/J mice, and μ MT B6.129S2-*Ighm^{tm1Cgn}*/J. OT-II transgenic C57BL/6-Tg(TcraTcrb)425Cbn/Crl mice were purchased from Charles River. Some *Foxp3^{GFP}* reporter mice were a generous gift from Alexander Rudensky. MJ23tg mice, RT83tg mice, and TCR β tg mice were generated at the University of Chicago Transgenic Core Facility as described below.

ⁱ This section is reproduced here, from the referenced citations, with minimal modification under the licenses granted by the AAAS Author License to Publish Policy and Elsevier. Materials and Methods sections from the referenced papers have been combined for brevity with additional details added for clarity and completeness.

Generation of TCR transgenic mice

TCR transgenic mice were generated by standard methods using the TCR cassette vectors of Kouskoff et al. (80). The TCR cassette vectors pT α cass and pT β cass were a gift from C. Benoist. The TCR chains are as follows, with the CDR3 amino acid sequences indicated.

a) “TCR β tg” mice:

V β 3(TRBV26)-ASSLGSSYEQY, utilizing TRBJ2-7

b) “MJ23tg” mice:

V α 2(TRAV14D-3)-LYYNQGKLI, utilizing TRAJ23

V β 3(TRBV26)-ASSLGSSYEQY, utilizing TRBJ2-7

c) “RT83tg” mice:

V α 8(TRAV12D-3)-ALRDSNNRIF, utilizing TRAJ31

V β 3(TRBV26)-ASSLGSSYEQY, utilizing TRBJ2-7

The rearranged TCR α and TCR β chains were cloned into pT α cass and pT β cass, respectively. Rearranged TCR α chains was generated by gene synthesis (Genscript), and cloned into the XmaI/SacII sites of the pT α cass vector using STBL4 cells (Invitrogen). The resulting TCR α constructs were excised from the vector using Sall. The rearranged TCR β chain was generated via splicing by overlap extension, cloned into pBSII (Stratagene) using XhoI/SacII sites, and subcloned into pT β cass using STBL4 cells. The resulting TCR β construct was excised from the vector using KpnI.

Excised linear TCR α and TCR β constructs were purified and either injected singly (for TCR β tg) or co-injected (for MJ23tg and RT83tg) into blastocysts using standard methods. Transgenic mice were generated on either a pure B6 background or on a (CBA x B6)F2 background and crossed to the B6 background for at least 12 generations. Genotyping of transgenic mice was performed by PCR amplification of earpunch DNA using the following primers:

V α 2(TRAV14D-3)-LYYNQGKLI forward 5'-CGGGGGGAatggacaagatc-3'

V α 2(TRAV14D-3)-LYYNQGKLI reverse 5'-AAAGATAAGCTTCCCCTGGTTATAATAGAG-3'

V α 8(TRAV12D-3)-ALRDSNNRIF forward 5'-CATCTCCCGGGGGGAATGCGTC-3'

V α 8(TRAV12D-3)-ALRDSNNRIF reverse 5'-AGATTCTGTTATTGCTATCTC-3'

V β 3(TRBV26)-ASSLGSSYEYQ forward 5'-CCAGTATCTCGAGCGGATGG-3'

V β 3(TRBV26)-ASSLGSSYEYQ reverse 5'-TTCATAGGAGCTACCCAGAC-3'

TCR CDR3 length distribution analysis

T cells were FACS-sorted into TRI reagent (Sigma), and RNA was isolated by standard methods using glycogen (Roche) as a carrier for precipitation. RNA was reverse transcribed using oligo dT primer (IDT) and Superscript II reverse transcriptase (Invitrogen). cDNA was subjected to PCR amplification with Platinum Taq (Invitrogen) using a 6-FAM-labeled C α -specific primer (5'-CCATGGTTTTTCGGCACATTG-3') paired with a V α 2(TRAV14)-specific primer (5'-GAGAAAAAGCTCTCCTTGAC-3'). 40 cycles of PCR amplification were performed with annealing at 55°C. Amplification products

were resolved and quantified on an Applied Biosystems 3730XL automated sequencer, using an internal calibration control to determine fragment length. CDR3 size spectra and peak areas were analyzed using Peak Scanner software (Applied Biosystems).

TCR sequencing and analysis

454 Deep Sequencing of $V\alpha 2$ (TRAV14)⁺ TCR α chains and $V\beta 3$ (TRBV26)⁺ TCR β chains

For the sequence analysis of $V\alpha 2$ (TRAV14)⁺ TCR α or $V\beta 3$ (TRBV26)⁺ TCR β chains, cDNA from FACS-sorted T cell subsets was PCR-amplified using the following primers. The forward fusion primers follow the sequence PrimerA-Barcode-mVregion, and the reverse fusion primers follow the sequence PrimerB-Barcode-mCregion. Sequences are as follows:

PrimerA 5'-CCATCTCATCCCTGCGTGTCTCCGACTCAG-3'

PrimerB 5'-CCTATCCCCTGTGTGCCTTGCCAGTCTCAG-3'

mV $\alpha 2$.P2 5'-GAGAAAAAGCTCTCCTTGAC-3'

mC α .P2 5'-CCATGGTTTTTCGGCACATTG-3'

mV $\beta 3$.P1 5'-CCTTGCAGCCTAGAAATTCAG-3'

mC β .P1 5'-CTTGGGTGGAGTCACATTTCTC-3'

The barcodes used were those recommended by the manufacturer for use with GS FLX Titanium emPCR (LIB-L) chemistry (Roche). PCR amplicons were gel-purified using a Gel Extraction Kit (Qiagen), and samples were processed for sequencing.

Sequencing was performed at the Utah State University Center for Integrated Biosystems using the Titanium sequencing chemistry on a Roche GS FLX system. The use of barcoded samples permitted the multiplexing of up to 14 different samples. Each sequence read was processed using a custom written python script to demultiplex the sample barcodes and parse out and translate the CDR3 regions. Using the parsed CDR3 sequences we generated a count table which had for each CDR3 and each sample a count of how many times that CDR3 element appeared. Typically, 1,000-2,000 sequence reads were obtained per sample.

iRepertoire complete TCR α chain analysis

CD4⁺Foxp3⁺ Treg cells were FACS-purified from different anatomical sites of 9-week-old TCR β transgenic *Foxp3*^{GFP} males on a wild type (*Batf3*^{+/+} and *Aire*^{+/+}), *Batf3*^{-/-} or *Aire*^{-/-} background, and cDNA was subjected to TCR α sequence analysis. RNA from FACS-sorted T cell subsets was subjected to TCR α sequencing using the Amp2Seq service from iRepertoire, a platform based on semi-quantitative multiplex PCR coupled with Illumina sequencing. This approach allows analysis of the complete TCR α repertoire, regardless of variable-region usage. Typically, >8 x 10⁵ TCR sequence reads were obtained per sample. We used edgeR from the R/Bioconductor package, a standard method from RNAseq analysis. TCRs were analyzed solely based on the predicted CDR3 sequence, regardless of V-region usage. We first filtered for TCRs with CDR3 segments between 7-17 amino acids in length and removed those TCRs with counts that were less than 10 in *Ns*-1 samples where *Ns* was the size of the smallest group. For example, when comparing two data sets with *N* = 4 and *N* = 5, *Ns*-1 = 3. In

this case, TCRs with fewer than 10 counts in 3 or more samples were removed from the differential analysis. This approach allowed focusing the analysis on recurrent TCRs. The samples were then normalized using the standard edgeR normalization routine (calcNormFactors) and p-values were computed using the edgeR standard test. P-values were corrected using the FDR method and the standard threshold of 0.05 was set. To enable fold-change calculations, a pseudocount approach was used. Differential representation of recurrent TCRs was displayed in “volcano plots” depicting FDR vs. log2 fold-change.

Analysis of TCR repertoire similarity

To analyze TCR repertoire similarity, we also analyzed CDR3 elements using the Morisita-Horn similarity index(81). The index computes the similarity between two populations of “species”, originally taxonomic species, but here CDR3 species. If x_i is the number of time species “i” occurs in sample X and y_i the number in sample Y then the index is defined as:

$$C_H = \frac{2 \sum_{i=1}^S x_i y_i}{\left(\frac{\sum_{i=1}^S x_i^2}{X^2} + \frac{\sum_{i=1}^S y_i^2}{Y^2} \right) XY}$$

Where X is the sum of x_i , Y is the sum of y_i and S is the number of species. The resulting matrix of pair-wise similarities between all samples was then clustered using standard hierarchical clustering using $1-C_H$ as the distance metric and using average linkage for the joining.

Antibodies, flow cytometry and fluorescence-activated cell sorting

All antibodies were purchased from eBioscience, Biolegend, BD Biosciences or Miltenyi Biotec. Typically, cells were stained for 20 minutes on ice in staining buffer (phosphate-buffered saline with 2% FCS, 0.1% NaN₃, 5% normal rat serum, 5% normal mouse serum, 5% normal rabbit serum (all sera from Jackson Immunoresearch), and 10 µg/mL 2.4G2 antibody). Intracellular staining for Foxp3 and Egr2 was performed using fixation/permeabilization buffers from eBioscience. For the analysis of Treg cell thymic development and thymocyte cell sorting, thymocytes were enriched for CD4⁺CD8α^{neg} cells by depleting CD8α⁺ cells utilizing biotinylated anti-CD8α (53-6.7) antibodies and streptavidin magnetic beads (STEMCELL) in accordance with manufacturer's protocols. Flow cytometry was performed on either an LSR-II or an LSRFortessa flow cytometer (BD Biosciences), using FlowJo data analysis software (Tree Star). Fluorescence-activated cell sorting (FACS) was performed using a FACSAria (BD Biosciences).

Generation of mixed bone marrow chimeric mice

5 x 10⁶, CD90.2 MACS bead (Miltenyi) T cell-depleted, bone marrow cells were transferred by either tail vein or retro orbital injection into either sublethally (500 rads) or lethally (1100 rads) irradiated hosts, with irradiations performed one day prior to transfer. Mixed donor cells typically consisted of a low-frequency (5%) of TCRtg bone marrow (either MJ23tg or RT83tg on a *Rag1*^{-/-} CD45^{1/1} background) and polyclonal "filler" cells from various CD45^{1/2} or CD45^{2/2} donors. All donor cells were taken from female mice. This donor cell ratio consistently resulted in a clonal frequency of TCRtg

thymocytes of less than 1%, regardless of radiation. Unless otherwise noted, all mice were analyzed at 6 weeks post-engraftment.

T cell transfer experiments

CD4⁺ T cells isolated from MJ23tg *Rag1*^{-/-} CD45.1⁺ female donor mice were purified using MACS sorting (Miltenyi), and 1 x 10⁵ cells were transferred intravenously into 5-month-old TRAMP^{+/+} or B6 recipients. 30 days post-transfer, the fate of donor cells was assessed.

Thymocyte, splenocyte, lymphocyte and prostate dendritic cell isolations

For most analyses involving APC subsets, prostate tissue (all lobes, unless otherwise noted) or lymphoid organs were injected and digested with Liberase TL (400 µg/mL, Roche) and DNase (800 µg/mL, Roche) in RPMI for 30 min at 37°C. Digested tissues were mechanically disrupted and placed into single cell suspension using a 70 µm cell strainer. Thymocyte APC fractions were further enriched by layering digested thymocytes on top of a discontinuous Percoll gradient (GE Healthcare) at 1.115 g/mL in PBS, followed by centrifugation at 1350 g for 30 min at 4°C and isolation of cells settling at the Percoll interface(82).

MJ23tg T cell stimulation experiments

Prostates from 20-27-week-old TRAMP mice were dissected and injected with a solution containing liberase CI / DNase I (Roche). Tissue was then mechanically disrupted, and the immune cell fraction was enriched on a continuous Percoll (GE

Healthcare) gradient. CD45⁺CD11c⁺F4/80^{neg} cells from this fraction were then purified by FACS. Cell cultures were set up in 96-well round-bottom plates coated with collagen (Sigma). Cultures contained 3 x 10⁴ CD45⁺CD11c⁺F4/80^{neg} cells, 3 x 10⁴ CD4⁺Foxp3^{neg} MJ23tg T cells or OT-IItg cells labeled with CFSE (Molecular Probes), and 100 U/mL recombinant mouse IL-2 (Miltenyi). In addition, anti-MHC-II antibody clone M5 (eBioscience) or isotype control antibody was added to the culture at a final concentration of 10 µg/mL. Dilution of CFSE was assessed by flow cytometry on day 4.

***In Vitro* Treg suppression assays**

Cultures containing the following components were established in 96 well round-bottom plates: a) 5 x 10⁴ irradiated (3,000 rads) splenocytes, b) 2.5 x 10⁴ CD4⁺CD25^{neg} polyclonal “T responder” cells labeled with CellTrace-Violet dye (Invitrogen), c) either 2.5 x 10⁴ CD4⁺CD25^{neg} or 2.5 x 10⁴ CD4⁺CD25⁺ T cells isolated from polyclonal or MJ23tg *Rag1*^{-/-} males, and d) 0.25 µg/mL soluble anti-CD3 antibody clone 145-2C11 (BioXCell). Dilution of CellTrace-Violet dye by T responder cells was assessed by flow cytometry on day 4.

Thymocyte transfer and intrathymic injections

Bulk thymocytes were harvested from 4-6 week old female TCRtg donor mice (either MJ23tg or RT83tg on a *Rag1*^{-/-} CD45^{1/1} background, which are devoid of Foxp3⁺ cells) and depleted of dendritic cells using CD11c MACS beads (Miltenyi). 4 x 10⁶ cells were then injected via intra-thymic injection into 4-6 week old CD45^{2/2} hosts. Host mice

were analyzed at either seven days, to evaluate thymic development, or three weeks, to evaluate the anatomical distribution and activation of TCRtg cells.

***In Vitro* MJ23tg thymocyte stimulation assay**

Thymic cDCs and splenic DCs were isolated from 4-6 week old male B6 donors as described above. Thymic cDCs (CD11c⁺SiglecH^{neg} TCRβ^{neg}CD19^{neg}F4/80^{neg}) were then FACS sorted into CD8α⁺ (CD8α⁺Sirpα^{neg}) and Sirpα⁺ (CD8α^{neg}Sirpα⁺) subsets. Splenic DCs were isolated using CD11c MACS beads (Miltenyi) and utilized as a negative control. MJ23tg thymocytes were harvested from 4-6 week old male MJ23tg *Rag1*^{-/-} CD45^{1/1} donor mice (which are devoid of Foxp3⁺ cells), enriched for CD4 single positive cells using a CD4⁺ T cell isolation MACS kit (Miltenyi) and labeled with CellTrace-Violet (Life Technologies) per manufactures instructions. This resulted in a MJ23tg thymocyte input devoid of thymic APCs and containing ~4% MJ23tg CD4 single positive cells. Prostate-tissue extracts were prepared by isolating prostate lobes of a TRAMP tumor bearing mouse, incubating lobes in PBS for 5 minutes and collecting the resultant supernatant. 1 x 10⁵ CellTrace-Violet-labeled MJ23tg thymocytes in the presence of IL-2 (Miltenyi) and IL-7 (Biolegend) in 384-well plates were cultured with: a) 5 x 10⁴ FACS-purified Sirpα⁺ or CD8α⁺ thymic cDCs or MACS-enriched splenic DC controls, b) with or without anti-MHC-II (IA/IE) (Biolegend), c) with or without prostate-tissue extracts. Following three days of culture, proliferation, CD69 expression, and Foxp3 upregulation by MJ23tg thymocytes were analyzed.

Castration

Sublethally irradiated MJ23tg bone marrow chimeras were generated as described above. Six weeks post-engraftment, mice were anesthetized utilizing ketamine/xylazine and either surgically castrated via removal of the testes or sham castrated by performing all steps of the castration procedure (e.g. incision and suture) while leaving testes intact. Four weeks post-procedure, testosterone levels were restored in half of the castrated mice via subcutaneous implantation of a testosterone slow-release capsule. All mice were analyzed four weeks post-implantation (8 weeks post-castration or post-sham castration).

Statistical analysis

Data were analyzed using Prism software (GraphPad). For the comparison of two groups, the Student's t-test (two-tailed) or the nonparametric Mann-Whitney test were used, depending on whether data were normally distributed. For comparison of multiple groups, one-way ANOVA couple with Tukey's multiple comparison test were employed when appropriate.

RESULTS: Aire-dependent thymic development of tumor-associated regulatory T cells (79)ⁱ

Summary

Despite considerable interest in the modulation of tumor-associated Foxp3⁺ regulatory T cells (Tregs) for therapeutic benefit, little is known about the developmental origins of these cells and the nature of the antigens that they recognize. Here, we identified an endogenous population of antigen-specific Tregs (termed “MJ23” Tregs) found recurrently enriched in the tumors of mice with oncogene-driven prostate cancer. MJ23 Tregs were not reactive to a tumor-specific antigen, but instead recognized a prostate-associated antigen that was present in tumor-free mice. MJ23 Tregs underwent Aire-dependent thymic development in both male and female mice. Thus Aire-mediated expression of peripheral tissue antigens drives the thymic development of a subset of organ-specific Tregs, which are likely co-opted by tumors developing within the associated organ.

Introduction

Treg cells are critical for the prevention of autoimmunity, the maintenance of immune homeostasis, and the suppression of antitumor immune responses (17, 83). For many human cancers, the density of Tregs within tumor lesions is predictive of poor clinical outcome (36), suggesting that Tregs play a functional role in cancer progression.

ⁱ This section is reproduced here, from the referenced citation, with minimal modification under the license granted by the AAAS Author License to Publish Policy. Changes include renumbering of figures, inclusion of supplemental text and figures, renaming of section subheadings to conform with this document, and the inclusion of additional section subheadings to facilitate reader comprehension.

In this study, we set out to establish a tractable animal model in which a single specificity of naturally occurring tumor-associated Tregs could be studied in the context of a genetically-driven mouse model of autochthonous cancer.

Results

T cell receptor sequencing of Tregs from TRAMP prostate tumors identifies a conical and recurrently enriched TCR

In order to identify an endogenous tumor-associated Treg response, we analyzed the immune response in TRAMP mice, which develop prostatic adenocarcinoma due to the transgenic expression of the model oncogene SV40 T antigen in the prostate (84, 85). Unlike the prostates of tumor-free mice, which contain very few Treg cells (which are identified as CD4⁺ Foxp3⁺), a substantial population of Tregs can be detected in the prostate tumors of TRAMP mice (Fig. 1). We employed an experimental system involving T cell antigen receptor alpha chain (TCR α) repertoire analysis of T cell populations from TRAMP mice expressing the Foxp3^{gfp} reporter (86) and a fixed (transgenic) TCR β chain. The fixed TCR β used in this study was a TCR β chain that was found to be recurrently expressed by CD4⁺Foxp3⁺ Tregs isolated from the prostates of TRAMP mice (Fig. 2), and will be referred to hereafter as “TCR β tg”. TCR complementarity determining region 3 (CDR3) length distribution analysis of cDNA from purified CD4⁺Foxp3⁺ and CD4⁺Foxp3^{neg} T cells from the prostate tumors of TRAMP^{+/-} Foxp3^{gfp} TCR β tg males revealed a substantial overrepresentation of CD4⁺Foxp3⁺ T cells expressing a V α 2 (TRAV14) TCR α chain with a CDR3 of nine amino acids in length (as defined by IMGT, <http://www.imgt.org>) (Fig. 3A, denoted in red). Deep

sequencing of these samples revealed that the identical TCR α chain, of CDR3 sequence LYYNQGKLI, was recurrently expressed by Foxp3⁺ Tregs (Fig. 3B), indicating that Tregs of a single specificity are recurrently enriched within TRAMP prostate tumors. Strikingly, in many prostate samples, the V α 2-LYYNQGKLI TCR chain was encoded by a single nucleotide sequence (Fig. 4), suggesting that in many cases, tumor-infiltrating Tregs of this specificity may originate from a single clone.

A survey of different anatomical sites of TRAMP^{+/-} Foxp3^{gfp} TCR β tg mice using CDR3 length distribution analysis revealed that the overrepresentation of Tregs expressing a V α 2⁺ TCR α chain of nine amino acids in length was observed in the prostate tumor and prostate-draining periaortic lymph nodes, but was not detected over background in non-draining brachial lymph nodes (Fig. 3C). Thus, Tregs of this specificity are not expanded systemically in tumor-bearing mice, but are instead selectively enriched in the prostate tumor environment.

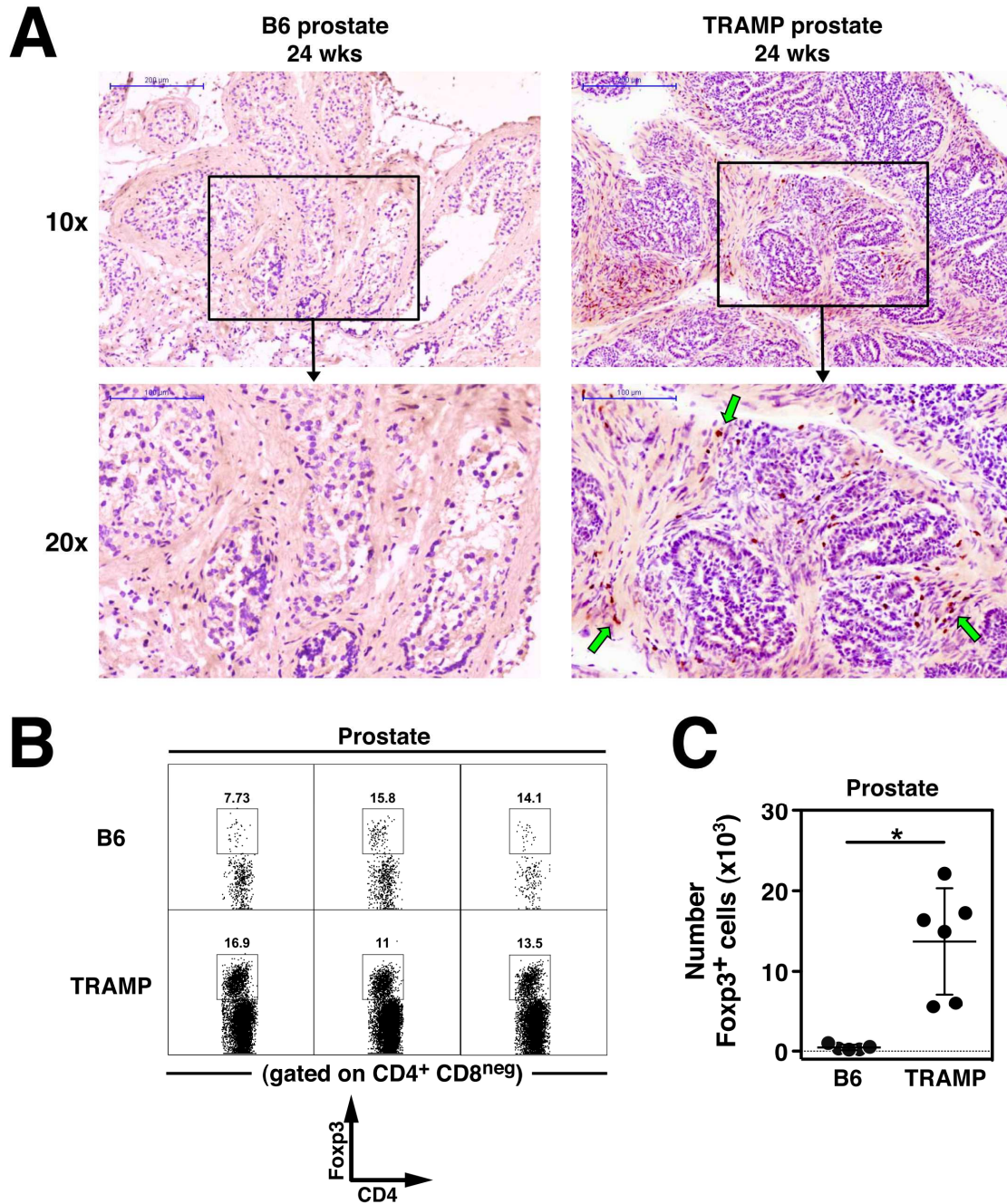


Figure 1: Enrichment of Tregs in TRAMP prostate tumors. (A) Immunohistochemical analysis of Fcpx3 expression in the prostatic dorsolateral lobes of 24-week-old B6 and TRAMP mice. Magnification is indicated. Green arrows denote Fcpx3-expressing cells. **(B)** Representative flow cytometric analysis of Fcpx3 expression by CD4⁺ T cells isolated from the prostates of 24-week-old B6 and TRAMP mice. **(C)** Quantification of the absolute number of Fcpx3⁺CD4⁺ cells isolated from 24-week-old B6 and TRAMP prostates. The mean \pm SEM is indicated. The asterisk denotes $p < 0.05$.

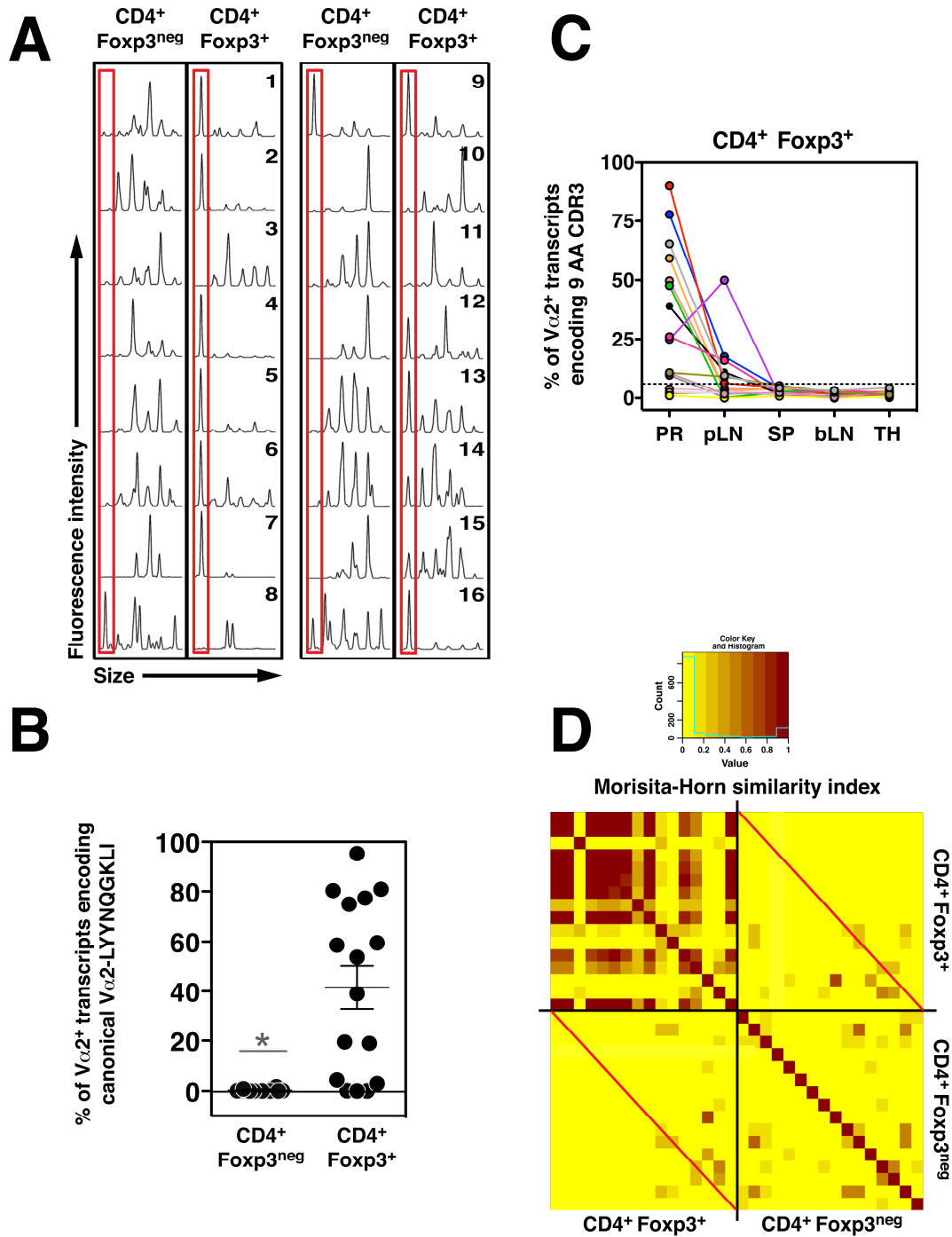


Figure 3: CD4⁺Foxp3⁺ Tregs expressing a canonical TCR are recurrently enriched in TRAMP prostate tumors. Analysis of V_α2 (TRAV14)⁺ TCR_α chains in tumor-bearing TRAMP^{+/-} Foxp3^{gfp} TCR_βtg mice. CD4⁺Foxp3^{neg} and CD4⁺Foxp3⁺ T cells were FACS-purified from different anatomical sites of ~27-week-old male mice, and cDNA was subjected to molecular analysis. **(A)** CDR3 length distribution analysis of V_α2⁺ TCR_α chains of T cell subsets isolated from prostate tumors.

Figure 3 Continued: The mouse number is indicated. The red boxes denote TCR α transcripts encoding a CDR3 of 9 amino acids (AA) in length. **(B)** V α 2⁺ TCR α transcripts from the indicated populations were PCR amplified and subjected to deep sequencing (see Methods (87)). The percentage of all V α 2⁺ TCR α transcripts encoding the canonical V α 2-LYYNQGLI chain is plotted for each sample. The mean \pm SEM is indicated. The asterisk indicates $p < 0.05$ (t-test). **(C)** Plots of the percentage of V α 2⁺ transcripts encoding a CDR3 of 9 AAs (based on peak area) for CD4⁺Foxp3⁺ T cells isolated from different anatomical sites of the mice depicted in panel (A). PR, prostate; pLN, periaortic lymph nodes; SP, spleen; bLN, brachial lymph nodes; TH, thymus. Samples from each mouse are color-coded. The plot does not depict data from mice 1 and 2, and includes data from two additional mice (numbers 17 and 18). Samples with values above the indicated threshold (dashed line) are considered “overrepresented”. This threshold is defined as the mean percent peak area plus three standard deviations for V α 2⁺ TCR α transcripts encoding a 9 AA CDR3 from the spleen of female TCR β tg mice. **(D)** Heat map of the Morisita-Horn (MH) similarity index for prostatic T cell subsets from mice 1-16. Samples are oriented in ascending numerical order, from top to bottom and left to right (not shown). A motif table of predicted amino acid sequences is presented in Table S1. CD4⁺Foxp3^{neg} and CD4⁺Foxp3⁺ subsets from the same prostate tumor intersect at the red diagonal lines. Data are pooled from $N = 3$ independent FACS-sorting experiments.

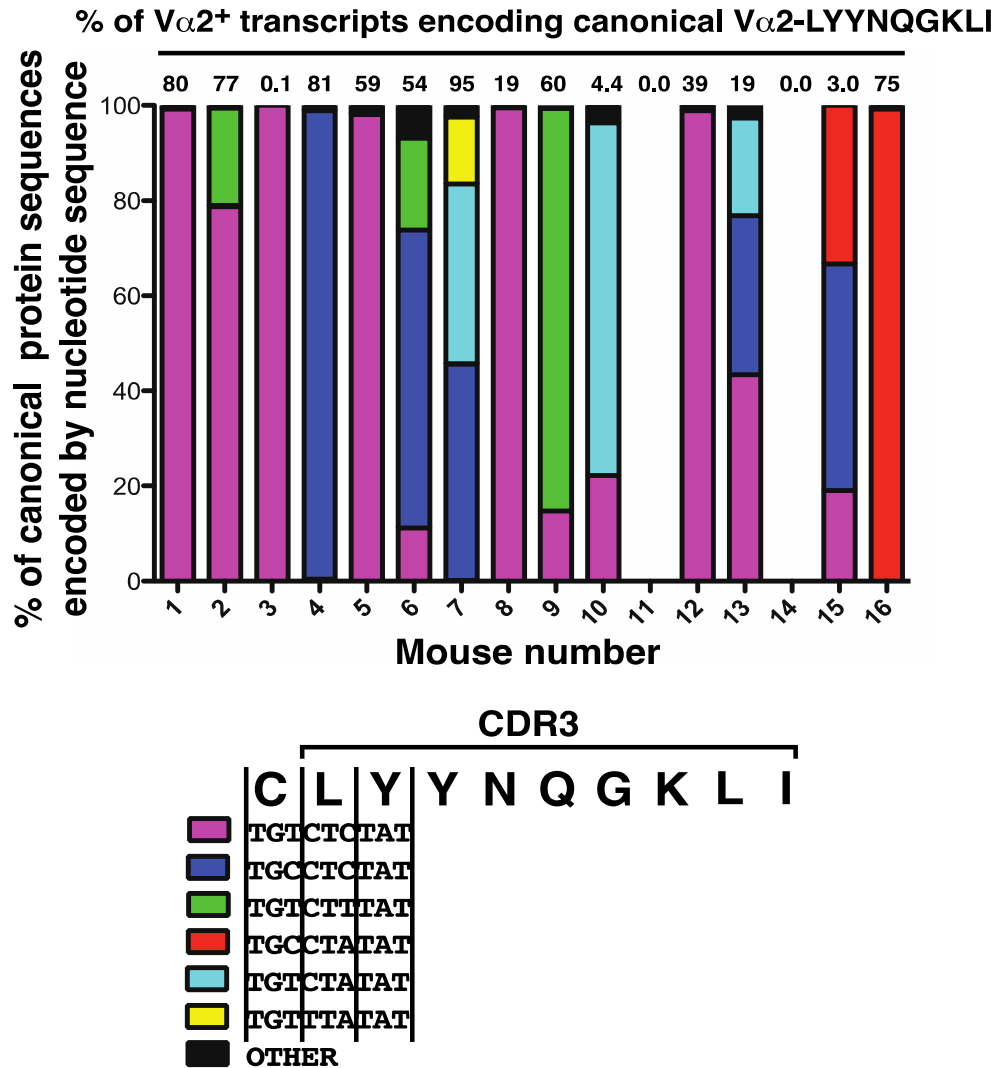


Figure 4: In many TRAMP^{+/-} Foxp3^{gfp} TCR β tg mice, the canonical V α 2-LYYNQGKLI chain is encoded by a single nucleotide sequence. Data are from the same mice presented in Fig. 1. There are six possible nucleotide sequences that encode the canonical V α 2-LYYNQGKLI chain (indicated by different colors). These nucleotide sequences vary only at the codons encoding the conserved cysteine N-terminal to the CDR3, and the leucine and tyrosine at the first two CDR3 positions. Nucleotides encoding the remaining YNQGKLI residues are invariant because they are derived from the TRAJ23 segment. Across the top, for each mouse, the percentage of V α 2⁺ transcripts that encode the canonical V α 2-LYYNQGKLI is indicated. The distribution of nucleotide sequences encoding these canonical chains is indicated in the colored bar graphs. For example, for mouse #1, 80% of V α 2⁺ transcripts encode the canonical V α 2-LYYNQGKLI chain, and >99% of these are encoded by the magenta nucleotide sequence. Data are pooled from *N* = 3 independent FACS sorting experiments.

The TCRs of Treg and Tconv tumor infiltrating cells are distinct and non-overlapping

In order to gain insight into the antigen specificities of polyclonal tumor-infiltrating CD4⁺ T cells, we determined the extent of overlap of the V α 2⁺ TCR repertoire for T cell subsets isolated from the prostate tumors of TRAMP^{+/-} Foxp3^{gfp} TCR β tg mice. Repertoire overlap was assessed using the Morisita-Horn (MH) similarity index (81, 88-91), for which a value of 1 indicates identity, and a value of 0 denotes complete dissimilarity (Fig. 3D). The analysis revealed that the TCR repertoire of CD4⁺Foxp3⁺ and CD4⁺Foxp3^{neg} populations isolated from a particular prostate tumor were largely distinct and non-overlapping (MH = 0.07 \pm 0.10 SD, Fig. 3D, samples intersecting at red lines), implying that the antigens recognized by tumor-infiltrating Tregs are different from those recognized by conventional CD4⁺ T cells. Second, the TCR repertoire of CD4⁺Foxp3⁺ cells isolated from the prostates of different mice exhibited a high degree of similarity from mouse to mouse (MH = 0.38 \pm 0.39 SD, Fig. 3D, upper left quadrant). While a substantial proportion of this similarity was due to the recurrent enrichment of the V α 2-LYYNQGKLI TCR, additional TCR α chains were identified that were recurrently expressed by prostatic Foxp3⁺ Tregs (Fig. 5). This finding suggests that TRAMP prostate tumors do not recruit polyclonal Tregs of arbitrary specificity, but instead are associated with the reproducible enrichment of Tregs of distinct specificities.

Figure 5: Five most common V α 2+ TCR α chains expressed by prostatic CD4⁺Foxp3⁺ T cells from TRAMP^{+/-} Foxp3^{gfp} TCR β tg mice. Analysis of V α 2 (TRAV14)⁺ TCR α chains in tumor-bearing TRAMP^{+/-} Foxp3^{gfp} TCR β tg mice. Data are from the same mice presented in Fig. 1B. CD4⁺Foxp3^{neg} and CD4⁺Foxp3⁺ T cells were FACS-purified from the prostates of ~27-week-old male mice, and V α 2⁺ TCR α transcripts were PCR-amplified and subjected to deep sequencing. The percentage of all V α 2⁺ TCR α transcripts encoding the indicated TCR α chain is plotted. The mean \pm SEM is indicated. Asterisks indicate $p < 0.05$. Data are pooled from $N = 3$ independent FACS sorting experiments.

Tumor-associated MJ23 Tregs are reactive to a prostate-associated self antigen

To facilitate the study of T cells expressing the canonical V α 2-LYYNQGKLI TCR α chain paired with the fixed TCR β chain (hereafter referred to as “MJ23” T cells), we generated transgenic (tg) mice expressing the MJ23 TCR $\alpha\beta$ heterodimer. In female MJ23tg *Rag1*^{-/-} mice, CD4⁺ T cells in the periphery were phenotypically naïve (Fig. 6A and Fig. 7). Moreover, Foxp3⁺ MJ23tg cells were not detected above background in the thymus and periphery of these mice (Fig. 6, A and B, and Fig. 7). In contrast, analysis of tumor-free male MJ23tg *Rag1*^{-/-} mice revealed spontaneous accumulation of activated CD44^{hi} CD4⁺ MJ23tg T cells in the prostate and prostate-draining periaortic lymph nodes (Fig. 6 A and B, and Fig. 7), indicative of MJ23 reactivity to an autoantigen at these sites. In the prostate, T cell accumulation was observed in both the stroma and the epithelium, and was associated with disruption of the basement membrane of prostatic glands (Fig. 6C). The presence of activated CD4⁺ T cells was accompanied by the concomitant appearance of a percentage of CD4⁺Foxp3⁺ T cells (Fig. 6, A and B, and Fig. 7). Foxp3⁺ cells exhibited *in vitro* suppressive activity (Fig. 8) and phenotypic characteristics of Tregs (Fig. 9), including expression of neuropilin-1. Taken together, our data demonstrate that MJ23 Tregs, identified based on their enrichment in mouse prostate tumors, are not reactive to a unique tumor-specific antigen, but instead recognize a self antigen associated with the organ of cancer origin.

In other experiments, CD11c⁺ dendritic cells isolated from TRAMP prostate tumors induced robust proliferation of MJ23tg T cells *ex vivo* (Fig. 6D), but did not stimulate OT-IItg T cells expressing an irrelevant TCR (92). These data provide direct evidence that prostate tumors contain the antigen recognized by MJ23 T cells.

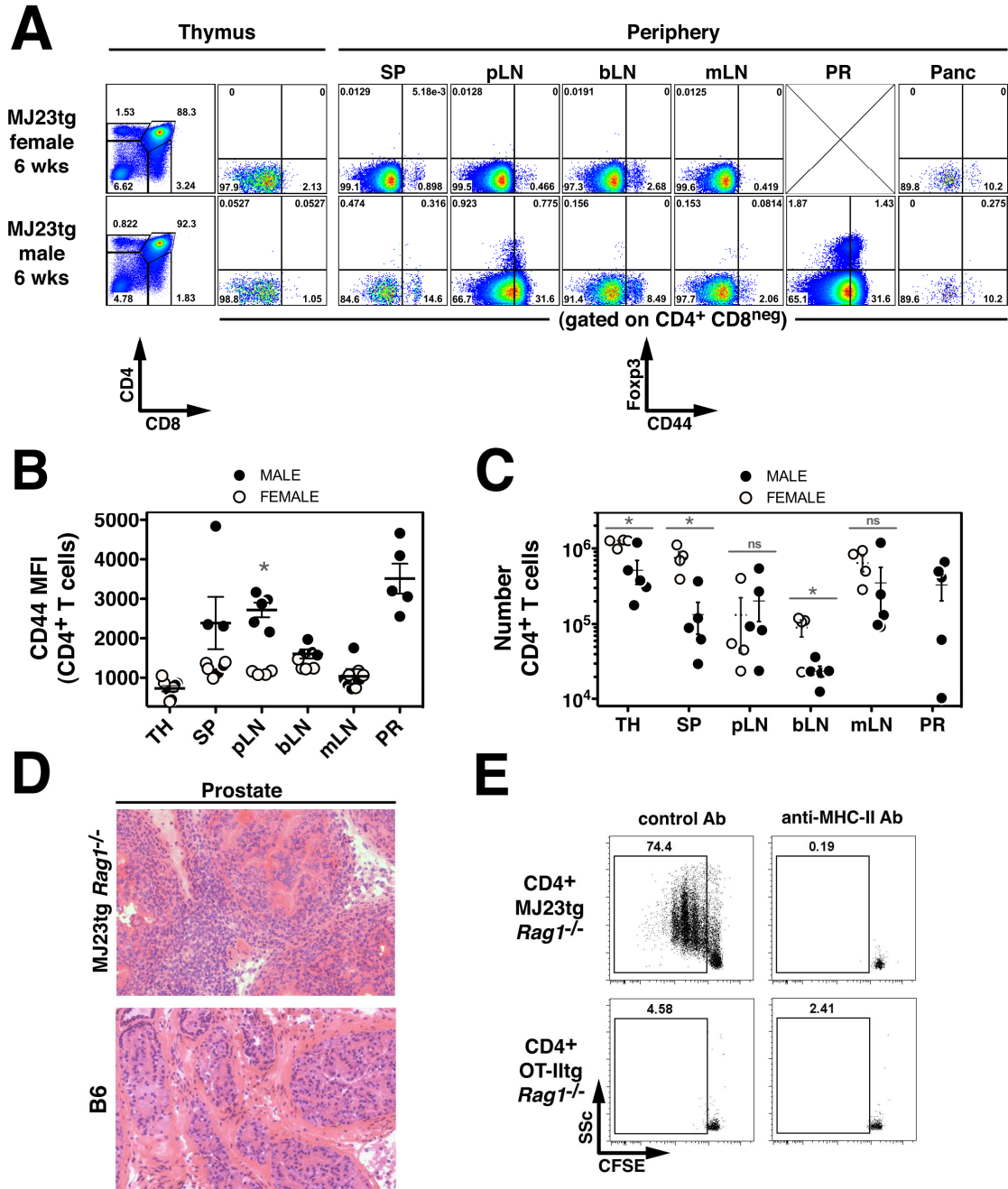


Figure 6: MJ23 T cells recognize a prostate-associated self antigen. (A-C) Spontaneous T cell autoreactivity in the prostates of tumor-free male MJ23tg *Rag1*^{-/-} mice. **(A)** Representative flow cytometric analyses of T cells isolated from the indicated organs of 6-week-old male or female mice. SP, spleen; pLN, periaortic lymph nodes; bLN, brachial lymph nodes; mLN, mesenteric lymph nodes; PR, prostate; Panc, pancreas. **(B)** Summary plot of the absolute number of CD4⁺Foxp3⁺ T cells from the indicated organs of 6-week-old male or female mice. **(C)** Hematoxylin and eosin staining of dorsolateral prostatic lobes from 18-week-old MJ23tg *Rag1*^{-/-} and B6 mice.

Figure 6 Continued: Scale bar = 100 μm . **(D)** CFSE-labeled $\text{CD4}^+\text{Foxp3}^{\text{neg}}$ MJ23tg T cells or OT-IItg cells were cultured with FACS-purified $\text{CD45}^+\text{CD11c}^+\text{F4/80}^{\text{neg}}$ cells isolated from TRAMP prostate tumors in the presence of recombinant mouse IL-2. In addition, MHC-II antibody or isotype control antibody was added to the culture. Dilution of CFSE was assessed by flow cytometry on day 4. The mean \pm SEM is indicated. Asterisks indicate $p < 0.05$, ns = not significant. For (A-B), data are pooled from $N = 2$ independent experiments. For (B), t-tests were used to compare data from male and female mice at each site. Data in (D) are representative of $N = 7$ independent experiments.

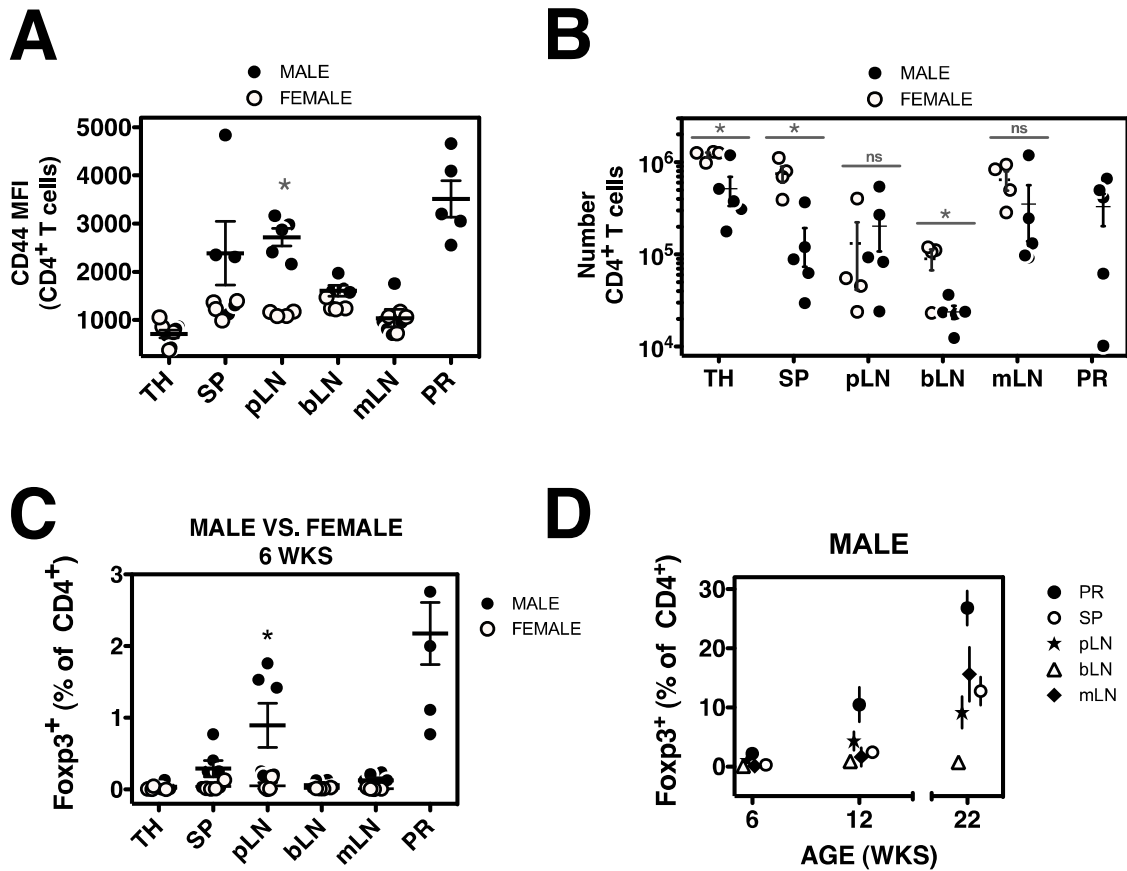


Figure 7: Analysis of CD4⁺FoXP3⁺ T cells in MJ23tg Rag1^{-/-} mice. Data are from the same mice presented in Fig. 6. TH, thymus; SP, spleen; pLN, periaortic lymph nodes; bLN, brachial lymph nodes; mLN, mesenteric lymph nodes; PR, prostate. **(A)** Summary plot of the mean fluorescence intensity (MFI) of staining for the CD44 activation marker on CD4⁺ T cells isolated from the indicated organs of 6-week-old male and female mice. **(B)** Summary plot of the absolute number of CD4⁺ T cells from different anatomical sites of 6-week-old male or female mice. **(C)** Summary plot of the frequency of FoXP3⁺ cells (as a percentage of CD4⁺ cells) from the indicated organs of 6-week-old male and female mice. **(D)** Summary plot of the frequency of FoXP3⁺ cells (as a percentage of CD4⁺ cells) from the indicated organs of male mice of various ages. The mean \pm SEM is indicated. Asterisks indicate $p < 0.05$, for comparisons of males vs. females at a given anatomical site. Data are pooled from $N = 2$ independent analyses.

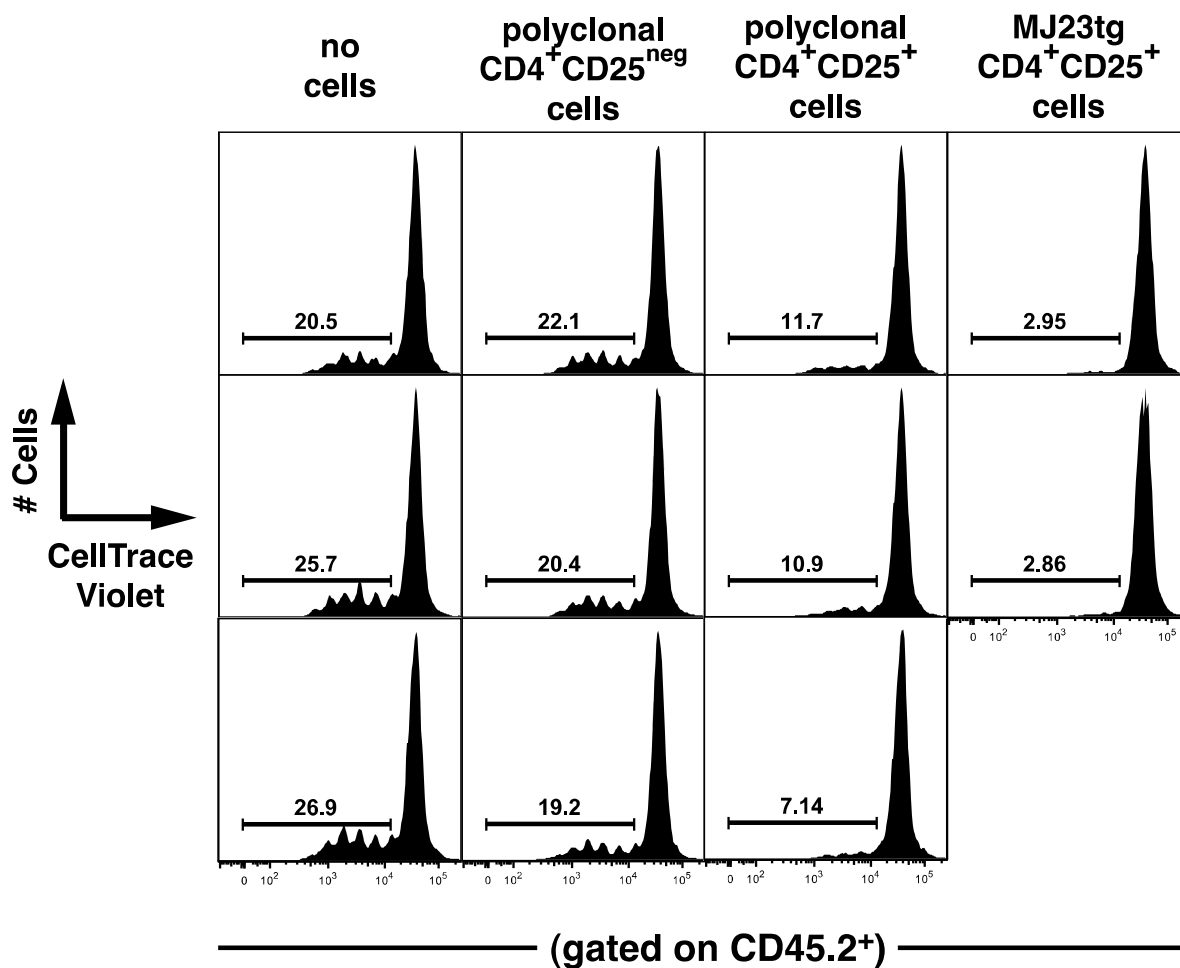


Figure 8: Suppressive function of Tregs from MJ23tg Rag1^{-/-} males. Suppressive activity of MJ23tg Tregs *in vitro*. 2.5×10^4 polyclonal CD45^{.2/.2}CD4⁺ CD25^{neg} T responder cells labeled with Cell Trace-Violet (CTV) were stimulated with 5×10^4 irradiated CD45^{.1/.1} splenocytes plus 0.25 $\mu\text{g}/\text{mL}$ soluble anti-CD3 antibody. In addition, 2.5×10^4 of the indicated FACS-purified CD45^{.1/.1} cells were added to the culture. CD4⁺CD25⁺ MJ23tg cells were isolated from the prostates of male MJ23tg Rag1^{-/-} mice. CD4⁺CD25⁺ polyclonal cells were isolated from the spleen and lymph nodes of B6.SJL mice. Dilution of CTV was assessed by flow cytometry at day 4. The percentage of CD45.2⁺ T responder cells with diluted CTV is indicated.

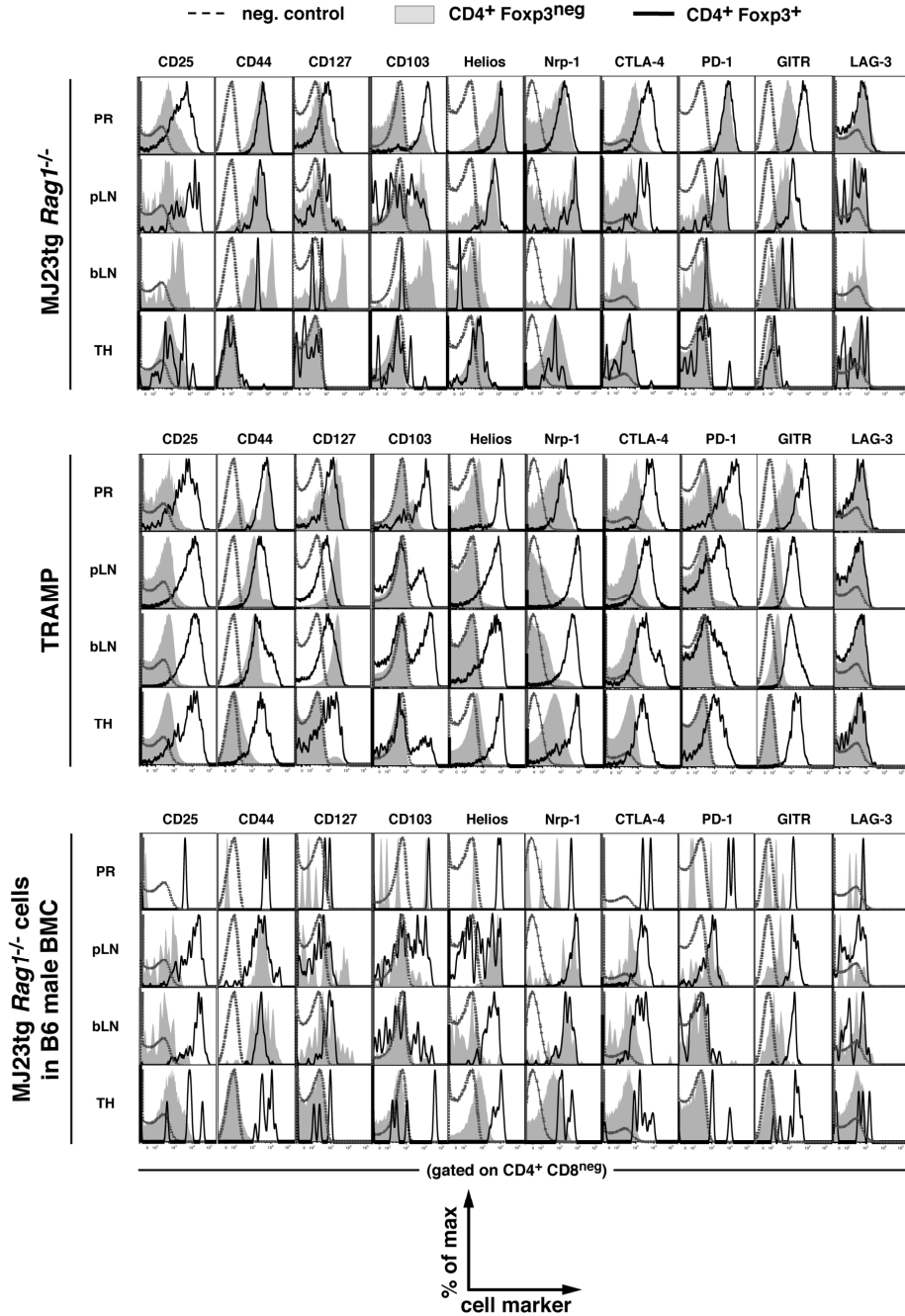


Figure 9: Phenotypic analysis of MJ23tg Tregs. Representative flow cytometric analysis of CD4⁺ T cells from the prostate (PR), periaortic lymph nodes (pLN), brachial lymph nodes (bLN), and thymus (TH) of the indicated mice. The cells analyzed are as follows: Top, T cells pooled from 12-week-old MJ23tg *Rag1*^{-/-} males; Middle, polyclonal T cells pooled from 27-week-old TRAMP males; Bottom, CD45.1⁺ MJ23tg donor cells pooled from MJ23tg bone marrow chimeras (BMCs) generated in B6 male hosts. Histogram overlays depict expression of the indicated marker by CD4⁺Foxp3^{neg} and CD4⁺Foxp3⁺ T cells.

MJ23 Tregs develop in the thymus and enrich in the prostate draining lymph nodes of male mice

In order to study the development of MJ23tg T cells at physiological clonal frequencies, we generated chimeric animals in which bone marrow cells from MJ23tg *Rag1*^{-/-} donors were engrafted into host mice at low frequencies (<1%), and the development and distribution of MJ23tg T cells was assessed (Fig. 10 and Fig. 11). Analysis of B6 male and tumor-bearing TRAMP male hosts revealed that Foxp3⁺ MJ23tg Tregs developed in the thymus (Fig. 10, A and B). The efficiency of development varied from mouse to mouse, and was inversely correlated with the frequency of MJ23tg precursors (Fig. 10B), a finding that is consistent with previously published studies (93, 94). In other experiments, OT-II *Rag1*^{-/-} precursors did not develop efficiently into Foxp3⁺ cells in the thymus, demonstrating the specificity of MJ23tg Treg development (Fig. 12).

In the periphery of male chimeras, Foxp3⁺ MJ23tg cells were distributed throughout the secondary lymphoid organs, but were preferentially enriched in the prostate-draining periaortic lymph nodes (Fig. 10C), a finding consistent with evidence of reactivity to a prostate-associated antigen (Fig. 6). Recent reports suggest that induced Tregs of extrathymic origin express low amounts of the marker neuropilin-1 (Nrp-1) (61, 62). Flow cytometric analyses of Foxp3⁺ MJ23tg Tregs in the lymph nodes and spleen of MJ23tg bone marrow chimeric mice revealed high expression of Nrp-1 by these cells (Fig. 9). Moreover, polyclonal T cells from the prostates of tumor-free B6 or tumor-bearing TRAMP mice exhibited unimodal, intermediate expression of Nrp-1 (Fig. 13). Comparatively, many Tregs from the colon, which is thought to contain a

substantial proportion of induced Tregs (32), expressed low amounts of Nrp-1 (Fig. 13). Together, these data are suggestive of a thymic origin for both MJ23 Tregs and polyclonal prostate tumor-infiltrating Tregs, consistent with our data demonstrating that the MJ23 TCR facilitates Treg development in the thymus (Fig. 10).

Very few donor-derived MJ23tg Tregs were observed in the prostate (Fig. 10, A and C), likely reflecting competition with endogenous MJ23 Tregs (Fig. 14). Data presented in Fig. 3 demonstrate that endogenous Tregs expressing the MJ23 TCR are recurrently enriched in TRAMP prostate tumors. However, in MJ23tg bone marrow chimeric mice generated in B6 or TRAMP male hosts, donor-derived MJ23tg Tregs were often not enriched in the prostate (Fig. 10, A and C). This effect was likely the result of two factors associated with the experimental approach utilized to generate chimeric mice, in which cells from MJ23tg mice were engrafted, along with an excess of polyclonal “filler” cells, into sublethally irradiated polyclonal hosts. First, chimeric mice exhibited a marked decrease in the total number of Tregs in the prostate relative to unmanipulated mice (Fig. 14A). These data indicate that radiation alters the prostatic Treg infiltrate, and induces a substantial reduction in the quantity of Tregs recovered. Second, prostatic infiltration by donor-derived MJ23tg cells was likely limited by competition with host-derived polyclonal MJ23 Tregs. In this scenario, endogenous Tregs that survive sublethal irradiation may occupy putative antigenic niches in the prostate, thereby restricting infiltration by donor-derived MJ23tg T cells that enter the peripheral pool following a time lag required for bone marrow engraftment and T cell development in the thymus. In support of this hypothesis, when MJ23tg bone marrow chimeras were analyzed at a later time point (20 weeks post-engraftment), donor-

derived MJ23tg Tregs were observed in the prostates of B6 male hosts (Fig. 14B), indicating that donor-derived MJ23tg Tregs access the prostate at later time points.

Upon intravenous transfer of naïve CD4⁺Foxp3^{neg} MJ23tg T cells into TRAMP males, the induction of Foxp3 expression by MJ23tg cells was negligible (Fig. 15), suggesting that antigen exposure in the periphery does not favor the development of induced Tregs. Taken together, our results demonstrate that expression of the MJ23 TCR facilitates Treg development in the thymus of male hosts. Thus, T cells of this specificity encounter the antigen(s) driving Treg development during maturation in the thymus, prior to their exposure to the prostate or tumor environment.

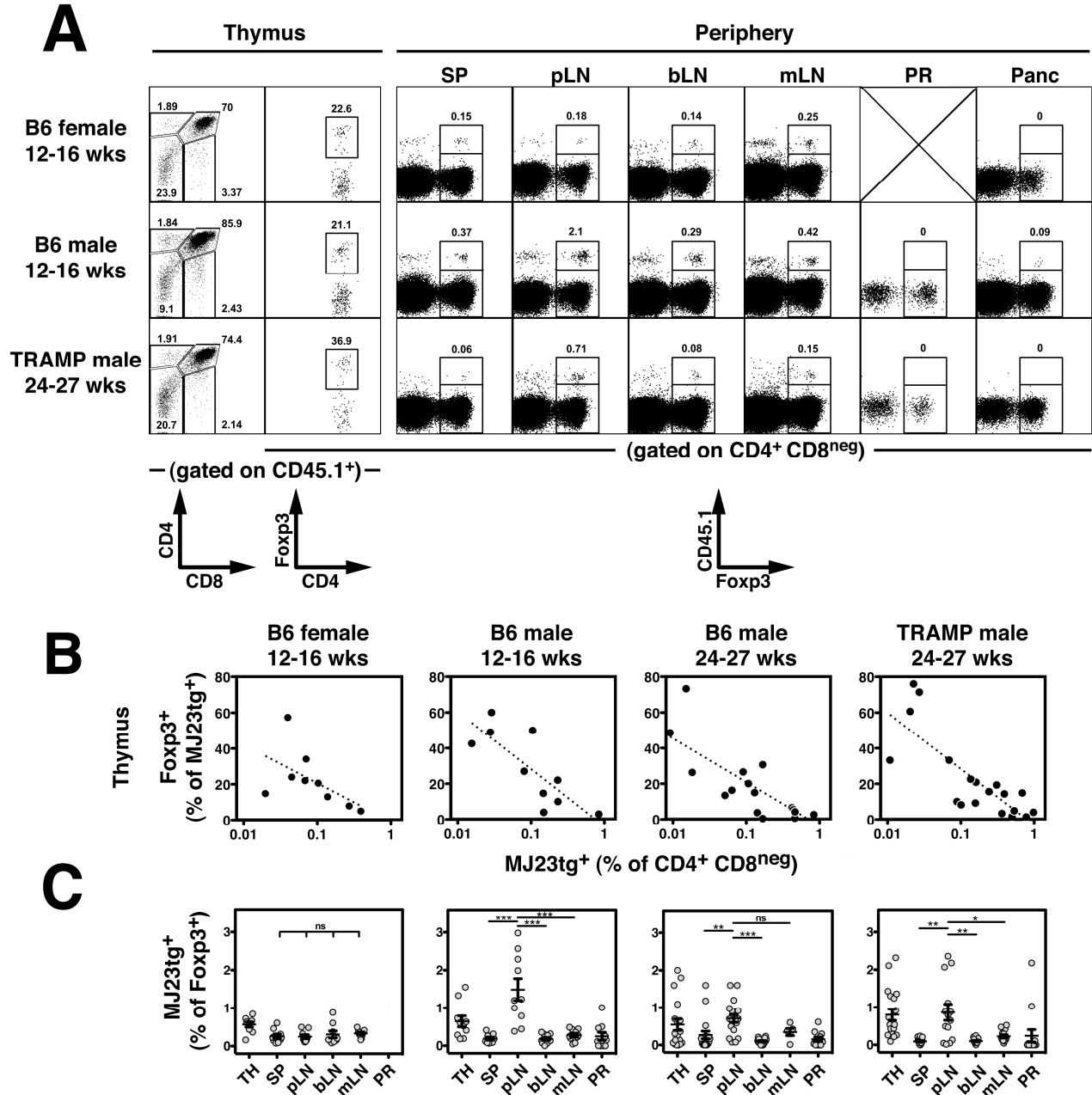


Figure 10: Thymic development of MJ23 Tregs. The MJ23 TCR facilitates thymic Treg development at low clonal frequencies. T cell-depleted bone marrow cells from MJ23tg *Rag1*^{-/-} CD45.1⁺ female donor mice were engrafted, along with polyclonal “filler” cells from B6 females (CD45^{.2/2}), into sublethally irradiated CD45^{.2/2} recipient mice. This approach resulted in seeding of MJ23tg precursors at a low frequency (<1%). 6 weeks post-engraftment, the fate of MJ23tg cells was analyzed. **(A)** Representative flow cytometric analyses of CD45.1⁺ MJ23tg T cells from different anatomical sites of male or female mice of the indicated ages and strain.

Figure 10 Continued: Abbreviations are the same as in Fig. 6. For the thymus, the left column (CD4 vs. CD8) depicts undepleted samples, the right column (Foxp3 vs. CD4) depicts CD8-depleted samples. For the periphery, the percentage of all CD4⁺Foxp3⁺ T cells that are CD45.1⁺ (MJ23tg⁺) is indicated. **(B)** Summary plots of the “efficiency” of MJ23tg Treg development in the thymus, in which the percentage of CD4⁺CD8^{neg} CD45.1⁺ MJ23tg cells that express Foxp3 is plotted vs. the frequency of CD45.1⁺ MJ23tg thymocytes (as a percentage of all CD4⁺CD8^{neg} cells) for cells isolated from host mice of the indicated strain, gender, and age. Dashed lines indicate best-fit semi-log curves. **(C)** Summary plots of the percentage of CD45.1⁺ MJ23tg T cells amongst all CD4⁺Foxp3⁺ cells isolated from various organs of the indicated hosts. The mean ± SEM is shown. Asterisks indicate $p < 0.05$. ANOVA was used to compare the secondary lymphoid sites (spleen and lymph nodes) within chimeric hosts of a given type. Data are pooled from at least $N = 3$ independent experiments.

Figure 11: Additional characterization of MJ23tg bone marrow chimeric mice. Data are from the same mice depicted in Fig. 3. T cell-depleted bone marrow cells from MJ23tg *Rag1*^{-/-} CD45.1⁺ female donor mice were engrafted, along with polyclonal “filler” cells from B6 females (CD45^{.2/2}), into sublethally irradiated CD45^{.2/2} recipient mice. This approach resulted in seeding of MJ23tg precursors at a low frequency (<1%).

Figure 11 Continued: 6 weeks post-engraftment, the fate of MJ23tg cells was analyzed. **(A)** Summary plot of the percentage of CD45.1⁺ MJ23tg thymocytes that fall within the CD4⁺CD8^{neg}, CD4^{neg}CD8⁺, and CD4⁺CD8⁺ subsets of 12-16-week-old B6 female (F) or male (M) hosts. **(B)** Summary plot of the absolute number of CD4⁺CD8^{neg}Foxp3⁺CD45.1⁺ MJ23tg T cells from the thymus of the indicated hosts. **(C)** Both CD4⁺Foxp3^{neg} and CD4⁺Foxp3⁺ MJ23tg cells are present in the periphery of chimeric hosts. Summary plots of the percentage of Foxp3⁺ cells amongst CD45.1⁺CD4⁺ MJ23tg T cells isolated from various organs of the indicated hosts. **(D)** CD8⁺CD4^{neg} MJ23tg T cells are present in the periphery of chimeric mice, and exhibit an antigen-inexperienced phenotype. Representative flow cytometric analyses of T cells from different anatomical sites of a male chimeric host. Top, plots of CD4 vs. CD8 expression by CD45.1⁺ MJ23tg T cells. Bottom, histogram overlays of CD44 expression by CD4⁺ and CD8⁺ T cells, both CD45.1⁺ MJ23tg cells and CD45.2⁺ polyclonal cells. **(E)** CD8⁺CD4^{neg} MJ23tg T cells are widely distributed in the periphery of chimeric hosts, and are not significantly enriched in the periaortic lymph nodes. Summary plots of the percentage of CD45.1⁺ MJ23tg T cells amongst all CD8⁺ cells isolated from various organs of the indicated hosts. The mean \pm SEM is indicated. Asterisks indicate $p < 0.05$. For A, a t-test was used to compare male vs. female of the indicated thymic subsets. For B, ANOVA was used to compare the four groups. For C and E, ANOVA was used to compare the secondary lymphoid sites (spleen and lymph nodes) within chimeric hosts of a given type. Abbreviations are the same as in Fig. 2. Data are pooled from $N = 3$ independent experiments.

Figure 12: The OT-II TCR does not facilitate Treg development in the thymus of mixed bone marrow chimeric mice. T cell-depleted bone marrow cells from MJ23tg *Rag1*^{-/-} CD45^{.1/1} female and OT-IItg *Rag1*^{-/-} CD45^{.1/2} female mice were engrafted, along with polyclonal “filler” cells from B6 females (CD45^{.2/2}), into sublethally irradiated B6 male or female (CD45^{.2/2}) recipient mice. Donor cell proportions were 5% MJ23tg, 5% OT-IItg, and 90% B6 filler. This approach resulted in seeding of MJ23tg and OT-IItg precursors at a low frequency (<1%). 6 weeks post-engraftment, the fate of donor cells was analyzed. **(A)** Representative flow cytometric analyses of CD4⁺CD8^{neg} thymocytes from the indicated hosts. Plots of CD45.1 vs. CD45.2 depict undepleted thymus samples. Plots of Foxp3 vs. CD4 depict CD8-depleted thymus samples. The percentage of cells within the indicated gates is shown. **(B)** Summary plots of the “efficiency” of Treg development, in which the percentage of CD4⁺CD8^{neg} TCRtg⁺ (MJ23tg or OT-IItg) cells that express Foxp3 is plotted vs. the frequency of TCRtg⁺ thymocytes (as a percentage of all CD4⁺CD8^{neg} cells) for cells isolated from the indicated hosts. Dashed lines indicate best-fit semi-log curves.

Figure 13: Polyclonal Tregs from TRAMP prostates express intermediate amounts of neuropilin-1. Flow cytometric analysis of CD4⁺ T cells isolated from different organs of 24-27-week-old TRAMP or B6 males. Left, plots of Foxp3 vs. neuropilin-1 (Nrp-1) expression are shown. The percentage of cells within each quadrant is indicated. Right, histograms of Nrp-1 expression are shown for Foxp3⁺ cells from the indicated organs of a TRAMP mouse.

Figure 14: Factors limiting the recovery of donor-derived MJ23tg T cells in chimeric mice. **(A)** Sublethal radiation substantially reduces the number of Tregs recovered from the prostates of tumor-bearing TRAMP mice. Summary plot of the absolute number of CD4⁺Foxp3⁺ T cells recovered from the prostates of 27-week-old TRAMP mice that had been subjected to 500 rads of radiation (rad) or no radiation (no rad) 6 weeks prior to analysis. **(B)** In MJ23tg bone marrow chimeric mice, donor-derived CD45.1⁺ MJ23tg T cells are observed in the prostate 20 weeks post-engraftment. MJ23tg chimeras were generated in B6 male hosts as described in Figure 10. Flow cytometric plots of CD45.1 vs. Foxp3 expression are shown for prostatic CD4⁺ T cells. The percentage of CD4⁺Foxp3⁺ T cells that are CD45.1⁺ (MJ23tg⁺) is indicated. The mean ± SEM is indicated. Asterisks indicate p < 0.05.

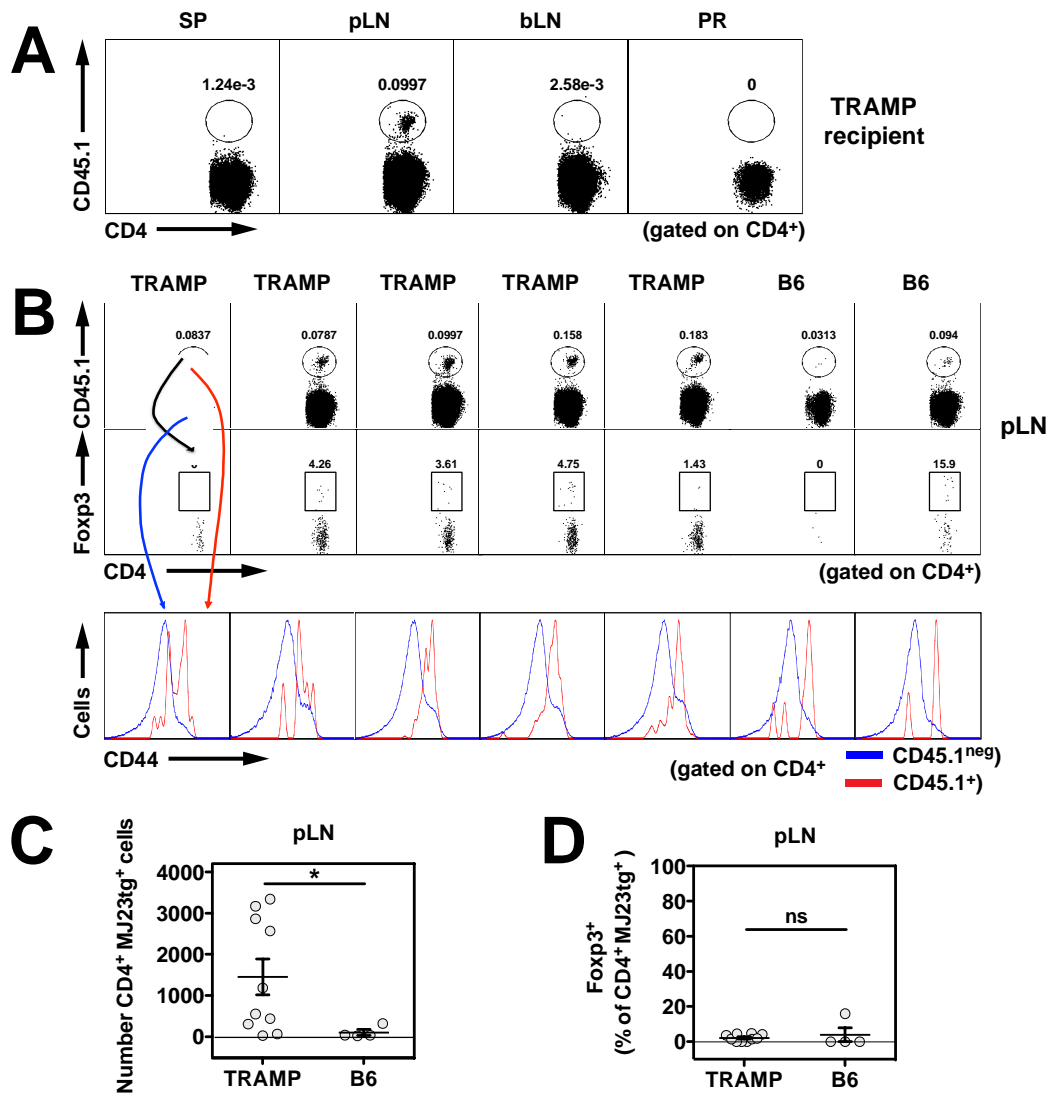


Figure 15: Negligible extrathymic development of MJ23tg Tregs. 1×10^5 $CD4^+$ T cells isolated from MJ23tg $Rag1^{-/-}$ $CD45.1^+$ female donor mice were transferred intravenously into 5-month-old TRAMP $^{+/+}$ or B6 male recipients. 30 days post-transfer, the fate of donor cells was assessed. **(A)** Representative flow cytometric analysis of the recovery of $CD45.1^+$ MJ23tg donor cells from a TRAMP male recipient, demonstrating that donor cells were exclusively recovered from the periaortic lymph nodes. SP, spleen; pLN, periaortic lymph nodes; bLN, brachial lymph nodes; PR, prostate. **(B)** Representative flow cytometric analysis of $CD45.1^+$ MJ23tg donor T cells in the pLN of the indicated recipient mice. Arrows indicate subgating. **(C)** Summary plot of the absolute number of $CD4^+CD45.1^+$ MJ23tg T cells recovered from the pLN of the indicated recipient mice. **(D)** Summary plot of the percentage of $CD4^+CD45.1^+$ MJ23tg T cells in the pLN that express Foxp3. The mean \pm SEM is indicated. Asterisks indicate $p < 0.05$. Data in (C) and (D) are pooled from $N = 2$ experiments.

MJ23 Treg development is Aire-dependent

On the basis of our data indicating that MJ23 T cells are reactive to a prostate-associated antigen, we anticipated that Foxp3⁺ MJ23tg Tregs would not develop in B6 female hosts. However, unexpectedly, Foxp3⁺ MJ23tg Tregs developed in the thymus of chimeric B6 females (Fig. 10, A and B, and Fig. 11). In the periphery of female mice, Foxp3⁺ MJ23tg T cells were broadly distributed in the spleen and all lymph nodes examined, but selective enrichment in the periaortic lymph nodes was not observed in female hosts (Fig. 10C). In order to elucidate the mechanisms underlying MJ23tg Treg development in both male and female mice, we examined the role of Aire in development. *Aire* encodes a transcriptional regulator that drives the ectopic expression of peripheral tissue-specific antigens by medullary thymic epithelial cells, and is critical for the maintenance of immune tolerance (95-97). Analysis of MJ23tg development in chimeric mice in which MJ23tg precursors were engrafted into *Aire*^{+/+} or *Aire*^{-/-} hosts revealed that Foxp3⁺ MJ23tg Tregs failed to develop in the thymus and periphery of *Aire*^{-/-} hosts, both male and female (Fig. 16, A and B). In addition, *Aire*^{-/-} hosts exhibited a reduction in the percentage of thymic Tregs relative to *Aire*^{+/+} hosts, consistent with previous reports (95, 98), but were not characterized by a complete deficiency of polyclonal Tregs (Fig. 16, A and C). Despite the lack of MJ23tg Treg development, mature CD4⁺Foxp3^{neg} MJ23tg T cells developed in *Aire*^{-/-} hosts (Fig. 16A and Fig. 17), indicating that T cells of this specificity are not dependent on Aire for their positive selection into the CD4⁺ lineage. This result also suggests that the thymic development of Tregs reactive to an Aire-dependent antigen may require both the recognition of self peptide/MHC ligands for positive selection, and the recognition of an additional Aire-

dependent antigen for commitment to the Treg lineage. Importantly, similar experiments utilizing a second naturally occurring tumor-infiltrating Treg TCR, termed “RT83”, demonstrated that Aire is required for the thymic development of RT83tg Tregs (Fig. 16D and Fig. 18). Thus, our data demonstrate that Aire is critical for the thymic development of multiple naturally occurring Treg specificities. These findings are consistent with a model in which the Aire-mediated expression of peripheral tissue-restricted antigens by thymic epithelial cells drives the development of a subset of tissue-specific or organ-specific Tregs (82).

While there is substantial evidence demonstrating that Aire plays a critical role in the deletion of autoreactive thymocytes reactive to peripheral tissue antigens (95, 99-101), a definitive role for Aire in the thymic selection of naturally occurring Tregs has not been previously established. Here, we provide direct evidence that Aire is critical for the thymic development of Tregs of naturally arising specificities. Thus, the integration of available evidence suggests a dual role for Aire in the maintenance of immune tolerance, in which Aire drives both the deletion of autoreactive T cells and the development of a subset of Foxp3⁺ Tregs.

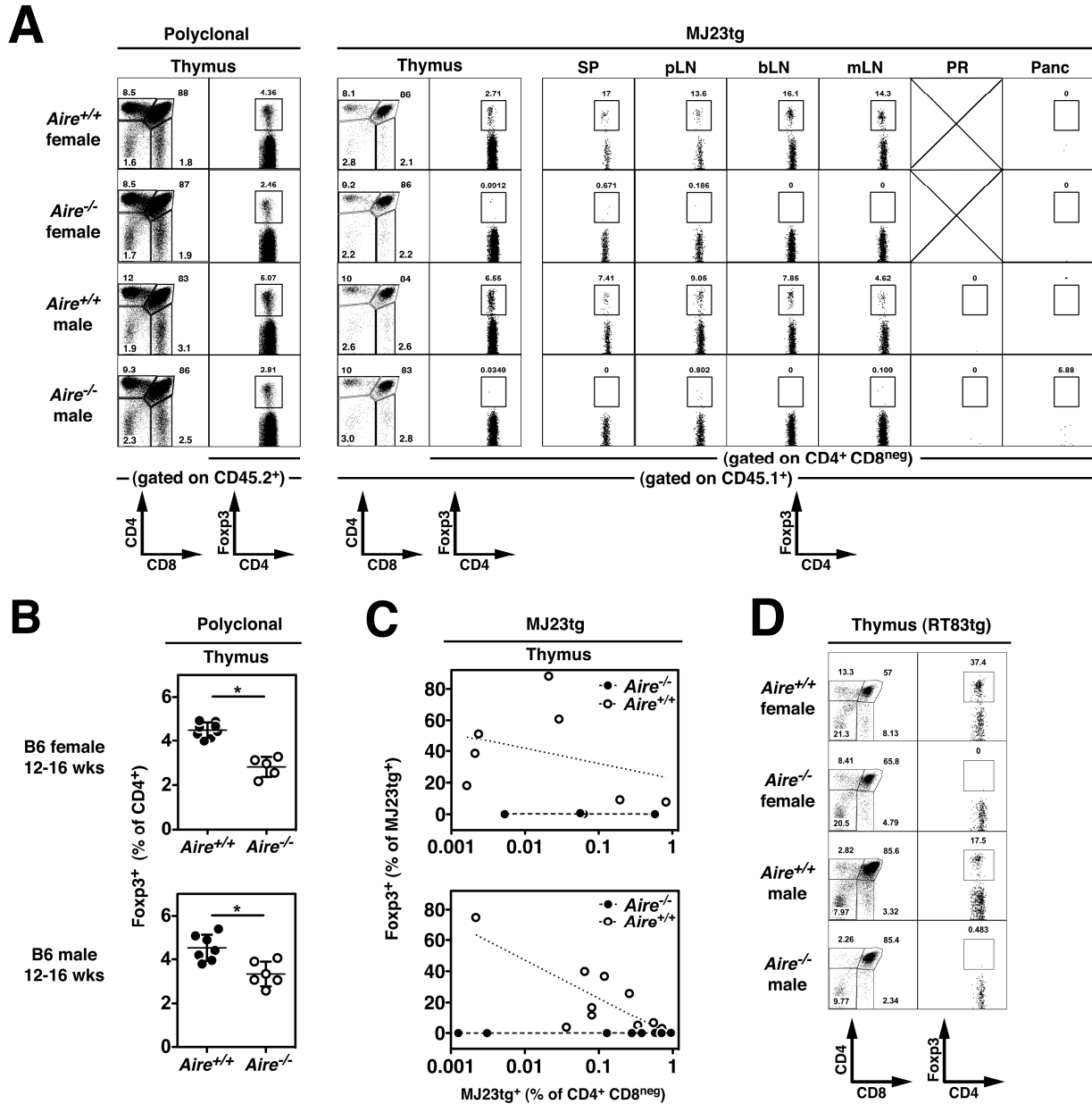


Figure 16: Aire-dependent thymic development of antigen-specific Tregs. (A-C). The thymic development of MJ23tg Tregs is Aire-dependent. T cell-depleted bone marrow cells from MJ23tg *Rag1*^{-/-} CD45.1⁺ female donor mice were engrafted, along with “filler” cells from *Aire*^{-/-} females (CD45^{2/2}), into sublethally irradiated *Aire*^{-/-} or *Aire*^{+/+} recipient mice (CD45^{2/2}), both male and female. 6 weeks post-engraftment, the fate of MJ23tg cells was analyzed. **(A)** Representative flow cytometric analyses of CD45.2⁺ polyclonal T cells (left) and CD45.1⁺ MJ23tg T cells from different anatomical sites of 12-16-week-old male or female mice of the indicated *Aire* genotype. Abbreviations are the same as in Fig. 2. The percentage of CD4⁺ cells that are Fcpx3⁺ is shown. For the thymus, the left column (CD4 vs. CD8) depicts undepleted samples, the right column (Fcpx3 vs. CD4) depicts CD8-depleted samples.

Figure 16 Continued: (B) Summary plots of the “efficiency” of MJ23tg Treg development, in which the percentage of CD45.1⁺ MJ23tg cells that express Foxp3 is plotted vs. the frequency of CD45.1⁺ MJ23tg thymocytes (as a percentage of all CD4⁺CD8^{neg} cells) for cells isolated from host mice of the indicated sex and genotype. Dashed lines indicate best-fit semi-log curves. **(C)** Summary plots of the percentage of CD45.2⁺ polyclonal CD4⁺CD8^{neg} thymocytes that express Foxp3 in chimeric mice of the indicated sex and genotype. The mean ± SEM is shown. Asterisks indicate $p < 0.05$ for the comparison of *Aire*^{-/-} vs. *Aire*^{+/+} mice (t-test). Data in (A-C) are pooled from $N = 3$ independent experiments. **(D)** Aire-dependent thymic development of “RT83tg” Tregs. RT83tg bone marrow chimeras were generated in *Aire*^{-/-} or *Aire*^{+/+} hosts, as described above for MJ23tg T cells. Representative flow cytometric analyses of CD45.1⁺ RT83tg T cells from the thymus of 12-16-week-old male or female mice of the indicated *Aire* genotype. The percentage of CD4⁺ cells that are Foxp3⁺ is shown. For the thymus, the left column (CD4 vs. CD8) depicts undepleted samples, the right column (Foxp3 vs. CD4) depicts CD8-depleted samples. Data in (D) are pooled from $N = 2$ independent experiments.

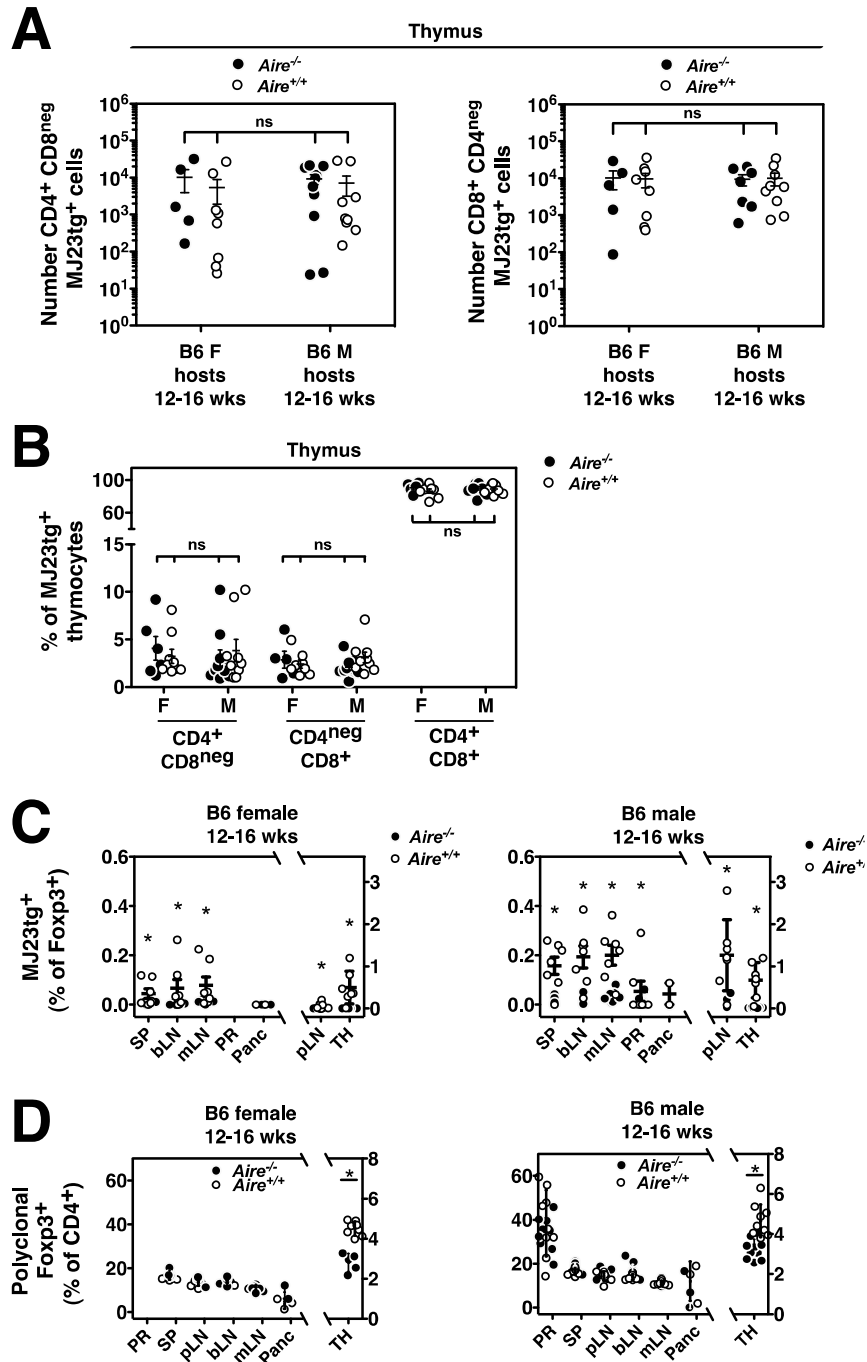


Figure 17: Further characterization of MJ23tg T cells in *Aire*^{-/-} and *Aire*^{+/+} chimeric hosts. Data are from the same mice depicted in Figure 16. T cell-depleted bone marrow cells from MJ23tg *Rag1*^{-/-} CD45.1⁺ female donor mice were engrafted, along with “filler” cells from *Aire*^{-/-} females (CD45^{2/2}), into sublethally irradiated *Aire*^{-/-} or *Aire*^{+/+} recipient mice (CD45^{2/2}), both male and female. 6 weeks post-engraftment, the fate of MJ23tg cells was analyzed.

Figure 17 Continued: **(A)** The absolute number of thymic CD4⁺CD8^{neg} and CD8⁺CD4^{neg} MJ23tg cells is not significantly altered in *Aire*^{-/-} hosts. Summary plots of the absolute number of MJ23tg T cells of the indicated phenotypic subset in the thymus of 12-16-week-old female or male hosts of the indicated genotype. **(B)** The distribution of thymic MJ23tg phenotypic subsets is not significantly altered in *Aire*^{-/-} hosts. Summary plot of the percentage of CD45.1⁺ MJ23tg thymocytes that fall within the CD4⁺CD8^{neg}, CD4^{neg}CD8⁺, and CD4⁺CD8⁺ subsets of female (F) or male (M) hosts of the indicated genotype. **(C)** MJ23tg Treg development is Aire-dependent. Summary plots of the percentage of CD45.1⁺ MJ23tg T cells amongst all CD4⁺Foxp3⁺ cells isolated from various organs of the indicated hosts. **(D)** The frequency of polyclonal Tregs is not altered in the periphery of *Aire*^{-/-} hosts. Summary plots of the percentage of Foxp3⁺ cells amongst all CD45.2⁺ polyclonal CD4⁺ cells isolated from various organs of the indicated hosts. The mean ± SEM is indicated. Asterisks indicate p < 0.05, ns = not significant. For (A-B), ANOVA was used to compare the four groups for each phenotypic T cell subset. For (C-D), t-tests were used to compare data from *Aire*^{-/-} vs. *Aire*^{+/+} hosts at the indicated anatomical sites. Data are pooled from N = 3 independent experiments.

Figure 18: Thymic development of Tregs expressing the “RT83” TCR is Aire-dependent. The RT83 TCR β chain, V β 3-ASSLGSSYEQY, was originally identified in polyclonal TRAMP mice based on recurrent expression by prostate tumor-infiltrating Tregs (defined by high-throughput sequencing of V β 3⁺ TCRs in fig. S2). The RT83 TCR α chain, V α 8-ALRDSNNRIF, was identified by single cell PCR and sequencing of TCRs expressed by V α 8⁺V β 3⁺CD4⁺CD25^{high} T cells sorted from TRAMP prostate tumors. This analysis identified multiple single cells that co-express the RT83 TCR α and TCR β chains in polyclonal TRAMP mice (not shown). The RT83 TCR β chain is the TCR chain expressed by “TCR β tg” mice utilized elsewhere in this study. (A-B) The thymic development of RT83tg Tregs is Aire-dependent. T cell-depleted bone marrow cells from RT83tg *Rag1*^{-/-} CD45.1⁺ female donor mice were engrafted,

Figure 18 Continued: along with “filler” cells from *Aire*^{-/-} females (CD45^{2/2}), into sublethally irradiated *Aire*^{-/-} or *Aire*^{+/+} recipient mice (CD45^{2/2}), both male and female. 6 weeks post-engraftment, the fate of RT83tg cells was analyzed. **(A)** Representative flow cytometric analyses of CD45.1⁺ RT83tg T cells from different anatomical sites of 12-16-week-old male or female mice of the indicated *Aire* genotype. Abbreviations are the same as in Fig. 2. The percentage of CD4⁺ cells that are Foxp3⁺ is shown. For the thymus, the left column (CD4 vs. CD8) depicts undepleted samples, the right column (Foxp3 vs. CD4) depicts CD8-depleted samples. **(B)** Summary plots of the “efficiency” of RT83tg Treg development, in which the percentage of CD45.1⁺ RT83tg cells that express Foxp3 is plotted vs. the frequency of CD45.1⁺ RT83tg thymocytes (as a percentage of all CD4⁺CD8^{neg} cells) for cells isolated from host mice of the indicated sex and genotype. Dashed lines indicate best-fit semi-log curves. Data are pooled from *N* = 2 independent experiments.

Conclusions

In sum, our data support a model in which a tumor does not drive the *de novo* conversion of tumor-specific CD4⁺ effector T cells into induced Foxp3⁺ Tregs, but instead recruits pre-existing thymic-derived Tregs reactive to Aire-dependent self antigens associated with the organ of cancer origin. Thus, a developing neoplasm co-opts endogenous mechanisms that have evolved to preserve the integrity of the host by maintaining organ-specific immune tolerance.

Results: Dendritic cells coordinate the development and homeostasis of organ-specific regulatory T cells (78)ⁱ

Summary

Whereas antigen recognition mediated by the T cell receptor (TCR) influences many facets of Foxp3⁺ regulatory T (Treg) cell biology, including development and function, the cell types that present antigen to Treg cells *in vivo* remain largely undefined. By tracking a clonal population of Aire-dependent, prostate-specific Treg cells in mice, we demonstrated an essential role for dendritic cells (DCs) in regulating organ-specific Treg cell biology. We have shown that the thymic development of prostate-specific Treg cells required antigen presentation by DCs. Moreover, Batf3-dependent CD8 α ⁺ DCs were dispensable for the development of this clonotype and had negligible impact on the polyclonal Treg cell repertoire. In the periphery, CCR7-dependent migratory DCs coordinated the activation of organ-specific Treg cells in the prostate-draining lymph nodes. Our results demonstrate that the development and peripheral regulation of organ-specific Treg cells are dependent on antigen presentation by DCs, implicating DCs as key mediators of organ-specific immune tolerance.

Introduction

CD4⁺Foxp3⁺ regulatory T (Treg) cells are required throughout life for the maintenance of immune homeostasis and the prevention of autoimmunity (43, 102). A

ⁱ This section is reproduced here, from the referenced citation, with minimal modification under the license granted by Elsevier. Changes include renumbering of figures, inclusion of supplemental figures, and modification of section subheadings to conform with this document. The Discussion section has also been moved and is expanded upon in the "Discussions, Future Directions and Conclusions" section of this document.

growing body of evidence suggests that the Treg cell repertoire contains organ-specific Treg cells reactive to tissue-restricted self antigens, and that these cells may be critical for the protection of organs from autoimmune attack. T cell receptor (TCR) profiling reveals an asymmetric distribution of Treg cell specificities in lymph nodes throughout the body, suggesting that the anatomical distribution of Treg cells is shaped by the presentation of regional organ-specific antigens (91). In transfer experiments, Treg cells isolated from organ-draining lymph nodes are more efficient than Treg cells from non-draining lymph nodes at suppressing organ-specific autoimmunity at multiple target sites (103-105). Recently, we identified a clonal population of prostate-specific Treg cells, named “MJ23” Treg cells, that are enriched in the prostate-draining lymph nodes and prostate tumor lesions of male mice (106), providing direct evidence of the existence of organ-specific Treg cells.

For some time, it has remained unclear whether organ-specific Treg cells originate in the thymus or develop extrathymically upon encounter with tissue-derived antigens. Recently, we and others demonstrated that the thymic development of some naturally occurring Treg cell specificities, including prostate-specific MJ23 Treg cells, is dependent on the expression of Autoimmune Regulator (Aire) (71, 106). Aire is a transcription factor expressed by medullary thymic epithelial cells (mTECs) that promotes the promiscuous expression of a variety of genes, many of which encode peripheral tissue-restricted antigens (TRAs) (96, 107). These findings provide mechanistic clarity, demonstrating that Aire-dependent mirroring of the “peripheral self” (96) plays a critical role in promoting the thymic development of Treg cells reactive to peripheral organ-specific antigens.

Substantial evidence indicates that *in vivo*, the development, differentiation, and function of Treg cells are dependent on TCR-mediated antigen recognition. In the thymus, Treg cell development is dependent on MHC-II-restricted antigen recognition, and occurs via a TCR-instructive process in which distinct TCR specificities facilitate efficient differentiation into the Treg cell lineage (93). In the periphery, a substantial proportion of Treg cells perceive TCR signals and actively divide at steady state (25, 76). Moreover, conditional ablation of the TCR on Foxp3-expressing cells disrupts Treg cell function, resulting in systemic autoimmunity (67, 68), demonstrating a crucial role for TCR-dependent signals in Treg cell-mediated immune tolerance. Thus, antigen recognition is critical for many aspects of the life cycle and lifestyle of Treg cells. Despite the importance of TCR engagement, little is known about the cell types that present antigen for recognition by Treg cells. These antigen presenting cells (APCs) are likely to orchestrate many aspects of Treg cell biology, providing antigenic and accessory signals that dictate Treg cell activation, anatomical distribution, spatial positioning within lymphoid and non-lymphoid organs (108), and access to distinct environmental cues. Thus, identifying the cellular interaction partners that interface with Treg cells in the thymus and periphery is critical for gaining a complete understanding of Treg cell biology and the mechanisms by which immune tolerance is established and maintained.

Antigen presentation by both mTECs and dendritic cells (DCs) is required to establish a replete Treg cell pool, suggesting that these presentation pathways collaborate to form a complete Treg cell repertoire (69-71). For the development of Aire-dependent Treg cells in the thymus, two models have been proposed to describe

the presentation of antigens encoded by Aire-dependent transcripts (69). In the first model, Aire-expressing mTECs function in a cell-autonomous fashion to directly present Aire-dependent antigens to thymocytes. In the second model, antigens expressed by mTECs are transferred to neighboring DCs, which then present acquired antigen to coordinate Treg cell differentiation. In this regard, the presence of multiple DC subsets in the thymic medulla, including plasmacytoid DCs, CD8 α ⁺ classical DCs (cDCs) and Sirp α ⁺ cDCs (15, 72), raises the possibility that a distinct DC subset may specialize in presenting Aire-dependent antigens to developing T cells.

Perhaps even less is known about the APCs that present antigen to Treg cells outside of the thymus, and the impact of these APCs on the peripheral homeostasis and function of Treg cells. In one study, it was demonstrated that following the depletion of CD11c-expressing cells or expansion of Flt3L-dependent DCs, the frequency of splenic Treg cells decreases or increases, respectively, suggesting that the homeostasis of some splenic Treg cells is orchestrated by CD11c⁺ cells (75). In a separate study, it was shown that expansion of Flt3L-dependent DCs or administration of anti-ICOSL antibody induces the selective expansion or reduction, respectively, of CD44^{high}CD62L^{low} splenic Treg cells (76). Since the spleen contains multiple subsets of CD11c-expressing cells (77), it is unknown whether a distinct DC subset supports Treg cell homeostasis at this site. Furthermore, it is unclear whether the same dependency on CD11c⁺ cells is operative in the lymph nodes, which contain various APC populations that are not found in the spleen (77). For the presentation of organ-derived antigens to organ-specific Treg cells in the draining lymph nodes, at least two possible scenarios can be envisioned (109). In the first scenario, lymph node resident DCs or

macrophages capture organ-derived antigen draining to the lymph nodes via the afferent lymphatics, and present this antigen to organ-specific Treg cells. In an alternate but not mutually exclusive scenario, DCs acquire antigen within the organ, migrate to the draining lymph nodes, and process and present antigen for recognition by organ-specific Treg cells (110).

Here, we demonstrate that DCs play a critical role in the thymic development and peripheral homeostasis of prostate-specific Treg cells. Our findings identify the cellular interaction partners of an archetypal population of Aire-dependent, organ-specific Treg cells, providing a conceptual framework for the broader understanding of organ-specific Treg cells of diverse specificities, and the APC types that choreograph the establishment and enforcement of organ-specific immune tolerance.

Results

In this study, we used two approaches to characterize the APCs required for the development and homeostasis of MJ23 Treg cells, a clonal population of Aire-dependent, prostate-specific Treg cells that has been identified previously (106). In the first approach, we generated bone marrow chimeric mice (BMCs) in which irradiated CD45.2⁺ hosts were reconstituted with donor cells of defined genotype, including a low frequency of bone marrow cells from CD45.1⁺ MJ23 TCR transgenic (MJ23Tg) mice on the *Rag1*^{-/-} background. In the second approach, we utilized intrathymic injection to introduce CD45.1⁺ MJ23Tg *Rag1*^{-/-} thymocytes, which are devoid of Foxp3⁺ Treg cells (106), into CD45.2⁺ recipients. Both approaches enabled us to track the development,

anatomical distribution, and activation of MJ23 T cells at low clonal frequencies post-transfer or engraftment.

Thymic development of MJ23 Treg cells requires antigen presentation and CD80 and/or CD86 expression by bone marrow-derived cells

Treg cell development in the thymus requires both MHC-II-dependent TCR stimulation and CD80 or CD86-dependent co-stimulation via the CD28 receptor (28). In addition, Aire is required for the thymic development of prostate-specific MJ23 Treg cells, implying that Aire-expressing mTECs are the most likely source of MJ23 antigen in the thymus (106). Using BMCs, the role of bone marrow-derived APCs and radioresistant host APCs (thymic epithelial cells, TECs) in coordinating Treg cell development could be assessed. We generated lethally irradiated BMCs in which wild-type, *Aire*^{-/-}, or *Cd80*^{-/-}*Cd86*^{-/-} host mice were reconstituted with bone marrow from wild-type mice, *Cd80*^{-/-}*Cd86*^{-/-} mice, or *H2*^{dIAb-Ea} homozygous mice deficient in all MHC-II genes (hereafter referred to as "MHC-II deficient" mice), and MJ23 Treg cell development was assessed. Given that positive selection of CD4⁺ T cells is substantially impaired in MHC-II null hosts (111) due to a lack of MHC-II on cortical TECs, we did not analyze MJ23 Treg cell development in MHC-II-deficient hosts. Instead, we assessed the role for TECs in Treg cell development using *Cd80*^{-/-}*Cd86*^{-/-} hosts lacking both CD80 and CD86, which are required for Treg cell development (28, 112) but do not impact positive selection at earlier stages of development. We found that MJ23 Treg cells did not develop in BMCs reconstituted with MHC-II deficient or *Cd80*^{-/-}*Cd86*^{-/-} bone marrow, but developed efficiently in BMCs generated in *Cd80*^{-/-}

Cd86^{-/-} hosts (Fig. 19, A and B and Fig. 20A). As expected, Aire expression by radioresistant host cells was crucial for MJ23 Treg cell development (Fig. 19B), confirming previous findings (106). These results suggest that MJ23 antigen is transferred from Aire-expressing mTECs to bone marrow derived APCs, which coordinate MJ23 Treg cell development by the provision of MHC-II-restricted antigen and co-stimulatory signals through CD28. Analysis of non-MJ23Tg polyclonal Treg cells revealed a similar pattern, in which BMCs reconstituted with MHC-II deficient or *Cd80*^{-/-} *Cd86*^{-/-} bone marrow exhibited a partial reduction of Treg cells (Fig. 19, A and C, and Fig. 20B), suggesting that these requirements may apply to a substantial fraction of the polyclonal Treg cell repertoire. Additionally, deficiency of CD80 and CD86 on radioresistant TECs led to a marked increase in the total number of polyclonal Treg cells in the thymus (Fig. 20B), suggesting a potential role for CD80 and/or CD86 expression by TECs in the negative selection of some specificities.

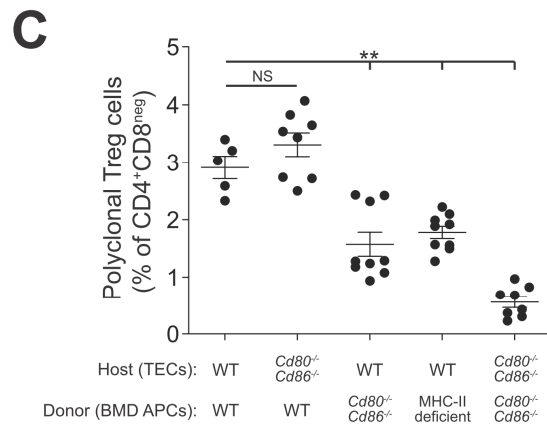
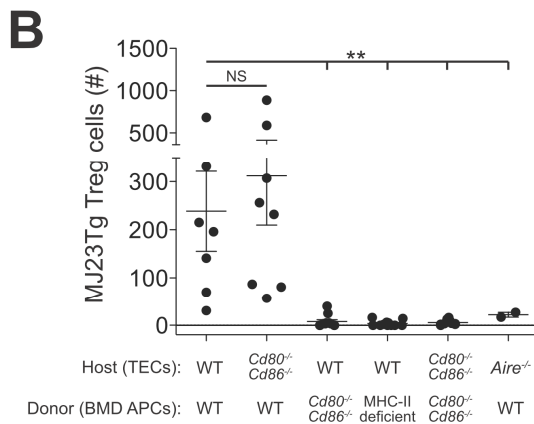
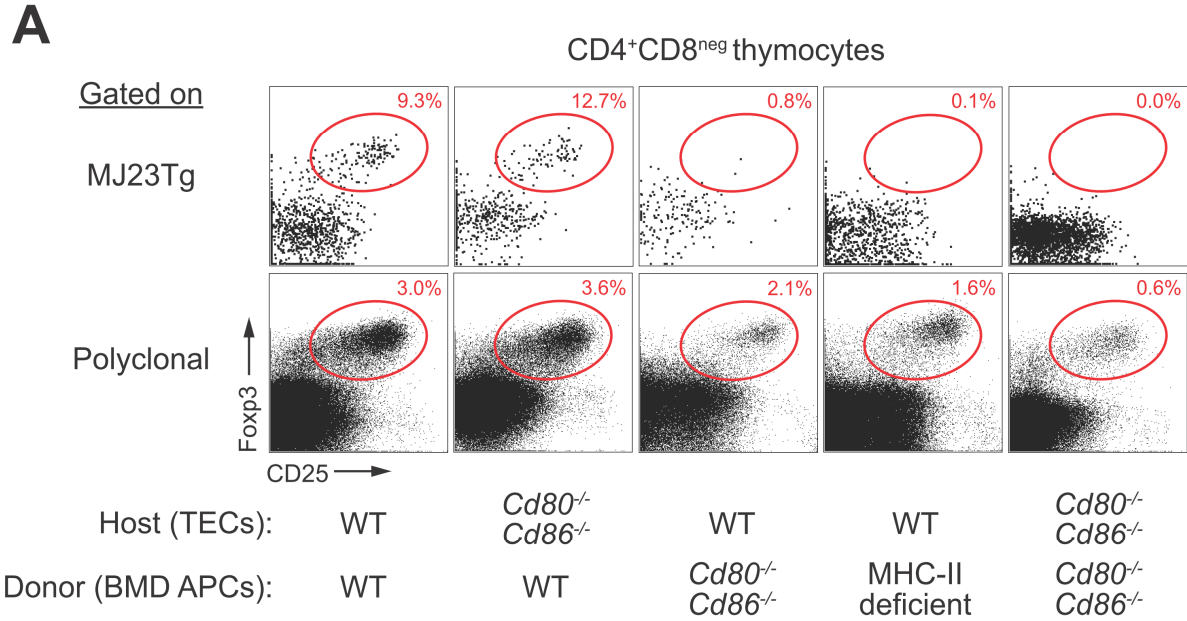


Figure 19: MJ23 Treg cell development is dependent on antigen presentation by bone marrow-derived cells. The thymic development of MJ23Tg Treg cells and a proportion of polyclonal Treg cells requires MHC-II and CD80 and/or CD86 expression by bone-marrow-derived antigen presenting cells. CD45.1⁺ MJ23Tg *Rag1*^{-/-} donor cells engrafted at low frequency, along with CD45.2⁺ polyclonal donor cells from the indicated genotype, into lethally irradiated CD45.2⁺ hosts of the indicated genotype. (A) Representative flow cytometric analysis (log-scale) of CD45.1⁺ MJ23Tg, *top row*, and CD45.2⁺ polyclonal Treg cells, *bottom row*, in the thymus of the indicated mice. The percentage of Foxp3⁺CD25⁺ Treg cells among CD4⁺CD8^{neg} thymocytes is indicated. WT, wild-type B6; MHC-II deficient, *H2*^{*dlab1-Ea*}. (B) Summary plot of the total number of thymic MJ23Tg Treg cells in chimeric mice of the indicated host and donor combinations. (C) Summary plot of the percentage of polyclonal Treg cells among CD4⁺CD8^{neg} thymocytes from the indicated chimeric mice. All data are pooled from *N* = 3 independent experiments. The mean ± SEM is shown. Asterisks indicate *P* values for *t* test for the comparison of the indicated groups, with ** = *P* < 0.005.

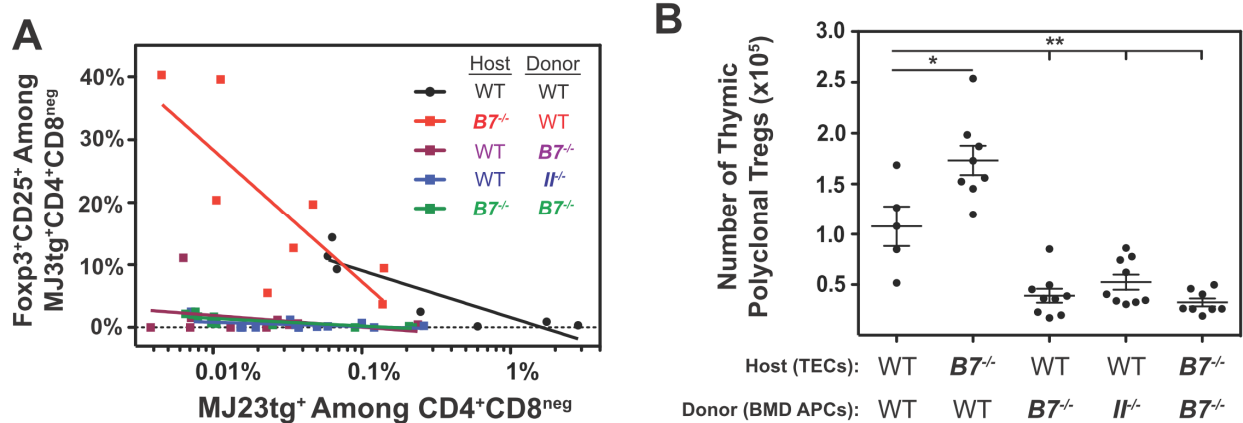


Figure 20: Efficiency of MJ23 Treg development and polyclonal Treg numbers are impacted by loss of MHC-II and B7-1/B7-2 on bone marrow-derived cells. Low frequency MJ23tg bone-marrow-chimeras were generated as described in Fig. 19. **(A)** Summary plot of the “efficiency” of CD45.1⁺ MJ23tg Treg development in the thymus of the indicated chimeric mice. The percentage of Fopx3⁺CD25⁺ cells among CD4⁺CD8^{neg} MJ23tg T cells is plotted versus the frequency of MJ23tg precursors (as a percentage of all CD4⁺CD8^{neg} thymocytes). Lines represent best-fit semi-log curves. WT, wild-type B6; *B7*^{-/-}, *B7-1/B7-2* double knockout; *II*^{-/-}, *MHC-II*^{-/-}. **(B)** Summary plot of the total number of CD45.2⁺ polyclonal Tregs among CD4⁺CD8^{neg} thymocytes from the indicated chimeric mice. All data are pooled from $N = 3$ independent experiments. The mean \pm SEM is shown. Asterisks indicate P values for t test for the indicated comparisons, with $*$ = $P < 0.05$ and $**$ = $P < 0.005$.

Antigen presentation by DCs is required for the thymic development of MJ23 Treg cells

In order to identify the bone marrow-derived APCs that coordinate MJ23 Treg cell development, we utilized models of inducible or constitutive APC deficiency. We assessed the requirement for antigen presentation by CD11c-expressing DCs, using both intrathymic injection and BMC approaches. First, we performed intrathymic injection of CD45.1⁺ MJ23Tg *Rag1*^{-/-} thymocytes into *Itgax-Cre*⁺ (also known as CD11c-Cre) *Ab1*^{flox/-} mice, which exhibit conditional deletion of the I-A^b MHC-II molecule on CD11c-expressing cells (Fig. 21A). MJ23 Treg cell development failed to occur in *Itgax-Cre*⁺ *Ab1*^{flox/-} hosts, but did occur in littermate controls lacking the *Itgax-Cre* transgene (Fig. 21, B and C, and Fig. 22A). MJ23 Treg cell development was lost in *Itgax-Cre*⁺ *Ab1*^{flox/-} mice despite detectable amounts of MHC-II remaining on the surface of CD11c⁺ cells (Fig. 21A), which may reflect the acquisition of MHC-II molecules from mTECs (113). Second, we generated BMCs in which lethally irradiated wild-type hosts were reconstituted with a mixture of *Itgax-DTR*⁺ (also known as CD11c-DTR) and MHC-II deficient bone marrow, together with a low frequency of CD45.1⁺ MJ23Tg *Rag1*^{-/-} bone marrow. *Itgax-DTR*⁺ mice express the human diphtheria toxin receptor (DTR) under the control of the *Itgax* promoter (114), permitting the inducible ablation of CD11c-expressing cells following administration of diphtheria toxin (DT). In these chimeras, DT administration induced the depletion of >95% of MHC-II-expressing DCs (Fig. 22C), allowing us to assess the role of antigen presentation by CD11c-expressing cells. Our data revealed that MJ23 Treg cell development was abrogated in DT-treated chimeras (Fig. 22, D and E), demonstrating that MHC-II expression by CD11c⁺ DCs is required for

MJ23 Treg cell development. In control experiments, injection of DT alone into MJ23Tg BMCs did not impact the number of MJ23Tg or polyclonal Treg cells in the thymus or periphery (Fig. 22, G through L). Loss of MHC-II on CD11c-expressing cells in either context (genetically or by DT administration) resulted in a reduction in the frequency of polyclonal thymic Treg cells (Fig. 21, B and D, and Fig. 22, D and F), suggesting that the development of a substantial fraction of Treg cells is dependent on antigen presentation by DCs. Finally, while recent reports demonstrate that a subpopulation of thymic B cells exhibits Aire expression (115) and may impact T cell selection (115, 116), MJ23 Treg cell development and polyclonal Treg cell frequencies were not impacted by B cell deficiency in *Ighm*^{-/-} mice (Fig. 21, C and D, and Fig. 23, B and C). Taken together, our results demonstrate that MHC-II-restricted antigen presentation by CD11c⁺ DCs is required to support MJ23 Treg cell development in the thymus.

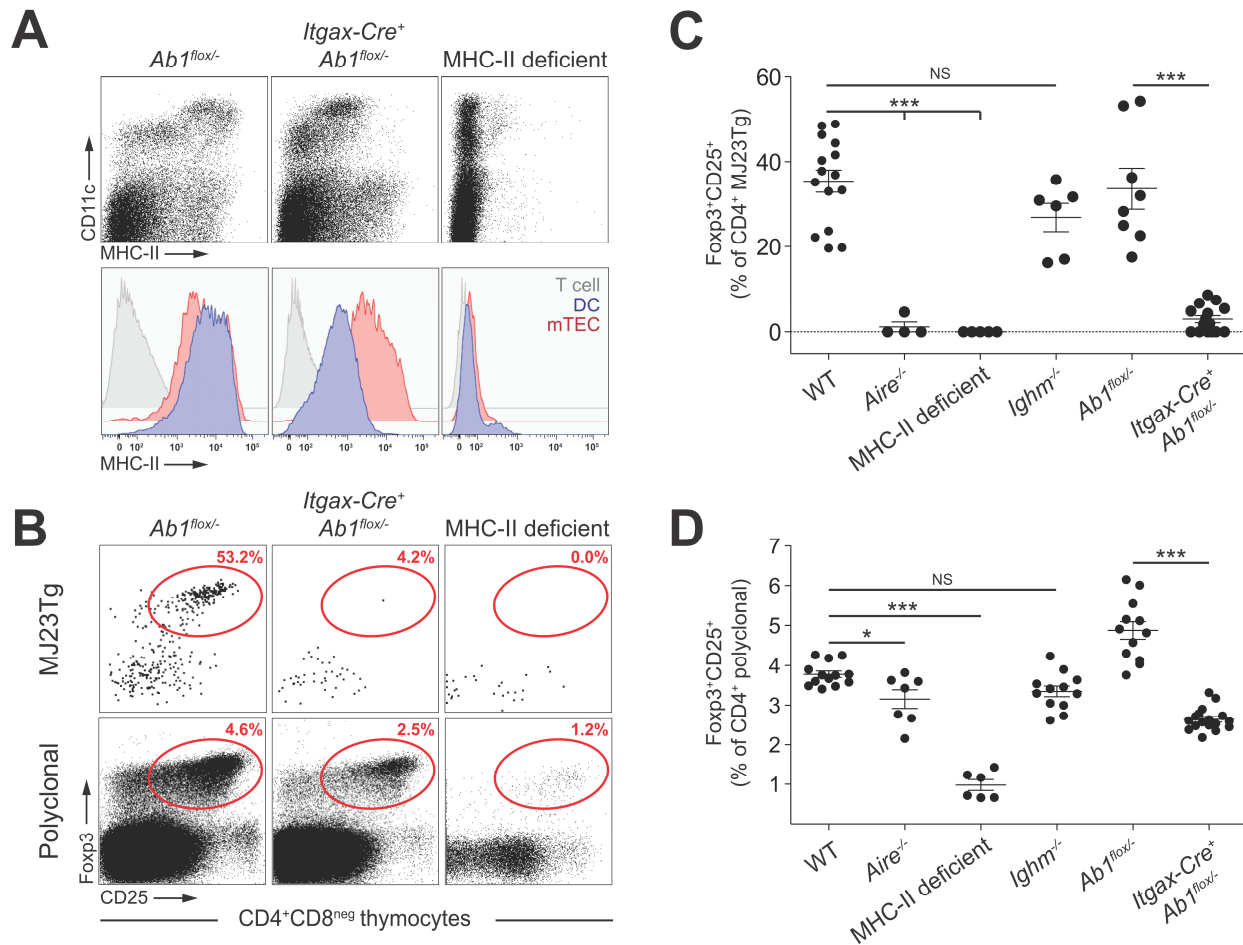


Figure 21: Antigen presentation by dendritic cells is required for the thymic development of MJ23 Treg cells. MJ23Tg Treg cell thymic development is dependent on MHC-II-expression by CD11c⁺ dendritic cells. CD45.1⁺ MJ23Tg *Rag1^{-/-}* thymocytes, were transferred via intrathymic injection into age-matched CD45.2⁺ mice of the indicated genetic backgrounds. Seven days post transfer, CD45.1⁺ MJ23Tg and CD45.2⁺ polyclonal Treg cell development was analyzed. **(A)** Representative flow cytometric analysis (log-scale) of MHC-II-expression of all thymocytes, *top row*, and the indicated thymic cell subsets, *bottom row*. T cells (TCRβ⁺); DC (CD11c⁺F4/80^{neg} TCRβ^{neg}); mTEC (EpCAM⁺Ly51^{neg}CD11c^{neg}). **(B)** Representative flow cytometric analysis (log-scale) of Treg cell development for donor MJ23Tg T cells, *top row*, and polyclonal CD4⁺CD8^{neg} thymocytes, *bottom row*, in recipients of the indicated genotypes. The percentage of Foxp3⁺CD25⁺ Treg cells among CD4⁺CD8^{neg} thymocytes is indicated. **(C-D)** Summary plot of the frequency of MJ23Tg **(C)** and polyclonal **(D)** Treg cells in the thymus following intrathymic injection into mice of the indicated genotypes. WT, wild-type; *Ab1^{flox/-}*, MHC-II^{flox/-}; *Itgax-Cre⁺*, CD11c-Cre⁺; MHC-II deficient, *H2^{dlab1-Ea}*; *Ighm^{-/-}*, B cell deficient. All data were pooled from *N* > 3 independent experiments. The mean ± SEM is shown. Asterisks indicate *P* values for *t* test for the indicated comparisons. * = *P* < 0.05 and *** = *P* < 0.0005.

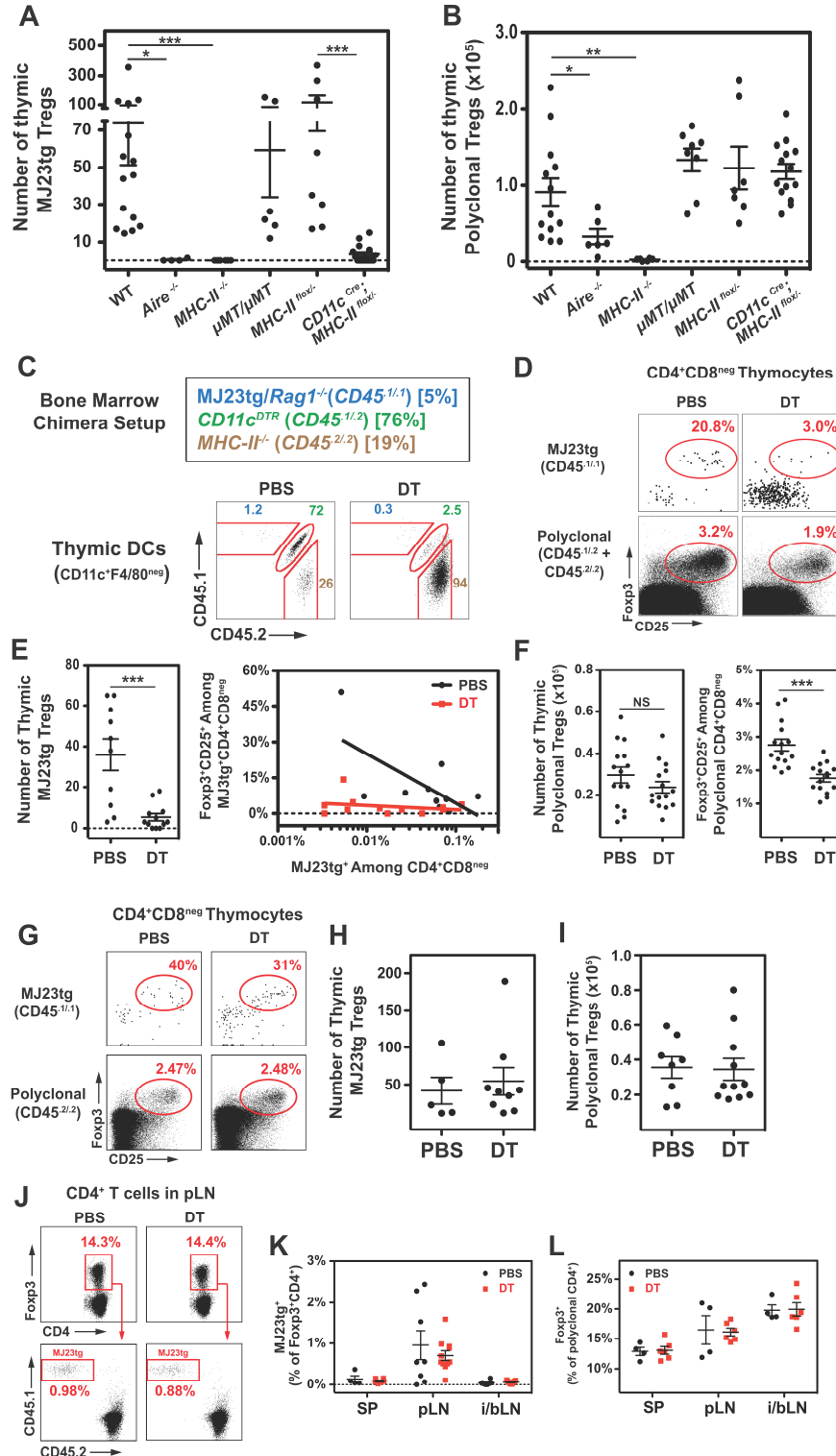


Figure 22: Antigen presentation by dendritic cells is required for the thymic development of MJ23 Tregs. (A-B) MJ23tg Treg thymic development is dependent on MHC-II-expression by CD11c⁺ dendritic cells.

Figure 22 Continued: MJ23tg, *A*, and polyclonal, *B*, Treg cells were quantified following intrathymic injection of Foxp3^{neg} MJ23tg *Rag1*^{-/-} *CD45*^{1/1.1} thymocytes into age-matched *CD45*^{2/2} mice of the indicated background as described in Figure 21. Summary plots of the total number of CD45.1⁺ MJ23tg (**A**) and CD45.2⁺ polyclonal (**B**) Tregs (Foxp3⁺CD25⁺) in the thymus of the indicated mice. All data were pooled from *N* > 3 independent experiments. The mean ± SEM is shown. Asterisks indicate *P* values for *t* test for the indicated comparisons, with * = *P* < 0.05, ** = *P* < 0.005 and *** = *P* < 0.0005. (**C-F**) Depletion of CD11c^{DTR} MHC-II^{+/+} DCs results in loss of MJ23tg Treg thymic development and a significant drop in the frequency of polyclonal thymic Tregs. T cell-depleted bone marrow cells from MJ23tg *Rag1*^{-/-} *CD45*^{1/1.1} donor mice were engrafted at low frequency (~ <1%), along with *CD11c*^{DTR} (*CD45*^{1/2}) and *MHC-II*^{-/-} (*CD45*^{2/2}) bone marrow at a 4:1 ratio, into lethally irradiated B6 hosts (*CD45*^{2/2}). Six weeks post-engraftment, chimeric mice were treated with either diphtheria toxin (DT), to deplete MHC-II⁺ DCs, or PBS every other day for 12 days. MJ23tg and polyclonal Treg development were analyzed on day 12 of treatment. (**C**) Experimental setup and representative flow cytometric analysis of the donor origin of thymic DCs (CD11c⁺ F4/80^{neg}) in PBS and DT treated mice. (**D**) Representative flow cytometric analysis of MJ23tg (*CD45*^{1/1.1}), *top row*, and polyclonal (*CD45*^{1/2} and *CD45*^{2/2}), *bottom row*, CD4⁺CD8^{neg} thymocytes in PBS and DT treated mice. (**E**) Summary plots of the total number of *CD45*^{1/1.1} MJ23tg thymic Tregs (Foxp3⁺CD25⁺), *left*, and the “efficiency” of MJ23tg Treg development, *right*, in the thymus of the indicated treatment groups. Lines represent best-fit semi-log curves. (**F**) Summary plots of the total number, *left*, and percentage, *right*, of CD45.2⁺ polyclonal Tregs among CD4⁺CD8^{neg} thymocytes from the indicated treatment groups. Data are pooled from *N* = 3 independent experiments. The mean ± SEM is shown. Asterisks indicate *P* values for *t* test for the indicated comparisons, with *** = *P* < 0.0005. (**G-L**) Treatment of MJ23tg bone marrow chimeras with diphtheria toxin (DT) does not impact MJ23tg or polyclonal Treg cells in the thymus or periphery. T cell-depleted bone marrow cells from MJ23tg *Rag1*^{-/-} *CD45*^{1/1.1} donor mice were engrafted at low frequency (<1%) along with polyclonal B6 “filler” (*CD45*^{2/2}) bone marrow into lethally irradiated B6 male hosts (*CD45*^{2/2}). Six weeks post-engraftment, chimeric mice were treated with either PBS or DT every other day for 12 days. MJ23tg and polyclonal Tregs in the thymus and secondary lymphoid organs were analyzed on day 12 of treatment. (**G**) Representative flow cytometric analysis of CD45.1⁺ MJ23tg, *top row*, and CD45.2⁺ polyclonal Tregs, *bottom row*, in the thymus of the indicated treatment groups. The percentage of Foxp3⁺CD25⁺ Treg cells among CD4⁺CD8^{neg} thymocytes is indicated. (**H-I**) Summary plots of the total number of thymic MJ23tg, *H*, and polyclonal, *I*, Foxp3⁺CD25⁺ Tregs in chimeric mice of the indicated treatment groups. (**J**) Representative flow cytometric analysis of CD4⁺ T cells from the prostate draining periaortic lymph nodes (pLN) with the frequency of Tregs among CD4⁺ T cells, *top row*, and MJ23tg Tregs among all Tregs, *bottom row*, indicated for each treatment group. (**K-L**) Summary plots of the percentage of MJ23tg Tregs among all Tregs, *K*, and frequency of polyclonal Tregs among CD4⁺ T cells, *L*, for the indicated anatomical sites and treatment groups. Data are pooled from *N* = 2 independent experiments. SP, spleen; i/bLN, pooled inguinal and brachial lymph nodes. The mean ± SEM is shown.

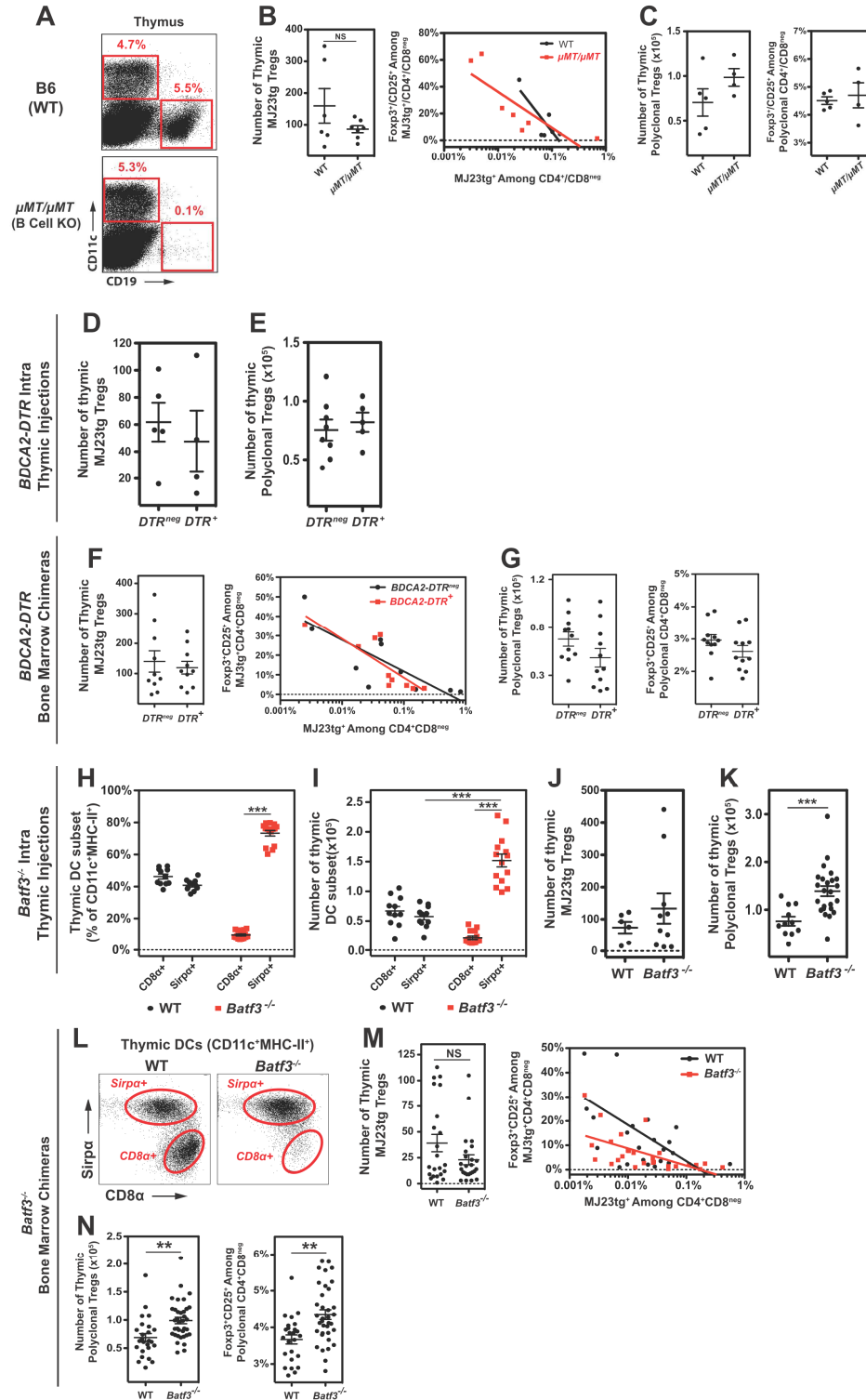


Figure 23: B cells, plasmacytoid DCs, and CD8 α ⁺ cDCs are dispensable for the thymic development of MJ23 Tregs. (A-C) Thymic development of MJ23tg and polyclonal Tregs is not impacted by the loss of B cells in μ MT/ μ MT mice.

Figure 23 Continued: T cell-depleted bone marrow cells from MJ23tg *Rag1*^{-/-} *CD45*^{1/1} donor mice were engrafted at low frequency (~ <1%), along with μ MT/ μ MT or wild-type, WT, (*CD45*^{2/2}) bone marrow, into sublethally irradiated μ MT/ μ MT or WT hosts (*CD45*^{2/2}), respectively. Six weeks post-engraftment MJ23tg and polyclonal Treg development were analyzed. **(A)** Representative flow cytometric analysis of thymic antigen presenting cells in WT or μ MT/ μ MT chimeric mice. **(B)** Summary plots of the total number of CD45.1⁺ MJ23tg Tregs (Foxp3⁺CD25⁺), *left*, and the “efficiency” of MJ23tg Treg development, *right*, in the thymus of the indicated chimeric mice. Lines represent best-fit semi-log curves. **(C)** Summary plots of the total number, *left*, and percentage, *right*, of CD45.2⁺ polyclonal Tregs among CD4⁺CD8^{neg} thymocytes from the indicated chimeric mice. Data are pooled from *N* = 2 independent experiments. The mean \pm SEM is shown. *t* test were performed between treatment groups with all differences having a *P* > 0.05. **(D-G)** Plasmacytoid DCs are dispensable for the thymic development of MJ23 Tregs. **(D-E)** CD11c-depleted thymocytes from MJ23tg *Rag1*^{-/-} *CD45*^{1/1} donor mice were transferred via intrathymic injection into *BDCA2-DTR*⁺ or *BDCA2-DTR*^{neg} (*CD45*^{2/2}) hosts. Mice were then treated with diphtheria toxin (DT) and analyzed seven days post-transfer as described in Figure 24. Summary plots of the total number of CD45.1⁺ MJ23tg Tregs (Foxp3⁺CD25⁺), *D*, or CD45.2⁺ polyclonal Tregs, *E*, from the indicated mice. Data are pooled from *N* = 2 independent experiments. **(F-G)** T cell-depleted bone marrow cells from MJ23tg *Rag1*^{-/-} *CD45*^{1/1} donor mice were engrafted at low frequency (~ <1%), along with either *BDCA2-DTR*⁺ or *BDCA2-DTR*^{neg} (*CD45*^{2/2}) bone marrow into sublethally irradiated *BDCA2-DTR*⁺ or *BDCA2-DTR*^{neg} (*CD45*^{2/2}) hosts, respectively. Six weeks post-engraftment, chimeric mice were treated with diphtheria toxin (DT) every other day for 12 days to deplete SiglecH⁺ pDCs. CD45.1⁺ MJ23tg and CD45.2⁺ polyclonal Treg development were analyzed on day 12 of treatment. **(F)** Summary plots of the total number of MJ23tg thymic Tregs (Foxp3⁺CD25⁺), *left*, and the “efficiency” of MJ23tg Treg development, *right*, in the thymus of the indicated chimeric mice. Lines represent best-fit semi-log curves. **(G)** Summary plots of the total number, *left*, and percentage, *right*, of polyclonal Tregs among CD4⁺CD8^{neg} thymocytes from the indicated chimeric mice. Data are pooled from *N* = 3 independent experiments. **(H-N)** *Batf3*-dependent CD8 α ⁺ cDCs are dispensable for the thymic development of MJ23 Tregs. **(H-K)** MJ23tg thymocytes were transferred into wild-type (WT) *Batf3*^{+/+} or *Batf3*^{-/-} mice and analyzed 7 days post-transfer as described in Figure 24. Summary plots of the percentage among CD11c⁺MHC-II⁺ cells, *H*, and total number, *I*, of the indicated cDC subsets in the indicated mice. Summary plots of the total number of thymic CD45.1⁺ MJ23tg Tregs, *J*, or CD45.2⁺ polyclonal Tregs, *K*, from the indicated mice. Data are pooled from *N* = 4 independent experiments. The mean \pm SEM is shown. Asterisks indicate *P* values for *t* test for the indicated comparisons, with *** = *P* < 0.0005. **(L-N)** MJ23tg BMCs were generated as described above into sublethally irradiated wild-type (WT) *Batf3*^{+/+} or *Batf3*^{-/-} (*CD45*^{2/2}) hosts. Six weeks post-engraftment MJ23tg and polyclonal Treg development were analyzed. **(L)** Representative flow cytometric analysis of thymic cDCs (CD11c⁺MHC-II⁺SiglecH^{neg}F4/80^{neg}) in the indicated chimeric mice. **(M)** Summary plots of the total number of MJ23tg Tregs, *left*, and the “efficiency” of MJ23tg Treg development, *right*, in the thymus of the indicated chimeric mice. Lines represent best-fit semi-log curves.

Figure 23 Continued: (N) Summary plots of the total number, *left*, and percentage, *right*, of polyclonal Tregs among CD4⁺CD8^{neg} thymocytes from the indicated chimeric mice. Data are pooled from $N = 5$ independent experiments. The mean \pm SEM is shown. Asterisks indicate P values for t test for the indicated comparisons, with ** = $P < 0.005$.

Plasmacytoid DCs and CD8 α ⁺ cDCs are dispensable for the thymic development of MJ23 Treg cells

The thymus contains three major classes of DCs, including plasmacytoid DCs (pDCs), Sirp α ⁺ cDCs, and CD8 α ⁺ cDCs (77, 117). To assess the role of pDCs in Treg cell development, we utilized *CLEC4C-DTR*⁺ (also known as BDCA2-DTR) mice, which express DTR exclusively in pDCs (118). In experiments in which MJ23Tg thymocytes were injected intrathymically into *CLEC4C-DTR*⁺ mice (Fig. 24, A through D, and Fig. 23, D and E), and in BMCs in which MJ23Tg bone marrow was introduced into *CLEC4C-DTR*⁺ hosts (Fig. 23, F and G), DT-mediated ablation of pDCs did not impact the development of MJ23 or polyclonal Treg cells, indicating that pDCs are dispensable for the development of these cells.

Batf3^{-/-} mice exhibit a deficiency of CD8 α ⁺ cDCs in the thymus (Fig. 24E, and Fig. 23, H and I) and secondary lymphoid organs (119), which allowed us to test the requirement for CD8 α ⁺ cDCs in orchestrating Treg cell development. In mice injected intrathymically with MJ23Tg thymocytes and in MJ23Tg BMCs, MJ23 Treg cells developed efficiently in *Batf3*^{-/-} hosts (Fig. 24, F and G, and Fig. 23, J and M), indicating that CD8 α ⁺ cDCs are dispensable for MJ23 Treg cell development. Thus, our data showing a requirement for antigen presentation by DCs (Fig. 21 and Fig. 24), coupled with our data demonstrating that pDCs and CD8 α ⁺ cDCs are dispensable for this process (Fig. 24, suggest either functional redundancy of multiple DC subsets, or a critical role for *Batf3*-independent Sirp α ⁺ cDCs in mediating MJ23 Treg cell development. It is currently not possible to test a specific requirement for thymic Sirp α ⁺ cDCs *in vivo* due to a lack of available models. These findings are inconsistent with the

conclusions of Perry and colleagues (71), who suggest that CD8 α ⁺ cDCs play a specialized role in coordinating the thymic development of Aire-dependent Treg cells. To determine whether our observed results are applicable to other Aire-dependent Treg cell specificities, we evaluated the thymic development of a second Aire-dependent Treg cell clone named RT83 (Malchow et al., 2013), which does not exhibit reactivity to a prostate-associated antigen. Using a combination of intrathymic injection and BMC approaches, we found that the thymic development of RT83Tg Treg cells was abrogated in MHC-II deficient or *Aire*^{-/-} hosts, but occurred efficiently in hosts lacking B cells, pDCs, or CD8 α ⁺ cDCs (Fig. 25).

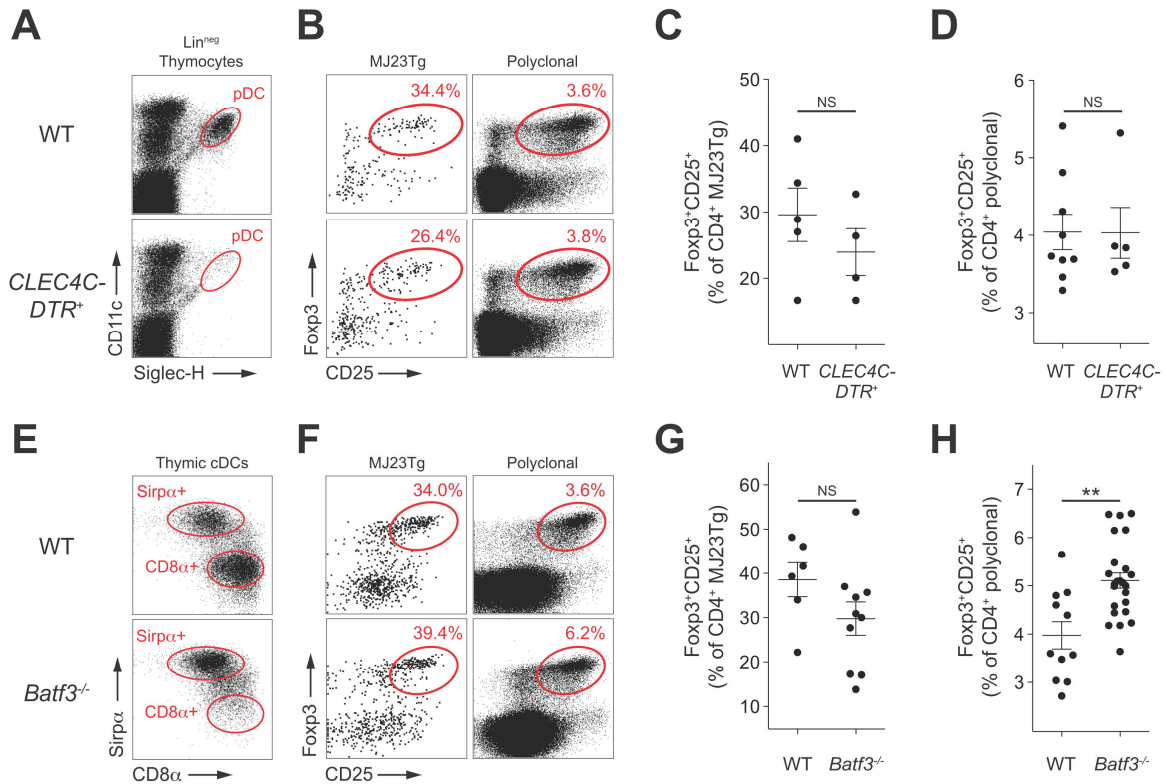


Figure 24: Plasmacytoid DCs and CD8 α ⁺ cDCs are dispensable for the development of MJ23Tg Treg cells. MJ23Tg Treg cell thymic development is not dependent on plasmacytoid DCs (pDCs) or Batf3-dependent CD8 α ⁺ classical DCs (cDCs). **(A-D)** CD45.1⁺ MJ23Tg *Rag1*^{-/-} thymocytes were intrathymically injected into CD45.2⁺ *CLEC4C-DTR*⁺ or *CLEC4C-DTR*^{neg} (WT) hosts. All mice were treated with diphtheria toxin (DT) every other day for 10 days, starting three days prior to thymocyte transfer, and analyzed seven days post-transfer. **(A)** Representative flow cytometric analysis of pDCs among "Lin^{neg}" thymocytes (F4/80^{neg}TCR β ^{neg}CD19^{neg}) in the indicated mice. **(B)** Representative flow cytometric analysis of Treg cell development for CD45.1⁺ MJ23Tg and CD45.2⁺ polyclonal CD4⁺CD8^{neg} thymocytes. The percentage of Fopx3⁺CD25⁺ Treg cells among CD4⁺CD8^{neg} thymocytes is indicated. Summary plots of the percentage of Treg cells among MJ23Tg **(C)** or polyclonal **(D)** CD4⁺CD8^{neg} thymocytes from the indicated mice. Data are pooled from *N* = 2 independent experiments. **(E-H)** CD45.1⁺ MJ23Tg thymocyte transfers were performed as described above into CD45.2⁺ *Batf3*^{+/+} (WT) or *Batf3*^{-/-} mice and analyzed seven days post-transfer. **(E)** Representative flow cytometric analysis of thymic cDCs (CD11c⁺MHC-II⁺Siglec-H^{neg}Lin^{neg}) in the thymus of the indicated mice. **(F)** Representative flow cytometric analysis of Treg cell development for MJ23Tg, *left*, and polyclonal, *right*, CD4⁺CD8^{neg} thymocytes. Summary plots of the percentage of Treg cells among MJ23Tg **(G)** or polyclonal **(H)** CD4⁺CD8^{neg} thymocytes from the indicated mice. Data are pooled from *N* = 4 independent experiments. All flow data are presented on log-scale. The mean \pm SEM is shown. Asterisks indicate *P* values for *t* test for the indicated comparisons, with ** = *P* < 0.005.

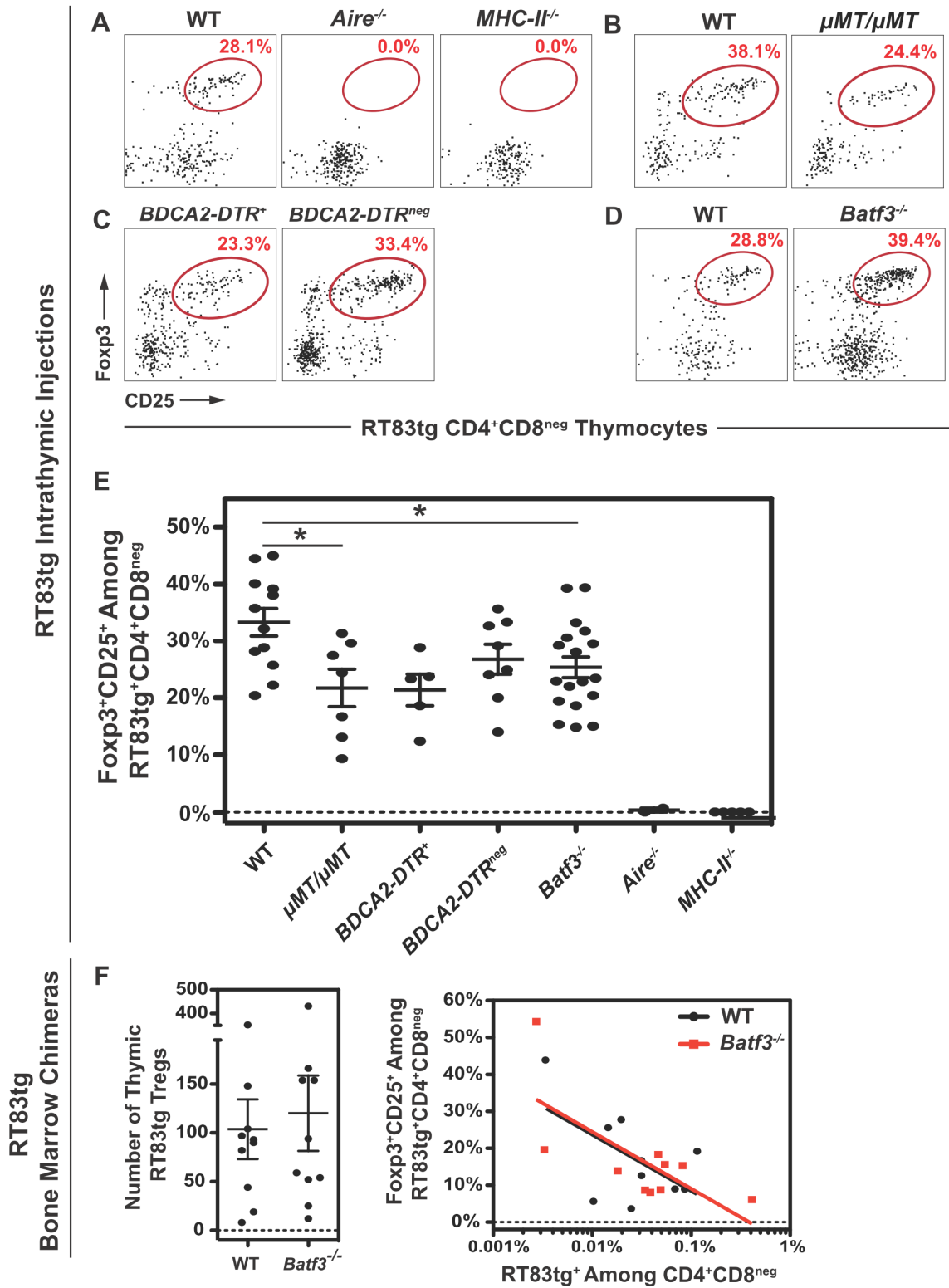


Figure 25: Plasmacytoid DCs and CD8 α ⁺ cDCs are dispensable for the thymic development of a second Aire-dependent Treg specificity.

Figure 25 Continued: The thymic development of RT83tg Tregs, a second Aire-dependent Treg specificity, occurs in the absence of pDCs or CD8 α^+ cDCs. (A-E) CD11c-depleted thymocytes from RT83tg *Rag1*^{-/-} *CD45*^{1/1} donor mice were transferred via intrathymic injection into the indicated hosts (*CD45*^{2/2}). For transfer into *BDCA2-DTR*⁺ or *BDCA2-DTR*^{neg} hosts, mice were treated with diphtheria toxin (DT) every other day for 10 days to deplete pDCs, starting three days prior to thymocyte transfer. For all mice, loss of the target APC subset, and thymic Treg development were analyzed at 7 days post transfer. (A-D) Representative flow cytometric analysis of Treg development for CD45.1⁺ RT83tg CD4⁺CD8^{neg} thymocytes in the thymus of the indicated mice and their controls. (E) Summary plot of the percentage of Tregs among RT83tg CD4⁺CD8^{neg} thymocytes from the indicated mice. Data are pooled from *N* = 5 independent experiments with approximately age-matched hosts. (F) T cell-depleted bone marrow cells from RT83tg *Rag1*^{-/-} *CD45*^{1/1} donor mice were engrafted at low frequency (~<1%), along with either wild-type (WT) *Batf3*^{+/+} or *Batf3*^{-/-} (*CD45*^{2/2}) bone marrow into sublethally irradiated WT or *Batf3*^{-/-} (*CD45*^{2/2}) hosts, respectively. Six weeks post-engraftment CD45.1⁺ RT83tg Treg development was analyzed. Summary plots of the total number of RT83tg Tregs, *left*, and the “efficiency” of RT83tg Treg development, *right*, in the thymus of the indicated chimeric mice. Lines represent best-fit semi-log curves. Data are pooled from *N* = 3 independent experiments. The mean \pm SEM is shown. Asterisks indicate *P* values for *t* test for the indicated comparisons, with * = *P* < 0.05.

The thymic Treg cell repertoire is not impacted by Batf3 deficiency

To broaden our analysis, we assessed the impact of Batf3 deficiency on the polyclonal Treg cell repertoire using a deep TCR sequencing approach (106). Briefly, we isolated Treg cells from the thymus of male *Batf3*^{+/+} or *Batf3*^{-/-} mice expressing a fixed transgenic TCR β chain and a *Foxp3*^{GFP} reporter, and performed sequencing of the complete TCR α repertoire, regardless of variable-region usage. Presence or loss of CD8 α ⁺ cDCs in the spleen was confirmed for all mice analyzed. On average, we isolated approximately 1.0×10^5 Treg cells from each thymus sample, yielding 1.0×10^6 TCR sequence reads per sample with a complexity of 9×10^3 unique TCRs, allowing us to assess the broad impact of Batf3 on the selection of thousands of Treg cell specificities.

Comparison of these Treg cell TCR catalogs revealed that Batf3 deficiency had negligible impact on the Treg cell repertoire in the thymus (Fig. 26). Of the 8,423 unique TCR clonotypes recurrently expressed by Treg cells in the thymus of either *Batf3*^{+/+} or *Batf3*^{-/-} mice, differential analysis of TCR frequency revealed a lack of Batf3-dependent specificities that were significantly underrepresented or absent in *Batf3*^{-/-} thymi (Fig. 26A, right arm of volcano plot). This finding was further illustrated by plotting the frequencies of the most prevalent thymic Treg cell specificities (Fig. 26B), which demonstrated that the frequency of these clonotypes was not significantly altered by Batf3 deficiency (when corrected for multiple comparisons). Analysis using the Morisita-Horn (MH) similarity index (81) also revealed a high degree of similarity between the thymic Treg cell TCR catalogs from *Batf3*^{+/+} and *Batf3*^{-/-} mice (Fig. 26C). Finally, unlike *Aire*^{-/-} mice that display diminished Treg cell frequencies in the thymus (Fig. 21D and

(95), *Batf3*^{-/-} mice exhibited elevated numbers and frequencies of polyclonal Treg cells in the thymus (Fig. 24H, Fig. 23, K and N), supporting the idea that *Batf3*-deficiency is not associated with a paucity of Treg cells. Our data suggest that *Batf3*-dependent CD8 α ⁺ cDCs do not play a specialized role in orchestrating Treg cell development.

To further examine the functional role of distinct thymic DC subsets in coordinating MJ23 Treg cell development, we performed *in vitro* assays in which fluorescence activated cell sorting (FACS)-purified thymic CD8 α ⁺ or Sirp α ⁺ cDCs were cultured with MJ23Tg thymocytes. Both thymic cDC subsets induced proliferation, CD69 expression, and Foxp3 induction by a fraction of MJ23Tg thymocytes (Fig. 27, A through C). This induction was blocked by addition of anti-MHC-II antibody, and was not conferred by co-culture with splenic CD11c⁺ cells (Fig. 27, A through C). Furthermore, when cultured with exogenous prostate-tissue extract, both CD8 α ⁺ and Sirp α ⁺ cDCs were able to process and present antigen, inducing robust stimulation and Foxp3 upregulation (Fig. 27, D through F). Thus, our cumulative data suggest that both cDC subsets are capable of acquiring antigen from mTECs and promoting MJ23 Treg cell development *in vitro*, suggesting possible functional redundancy of these DC subsets *in vivo*.

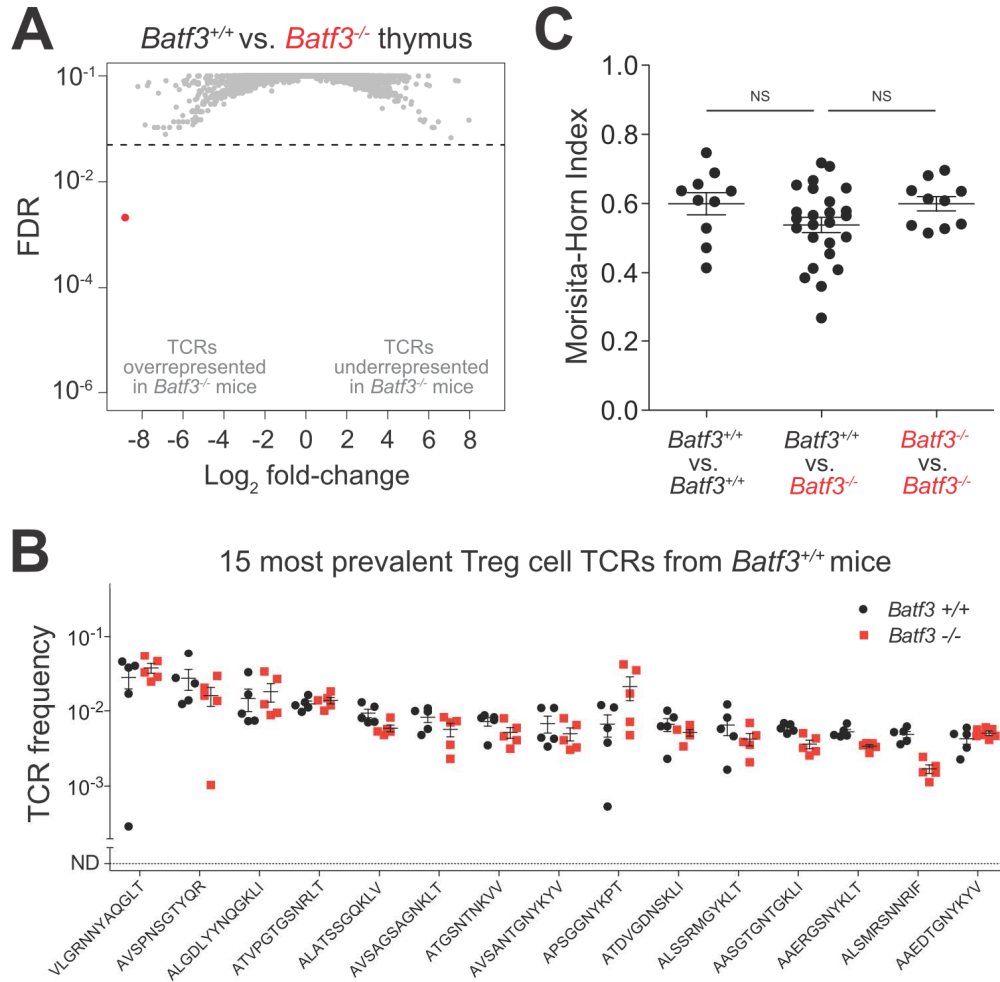


Figure 26: Loss of *Batf3*-dependent CD8 α ⁺ cDCs has negligible impact on the thymic Treg cell repertoire. CD4⁺CD25⁺Foxp3⁺ Treg cells were purified by FACS from 9-week-old TCR β Tg *Foxp3*^{GFP} males on a *Batf3*^{+/+} or *Batf3*^{-/-} background, and subjected to complete TCR α sequencing using the iRepertoire platform (see Experimental Procedures and Table S1). **(A)** For the TCR α chain sequences, a volcano plot of false discovery rate (FDR) versus differential TCR representation (log₂ fold-change) is shown for the 8,423 unique and recurrently expressed TCRs. The red dot denotes the single TCR that had a fold-change > 4 and FDR < 0.05. The horizontal dashed line indicates FDR cutoff. **(B)** For the 15 most prevalent TCRs recurrently expressed by Treg cells from the thymus of *Batf3*^{+/+} mice, a summary plot of the frequency of these TCRs in individual *Batf3*^{+/+} and *Batf3*^{-/-} thymic samples is shown, with the TCR α CDR3 sequences listed below. ND, not detected. **(C)** Repertoire overlap was assessed using the Morisita-Horn (MH) similarity index. Scatter plots of select MH pairwise comparisons are shown. For the MH index, a value of 1 indicates identity and a value of 0 denotes complete dissimilarity. A student *t* test was performed for the indicated comparisons, with none reaching statistical significance. *N* = 5 for *Batf3*^{-/-} thymi and *N* = 5 for *Batf3*^{+/+} thymi. The mean \pm SEM is shown.

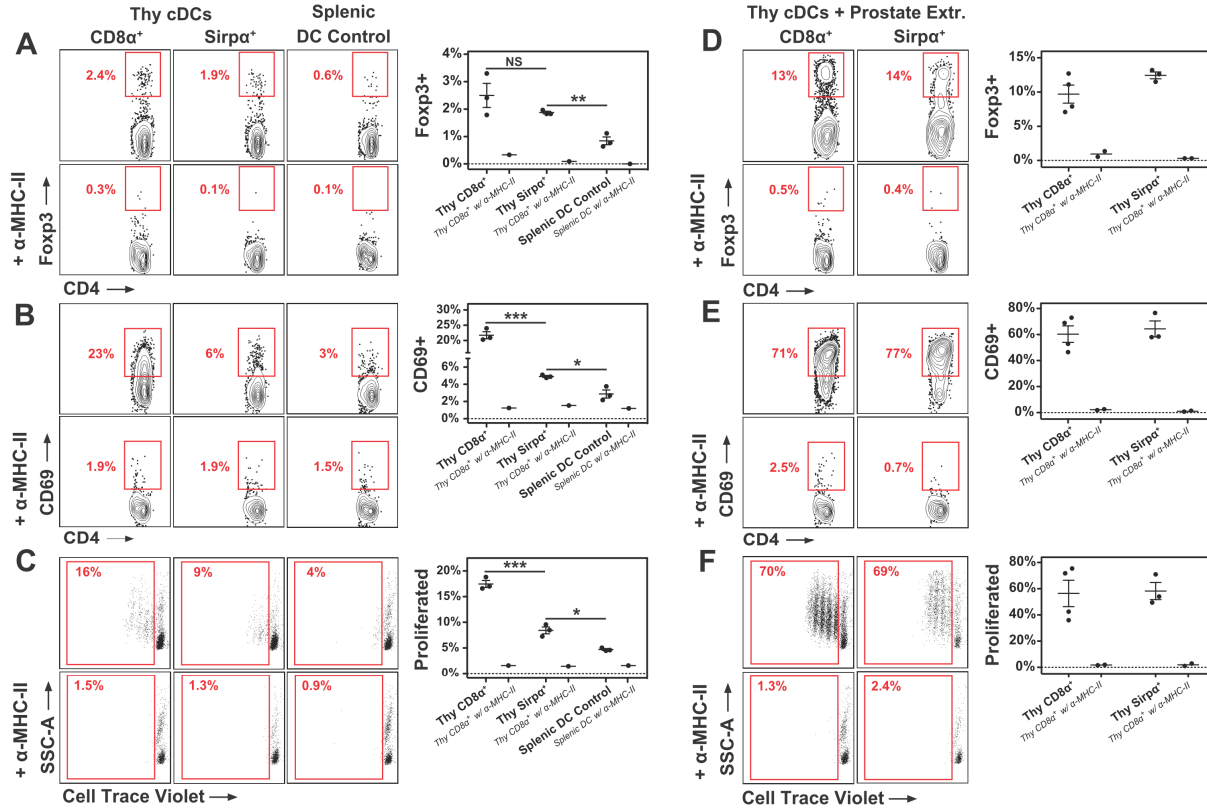


Figure 27: Both thymic CD8 α^+ and Sirpa $^+$ cDCs can promote activation and Foxp3 induction by MJ23tg thymocytes *in vitro*. Alone and in the presence of exogenous prostate tissue extracts, both CD8 α^+ and Sirpa $^+$ thymic DC subsets are capable of promoting activation and Foxp3 upregulation by MJ23tg thymocytes *in vitro*. DCs were harvested from the thymi and spleens of 3-to-4 week old male mice. Thymic CD8 α^+ Sirpa $^{\text{neg}}$ and Sirpa $^+$ CD8 α^{neg} DCs were FACS purified and co-cultured with CellTrace-Violet-labeled CD4 single-positive enriched MJ23tg thymocytes with, A-C, or without, D-F, extracts from TRAMP prostate tumor tissue (Prostate Extr.). Anti-MHC-II blocking antibody was added to the indicated wells. Splenic CD11c $^+$ DCs were enriched by magnetic sorting, and were utilized as a negative control. After 3 days of culture, thymocyte proliferation (CellTrace-Violet dilution), CD69 expression, and Foxp3 expression were assessed. (A-C) Representative flow cytometric analysis, *left*, and summary plots, *right*, of MJ23tg thymocytes co-cultured with the indicated DC populations with or without anti-MHC-II blocking antibody. The percentage of CellTrace-Violet-diluted, A, CD69 $^+$, B, and Foxp3 $^+$, C, cells are indicated. (D-F) Representative flow cytometric analysis, *left*, and summary plots, *right*, of MJ23tg thymocytes co-cultured with the indicated DC populations in the presence of prostate tumor extract with or without MHC-II blocking antibody. The percentage of CellTrace-Violet-diluted, A, CD69 $^+$, B, and Foxp3 $^+$, C, cells are indicated. The mean \pm SEM is shown. Asterisks indicate *P* values for *t* test for the indicated comparisons, with * = *P* < 0.05, ** = *P* < 0.005 and *** = *P* < 0.0005.

The enrichment of MJ23 Treg cells in the pLNs is abrogated by loss of antigen in castrated mice

Having identified a role for DCs in coordinating the thymic development of MJ23 Treg cells, we next aimed to elucidate the role of antigen recognition in dictating the peripheral homeostasis and anatomical distribution of MJ23 Treg cells. Previously, we demonstrated that MJ23 Treg cells are selectively enriched in the prostate-draining periaortic lymph nodes (pLNs) of male mice (106). Phenotypic analysis of MJ23Tg BMC mice revealed that MJ23 Treg cells in the pLNs of male mice expressed markers indicative of recent T cell activation, including CD69 and Egr2 (Fig. 28, A and B). In contrast, MJ23 Treg cells in female hosts or in the skin-draining lymph nodes and spleen of male hosts did not express these markers (Fig. 28, A and B).

To test the hypothesis that MJ23 Treg cell enrichment in the pLNs is dependent on continuous antigen recognition, we performed studies in which MJ23Tg BMCs were subjected to castration. We reasoned that castration, which leads to rapid involution of the prostate (Fig. 28C and (120)), would reduce prostate antigen density, thereby impacting MJ23 Treg cell enrichment. Thus, we assessed the frequency, anatomical distribution, and activation status of MJ23Tg Treg cells in castrated mice, sham castrated mice, or mice subjected to castration followed by testosterone supplementation, a procedure that leads to complete regeneration of the prostate (121). While MJ23 Treg cells in sham castrated mice expressed high amounts of CD69 and exhibited the expected enrichment in the prostate-draining pLNs, enrichment and activation of MJ23 Treg cells was lost upon castration and involution of the prostate (Fig. 28, D through F). Finally, the enrichment and activation of MJ23 Treg cells in the

pLNs was restored in castrated mice subjected to testosterone supplementation (Fig. 28, D through F). In sum, although antigen-independent hormonal effects of castration cannot be excluded, these findings suggest that the enrichment of prostate-specific MJ23 Treg cells in the pLNs requires the continued presence of antigen, and that antigen-driven enrichment in the organ-draining lymph nodes is reversible.

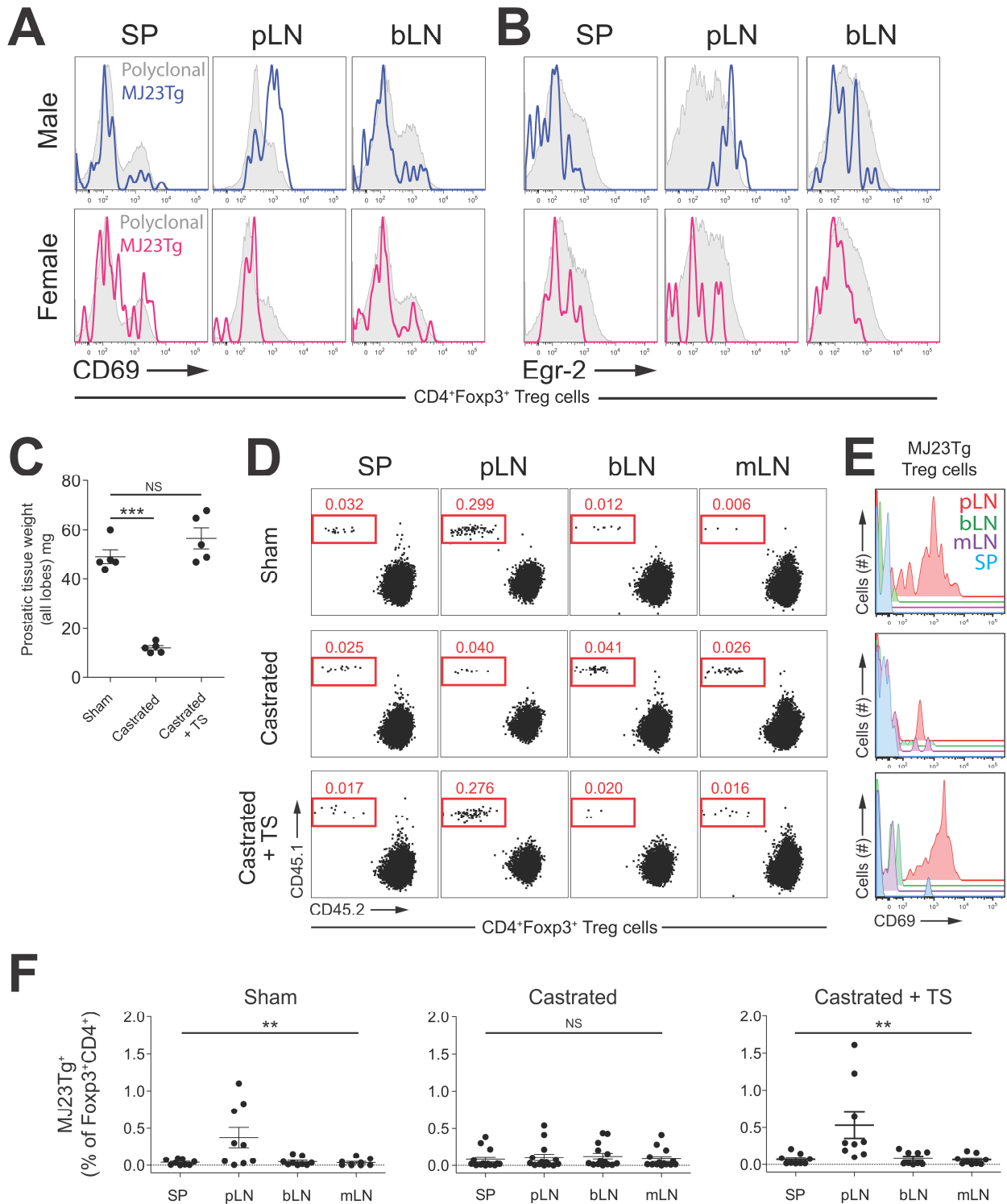


Figure 28: Castration abrogates the enrichment and activation of MJ23 Treg cells in the prostate-draining lymph nodes. The activation and enrichment of MJ23 Treg cells in the pLNs are dependent on continued availability of prostate antigen.

Figure 28 Continued: CD45.1⁺ MJ23Tg *Rag1*^{-/-} bone marrow cells were engrafted at low frequency, along with CD45.2⁺ B6 “filler” bone marrow into sublethally irradiated CD45.2⁺ B6 hosts. **(A-B)** Six weeks post-engraftment, the phenotype of CD4⁺Foxp3⁺ Treg cells was analyzed. Representative histograms of CD69 **(A)** and Egr-2 **(B)** expression for CD45.1⁺ MJ23Tg Treg cells, *solid blue or pink lines*, and CD45.2⁺ polyclonal Treg cells, *filled grey histograms*, for the indicated anatomical sites and mice. **(C-F)** MJ23Tg BMCs were generated into B6 males as described above. Six weeks post-engraftment, mice were either castrated or sham castrated as control. Four weeks post-procedure, half of the castrated mice received testosterone supplementation. Four weeks post-implantation, MJ23Tg Treg cell activation and anatomical distribution were analyzed. **(C)** Summary plot of prostatic tissue weight for the indicated treatment groups. Asterisks indicate *P* values for *t* test for the indicated comparisons, with *** = *P* < 0.0005 **(D-E)** Representative analysis (log-scale) of CD45.1⁺ MJ23Tg Treg cells, *D*, and CD69 expression by MJ23Tg Treg cells, *E*, at the indicated anatomical sites for the three treatment groups. **(F)** Summary plots of the percentage of MJ23Tg Treg cells among all Treg cells for the indicated sites and treatment groups. SP, spleen; bLN, brachial lymph node; mLN, mesenteric lymph node. The mean ± SEM is shown. Asterisks indicate *P* values for ANOVA tests, with ** = *P* < 0.005.

DCs are required for the optimal enrichment of MJ23 Treg cells in the pLNs

To determine the role of DCs in coordinating antigen-driven MJ23 Treg cell enrichment in the pLNs, we analyzed MJ23 Treg cell distribution in the periphery of BMCs reconstituted with a mixture of MJ23Tg, *Itgax-DTR*⁺, and MHC-II deficient bone marrow, described above. In these mice, DT-mediated ablation of MHC-II⁺ CD11c-expressing cells (Fig. 29A) led to a significant reduction of MJ23 Treg cell frequency and total number in the pLNs (Fig. 29B and Fig. 30A), indicating that MHC-II expression by CD11c⁺ DCs is required for optimal enrichment of MJ23 Treg cells in the pLNs. At the polyclonal level, DC depletion also induced a significant reduction of Treg cell frequency in the lymph nodes and spleen (Fig. 29C), suggesting that a fraction of polyclonal Treg cells at these sites are dependent on antigen presentation by DCs. In other experiments, we determined the impact of systemic DC expansion (Fig. 29D) induced by subcutaneous challenge with B16 melanoma cells producing Flt3L (122). B16-Flt3L tumor challenge induced significant increases in polyclonal Treg cell frequency in the spleen and inguinal & brachial lymph nodes, but did not induce further enrichment of MJ23 Treg cells in the pLNs (Fig. 29, E and F, and Fig. 30D) or thymus (Fig. 30H). Furthermore, as previously described for the spleen (75), we found that polyclonal Treg cell frequencies were positively correlated with DC abundance in the lymph nodes following DC depletion or expansion (Fig. 30, C and F). These findings suggest that MJ23 enrichment in the pLNs is limited by antigen availability, and is not further augmented by the systemic or local expansion of Flt3L-responsive DC populations.

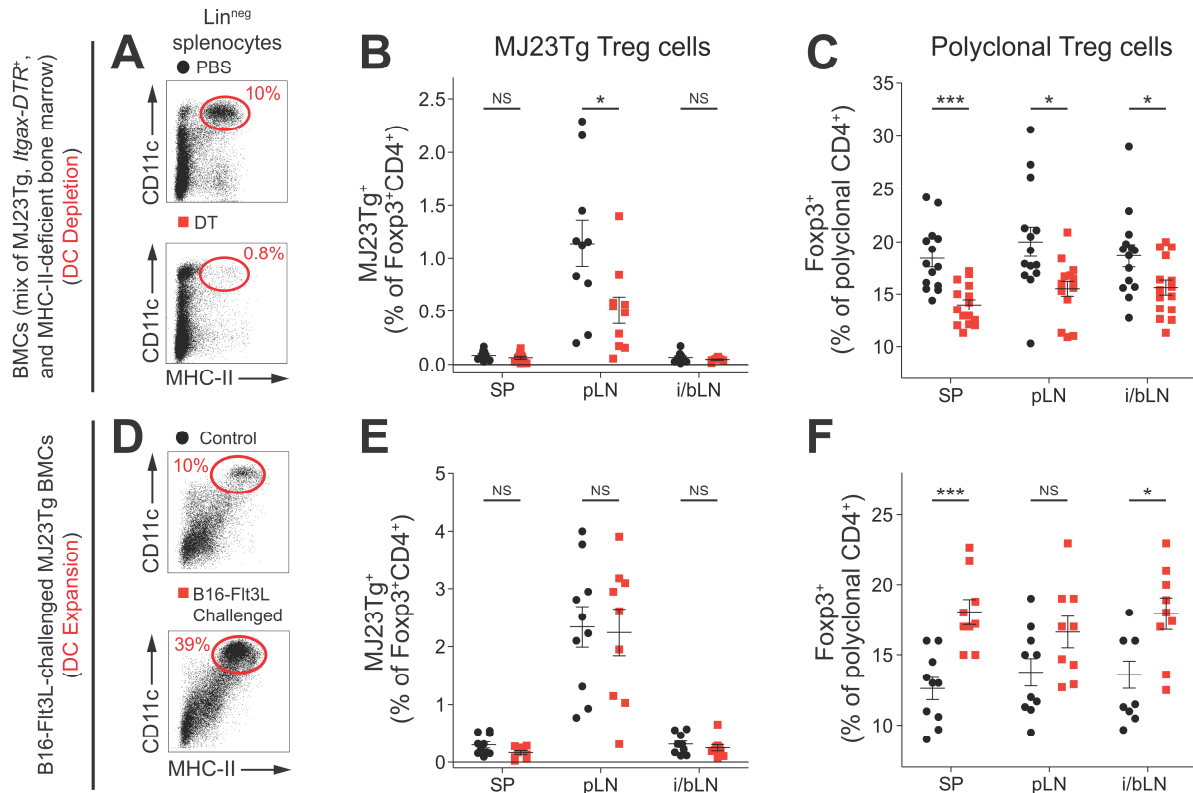


Figure 29: Dendritic cells coordinate MJ23Tg Treg cell enrichment in the prostate-draining lymph nodes. (A-C) The enrichment of MJ23 Treg cells in the pLNs is partially reversed by depletion of MHC-II-expressing $CD11c^+$ cells. $CD45^{1/1}$ MJ23Tg, $CD45^{1/2}$ *Itgax-DTR*⁺, $CD45^{2/2}$ *H2^{dIAb1-Ea}* MHC-II deficient mixed bone marrow chimeras were generated into lethally irradiated male $CD45^{2/2}$ B6 hosts as described in Figure 22. Six weeks later, chimeric mice were treated with either DT to deplete MHC-II⁺ DCs, or PBS every other day for 12 days and then analyzed. (A) Representative analysis (log-scale) of $TCR\beta^{neg}CD19^{neg}F4/80^{neg}DX-5^{neg}Ter119^{neg}$ (lineage^{neg}) splenocytes in PBS and DT treated chimeric mice. (B) Summary plots of the percentage of MJ23Tg Treg cells among all Treg cells at the indicated sites. (C) Summary plot of the percentage of $CD45.2^+$ polyclonal Treg cells among $CD4^+$ T cells in the indicated organs. Data are pooled from $N = 3$ independent experiments. (D-F) MJ23Tg BMCs were generated in male hosts as described in Figure 28. Six weeks post-engraftment, mice were subcutaneously injected with 1×10^6 B16 melanoma cells expressing Flt3 ligand (B16-Flt3L) to systemically expand DCs and analyzed 14 days post-challenge. (D) Representative flow cytometric analysis (log-scale) of lineage^{neg} splenocytes in control or B16-Flt3L-challenged chimeric mice. (E) Summary plots of the percentage of MJ23Tg Treg cells among all Treg cells at the indicated sites. (F) Summary plot of the percentage of $CD45.2^+$ polyclonal Treg cells among $CD4^+$ T cells in the indicated organs. Data are pooled from $N = 2$ independent experiments. SP, spleen; i/bLN, pooled inguinal and brachial lymph nodes. The mean \pm SEM is shown. Asterisks indicate P values for t test for the indicated comparisons, with * = $P < 0.05$ and *** = $P < 0.0005$.

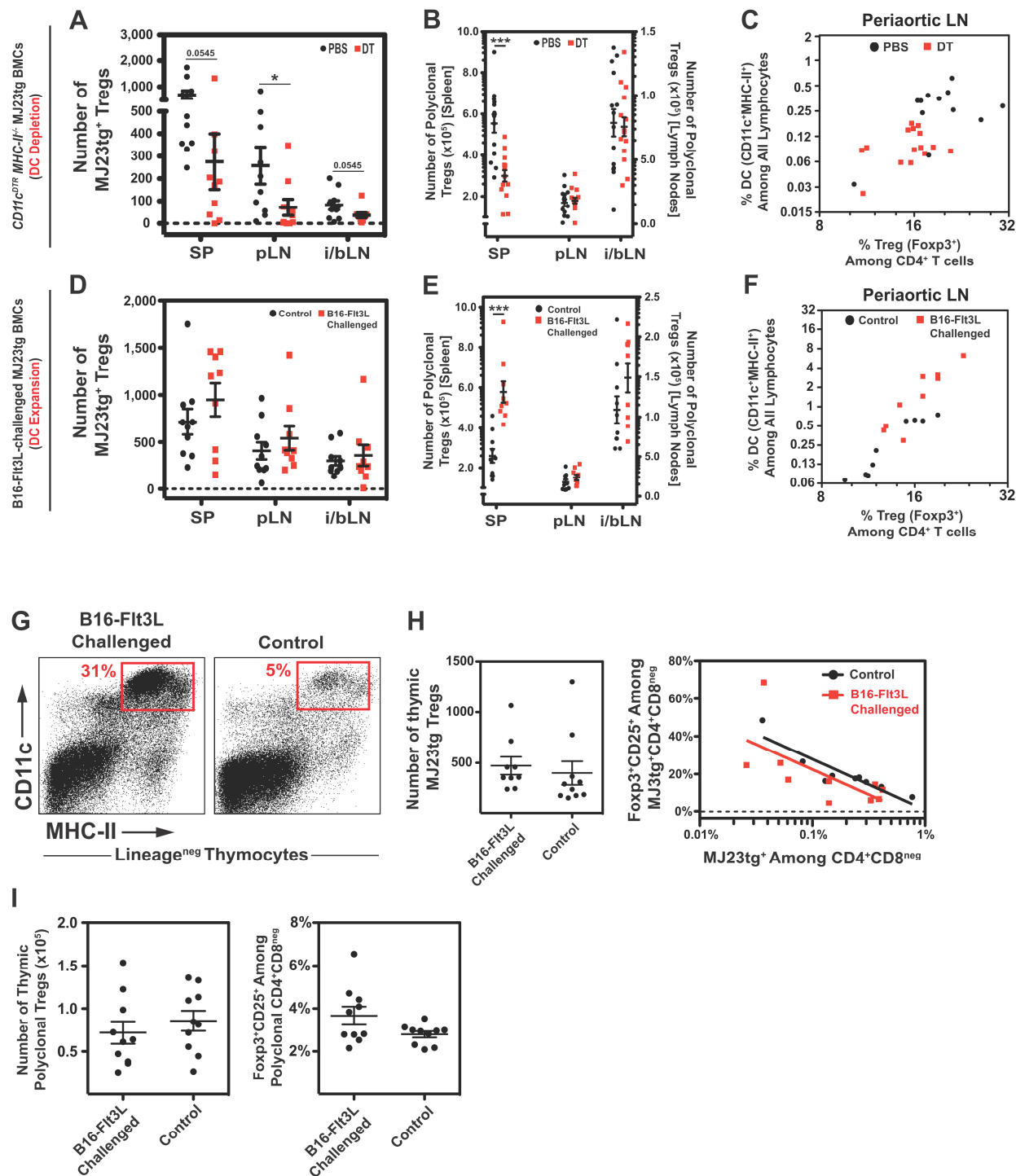


Figure 30: Dendritic cells coordinate MJ23tg Treg enrichment and impact polyclonal Treg frequencies in the prostate-draining lymph nodes. (A-C) Depletion of MHC-II-expressing CD11c⁺ cells negatively impacts the total number of MJ23tg Tregs in the pLN.

Figure 30 Continued: MJ23tg ($CD45^{1/1}$) $CD11c^{DTR}$ ($CD45^{1/2}$) $MHC-II^{-/-}$ ($CD45^{2/2}$) mixed bone marrow chimeras were generated into lethally irradiated male B6 ($CD45^{2/2}$) hosts, treated with diphtheria toxin (DT) to deplete $MHC-II^+$ DCs and analyzed 12 days post treatment as described in Figure 25. **(A)** Summary plot of the total number of $CD45^{1/1}$ MJ23tg $Foxp3^+CD4^+$ Tregs at the indicated sites of the indicated treatment groups. **(B)** Summary plot of the total number of $CD45.2^+$ polyclonal Tregs in the indicated organs of the indicated treatment groups. **(C)** Summary plot of the percentage of $CD45.2^+$ polyclonal Tregs among $CD4^+$ T cells compared to percentage of DCs ($CD11c^+MHC-II^+$) among all lymphocytes in the periaortic lymph nodes for DC depletion experiments. Data are pooled from $N = 3$ independent experiments. **(D-F)** Systemic expansion of dendritic cells via challenge with Flt3L-expressing B16 tumors does not increase the total number of MJ23 Tregs but does increase the frequency of polyclonal Tregs in the pLNs. T cell-depleted bone marrow cells from MJ23tg $Rag1^{-/-}$ $CD45^{1/1}$ donor mice were engrafted at low frequency ($\sim <1\%$), along with B6 “filler” ($CD45^{2/2}$) bone marrow into sublethally irradiated male B6 ($CD45^{2/2}$) hosts. Six weeks post-engraftment, mice were subcutaneously injected with 1×10^6 B16 melanoma cells expressing Flt3 ligand (B16-Flt3L) to systemically expand DCs, and mice were analyzed fourteen days post-challenge as described in Figure 27. **(D)** Summary plot of the total number of $CD45.1^+$ MJ23tg Tregs at the indicated sites of the indicated treatment groups. **(E)** Summary plot of the total number of $CD45.2^+$ polyclonal Tregs in the indicated organs of the indicated treatment groups. **(F)** Summary plot of the percentage of $CD45.2^+$ polyclonal Tregs among $CD4^+$ T cells compared to percentage of DCs among all lymphocytes in the periaortic lymph nodes for DC expansion experiments. Data are pooled from $N = 2$ independent experiments. SP, spleen; pLN, periaortic lymph nodes; i/bLN, pooled inguinal and brachial lymph nodes. The mean \pm SEM is shown. Asterisks or numbers indicate P values for t test for the indicated comparisons, with $*$ = $P < 0.05$ and $***$ = $P < 0.0005$. **(G-I)** Systemic expansion of dendritic cells via challenge with Flt3L-expressing B16 tumors does not increase MJ23 or polyclonal Treg development. T cell-depleted bone marrow cells from MJ23tg $Rag1^{-/-}$ $CD45^{1/1}$ donor mice were engrafted at low frequency ($<1\%$), along with B6 “filler” ($CD45^{2/2}$) bone marrow into sublethally irradiated male B6 ($CD45^{2/2}$) hosts. Six weeks post-engraftment, mice were subcutaneously injected with 1×10^6 B16 melanoma cells expressing Flt3 ligand (B16-Flt3L) to systemically expand DCs. Fourteen days post-challenge, DCs and Tregs were analyzed. **(G)** Representative flow cytometric analysis of $TCR\beta^{neg}CD19^{neg}F4/80^{neg}DX-5^{neg}Ter119^{neg}$ (lineage^{neg}) thymocytes in the thymus of control or B16-Flt3L-challenged chimeric mice. **(H)** Summary plots of the total of number of $CD45.1^+$ MJ23tg thymic Tregs ($Foxp3^+CD25^+$), *left*, and the “efficiency” of MJ23tg Treg development, *right*, in the thymus of the indicated treatment groups. Lines represent best-fit semi-log curves. **(I)** Summary plots of the total number, *left*, and percentage, *right*, of $CD45.2^+$ polyclonal Tregs among $CD4^+CD8^{neg}$ thymocytes from the indicated treatment groups. The mean \pm SEM is shown.

CCR7-dependent migratory DCs orchestrate MJ23 Treg cell enrichment in the pLNs

Given the emerging appreciation that DCs exhibit considerable functional and phenotypic heterogeneity (123, 124), we set out to determine whether a distinct DC subset is responsible for antigen presentation to MJ23 Treg cells. Lymph node mDCs, which are characterized by an MHC-II^{hi}CD11c^{int} phenotype (Fig. 31A), require CCR7-dependent signals to traffic from the tissues into the draining lymph nodes (125). Analysis of DCs in mouse prostate tissue revealed that both CD103⁺ and CD11b⁺ cDCs are present at steady state, and that these populations do not express CCR7 over background (Fig. 32, A and B). In contrast, mDCs in the pLNs exhibit a CCR7⁺ phenotype (Fig. 32, C and D), suggesting that mDCs upregulate CCR7 prior to or during transit from the tissues to the draining lymph nodes. To determine the extent to which mDCs are required for MJ23 Treg cell accumulation in the pLNs, we evaluated the anatomical distribution and phenotype of MJ23 Treg cells following intrathymic injection of CD45.1⁺ MJ23Tg *Rag1*^{-/-} thymocytes into *Ccr7*^{+/+} or *Ccr7*^{-/-} mice. In *Ccr7*^{+/+} hosts, MJ23 Treg cells developed efficiently (Fig. 32, E through G), preferentially accumulated in the pLNs, and adopted a CD69⁺ phenotype indicative of TCR signaling (Fig. 31, B through D). In contrast, in *Ccr7*^{-/-} mice, MJ23 Treg cells developed efficiently in the thymus (Fig. 31, E through G), but failed to accumulate in the pLNs and did not exhibit hallmarks of TCR signaling (Fig. 31, B through D). Notably, this effect was specific to the pLNs, as MJ23Tg Treg cell frequency was not reduced in the non-draining lymph nodes of *Ccr7*^{-/-} mice. In parallel experiments using RT83Tg T cells, which are not reactive to a prostate-specific antigen, the anatomical distribution of RT83 Treg cells did

not differ between *Ccr7*^{+/+} and *Ccr7*^{-/-} hosts (Fig. 31E). These findings suggest that CCR7-dependent mDCs are required for the enrichment of MJ23 Treg cells in the pLNs of male mice, implying that this DC subset may play a critical role in coordinating the peripheral homeostasis of prostate-specific Treg cells, thereby promoting immune tolerance to this anatomical site.

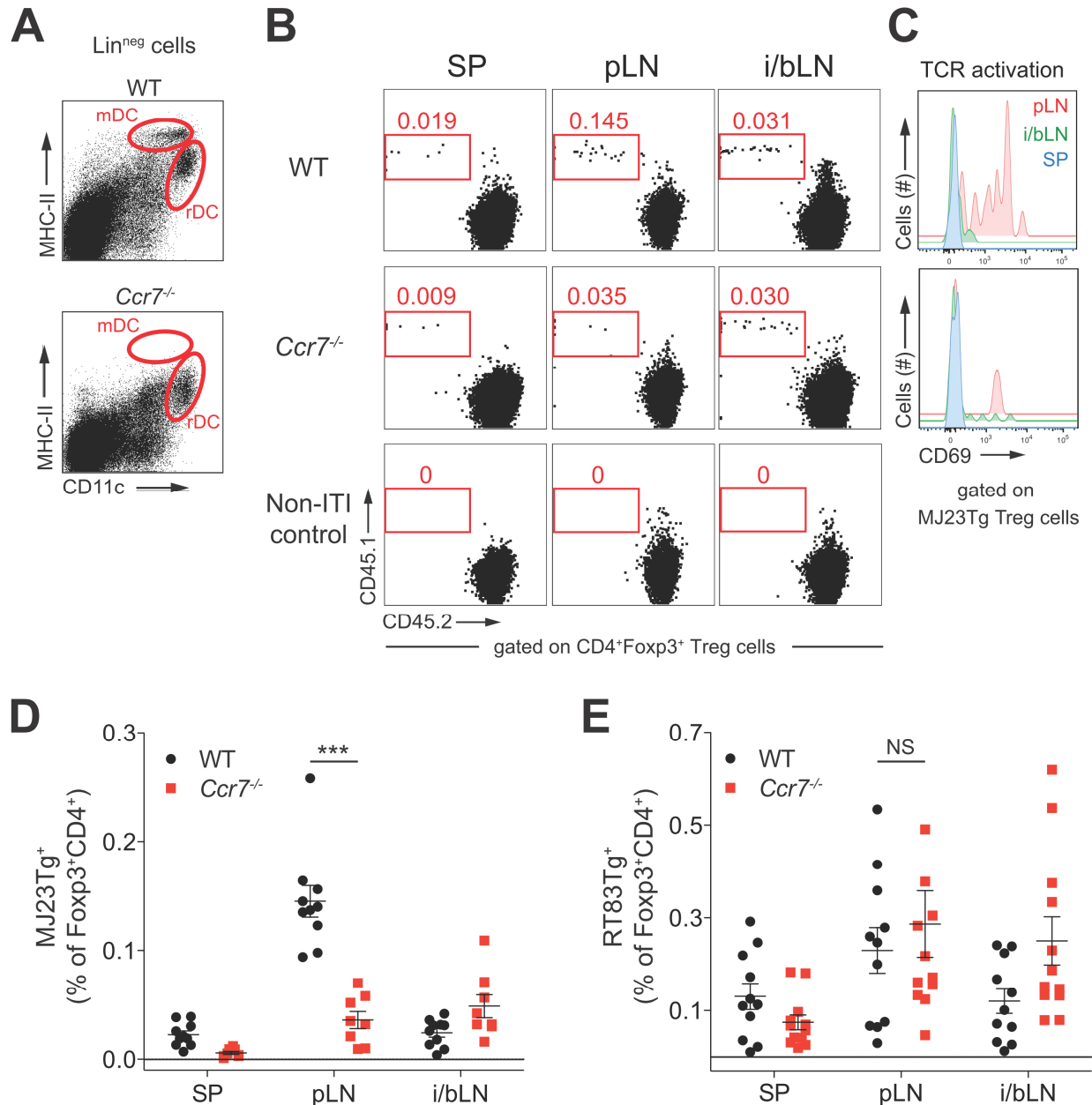


Figure 31: CCR7-dependent migratory DCs are required for the activation and enrichment of MJ23 Treg cells in the prostate-draining lymph nodes. The anatomical distribution and activation of MJ23 Treg cells are altered in the absence of CCR7-dependent migratory DCs, while the distribution of RT83Tg Treg cells are not. (A-D) CD45.1⁺ MJ23Tg Rag1^{-/-} thymocytes were intrathymically injected into age matched CD45.2⁺ Ccr7^{+/+} (WT) or Ccr7^{-/-} male hosts. Three weeks post-transfer, the anatomical enrichment and activation of CD45.1⁺ MJ23Tg Treg cells (CD4⁺Foxp3⁺) were analyzed. (A) Representative analysis (log-scale) of TCRβ^{neg}CD19^{neg}F4/80^{neg}DX-5^{neg}Ter119^{neg} (Lin^{neg}) lymphocytes in axillary lymph nodes of the indicated mice. mDC, migratory DC (CD11c^{int}MHC-II^{high}); rDC, resident DC (CD11c^{high}MHC-II^{int}).

Figure 31 Continued: (B-C) Representative analysis (log-scale) of MJ23Tg Treg cell frequency, *B*, and MJ23Tg Treg cell CD69 expression, *C*, at the indicated anatomical sites in the indicated host mice. Control mice not subjected to intrathymic injection (ITI) are shown as a staining control. **(D)** Summary plots of MJ23Tg Treg cell frequency, as a percentage of all Treg cells, at the indicated anatomical sites for WT and *Ccr7*^{-/-} hosts. SP, spleen; pLN, periaortic lymph nodes; i/bLN, pooled inguinal and brachial lymph nodes. Data are pooled from *N* = 3 independent experiments. **(E)** CD45.1⁺ RT83Tg *Rag1*^{-/-} thymocytes were transferred via intrathymic injection as described above. Summary plots of RT83Tg Treg cell frequency, as a percentage of all Treg cells, at the indicated anatomical sites. Data are pooled from *N* = 2 independent experiments. The mean ± SEM is shown. Asterisks indicate *P* values for *t* test for the indicated comparisons, *** = *P* < 0.0005.

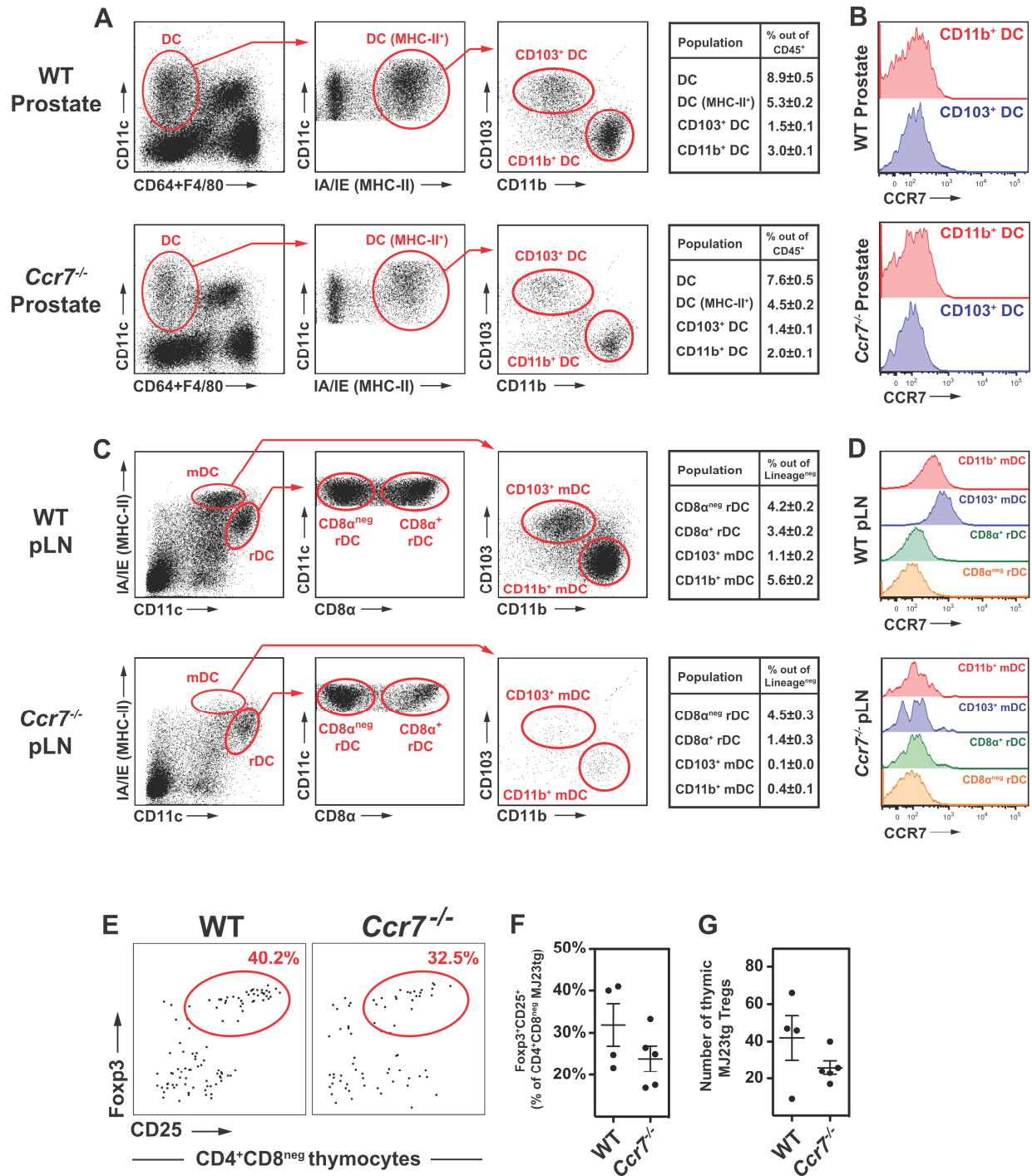


Figure 32: CD103⁺ and CD11b⁺ migratory DCs express CCR7 and are absent in the prostate draining pLNs of *CCR7*^{-/-} mice. (A-D) Characterization of CCR7 expression by CD103⁺ and CD11b⁺ cDCs in the prostate and pLNs of *Ccr7*^{+/+} and *Ccr7*^{-/-} mice. Cells were isolated from the prostate and pLNs of 8-week-old male *Ccr7*^{+/+} (WT) and *Ccr7*^{-/-} mice.

Figure 32 Continued: (A&C) Representative flow cytometry plots and gating strategies for identifying various DC subsets in the prostate, A, and pLNs, C, of the indicated mice. In the prostate, the percentage of DCs and indicated DC subsets among all CD45.2⁺ bone-marrow-derived cells (A) and expression of CCR7 (B) was determined for WT, *top*, and *Ccr7*^{-/-} mice. In the pLNs, the percentage of the various DC subsets among all TCRβ^{neg}CD19^{neg} F4/80^{neg}DX-5^{neg}Ter119^{neg} (lineage^{neg}) cells (C) and expression of CCR7 (D) was determined for WT, *top*, and *Ccr7*^{-/-} mice. mDC, migratory DC; rDC, resident DC. The mean ± SEM is shown for three mice per group. (E-G) MJ23tg Tregs develop efficiently in the thymus of *Ccr7*^{-/-} mice. CD11c-depleted MJ23tg *Rag1*^{-/-} CD45^{1/1} thymocytes were transferred via intrathymic injection into age matched WT or *Ccr7*^{-/-} (CD45^{2/2}) male hosts as described in Figure 31. Seven days post transfer, CD45.1⁺ MJ23tg Treg development was analyzed. (E) Representative flow cytometric analysis of Treg development for MJ23tg CD4⁺CD8^{neg} thymocytes. The percentage of Foxp3⁺CD25⁺ Treg cells among CD4⁺CD8^{neg} thymocytes is indicated. Summary plots of the frequency (F) and total number (G) of MJ23tg Foxp3⁺CD25⁺ Tregs in the thymus of the indicated genotypes is shown.

Conclusions

In this study, we identified the APCs that coordinate the thymic development and peripheral activation of a naturally occurring specificity of organ-specific Treg cells. Our results support a model in which DCs in the thymic medulla acquire promiscuously expressed prostate antigen from Aire⁺ mTECs, and promote the differentiation of MJ23 precursors into the Treg cell lineage. In the periphery, our results are consistent with a model in which DCs acquire antigen within the prostate, migrate to the draining lymph nodes via a CCR7-dependent process, and present antigen for recognition by MJ23 Treg cells, inducing TCR signaling and enrichment in the prostate-draining lymph nodes. Our data implicate DCs as key mediators of immune tolerance, choreographing the thymic development and peripheral homeostasis of organ-specific Treg cells. Moving forward, it will be important to determine the extent to which these principles apply to organ-specific Treg cells of diverse specificities, and the molecular and cellular properties that endow DCs with the capacity to coordinate Treg cell biology.

DISCUSSIONS, FUTURE DIRECTIONS AND CONCLUSIONS (78)ⁱ

Overview

TCR repertoires of tumor-associated Foxp3⁺ Tregs and CD4⁺ Tconv cells exhibit minimal overlap

We first sought to address the very broad question, “What are the fundamental biological principles which govern the development and function of tumor-associated Tregs?” We began by utilizing TRAMP prostate-tumor-bearing mice containing a fixed TCR β and performing high-throughput sequencing of the CDR3 regions of two commonly utilized TCR α chains (V α 2 and V α 8) for CD4⁺Foxp3⁺ Tregs and CD4⁺Foxp3^{neg} Tconv cells taken from prostate tumors and tumor-draining lymph nodes. By genetically fixing the β -chain of the TCR we were able to analyze and identify individual T cell clones on the TCR level while maintaining a high degree of T cell repertoire diversity. Utilizing sequencing data, we determined that the TCRs of Tregs and Tconvs infiltrating prostate tumors are distinct and exhibit minimal overlap, arguing that the peripheral conversion of Tconv cells to Tregs is most likely not a dominant mechanism in TRAMP prostate tumors. We also observed recurrent enrichment of certain Treg specificities within prostate tumors across many of the mice analyzed, with some TCRs representing a large proportion of all the Tregs recovered from that site.

ⁱ Some portions of this section are from a manuscript currently In Press at *Immunity* and expanded upon with permission under the license granted by Elsevier.

The prostate tumor-associated Treg specificity MJ23 is reactive to a prostate-specific antigen and is thymic derived

In order to further interrogate the fundamental biology of endogenous tumor-associated Treg cells, we generated TCRtg Rag-deficient mice expressing the fixed TCR β from our sequencing studies and one of the several TCR α sequences found recurrently on Tregs enriched in TRAMP prostate tumors. Two TCR α sequences were selected to generate TCRtg mice, the most highly enriched sequence among all V α 2⁺ Tregs, referred to as MJ23, and a sequence found recurrently represented within V α 8⁺ Tregs, referred to as RT83. Generation of the MJ23tg and RT83tg mice enabled us with tools to investigate critical aspects of the biology of these prototypical tumor-associated Treg specificities, including a determination of their developmental origin and antigenic specificity. We first evaluated the activation status, via the expression of CD44, and auto-infiltration of TCRtg T cells into various organs of MJ23tg Rag^{-/-} male or female mice. These analyses demonstrated that MJ23tg T cells become activated in the prostate-draining lymph nodes of male mice and auto-infiltrate the prostate of tumor-free mice, suggesting MJ23tg Tregs are reactive to a prostate-specific, tumor-independent antigen. In order to functionally evaluate the developmental origins of MJ23 Tregs, we next performed a series of low frequency BMCs utilizing bone marrow from MJ23tg Rag^{-/-} mice and adoptive transfer experiments where Foxp3^{neg} MJ23tg T cells were injected into tumor-free or TRAMP-prostate-tumor-bearing mice. While MJ23tg T cells developed into Foxp3⁺ Tregs with high efficiency in the thymus of both male and female BMCs, they failed to do so upon adoptive transfer regardless of sex or tumor status. These results indicate that MJ23 Tregs are primarily thymic derived and most likely not

a result of peripheral conversion at homeostatic steady state or in the context of a prostate tumor.

MJ23 Treg development is dependent on the transcription factor Aire

Having observed that MJ23tg T cells develop into Tregs in the thymus of male and female mice with similar efficiencies, we sought to determine the mechanism by which a prostate-organ specific antigen is expressed within the thymi of these mice, enabling their development into Tregs. Since the transcription factor Aire had been implicated in regulating the *in situ* expression of tissue-specific antigens within mTECs, we generated MJ23tg low frequency BMCs into *Aire*^{-/-} mice and determined that the development of MJ23tg Tregs is Aire-dependent. We then went on to perform additional analyses demonstrating that our second recurrently enriched tumor-associated Treg specificity RT83 was also primarily thymic derived and Aire-dependent.

Aire-dependent Treg development requires antigen presentation by thymic DCs

Finding that both the MJ23 and RT83 Treg specificities were primarily thymic derived and Aire-dependent, we sought to address critical gaps in our understanding for the mechanisms by which thymic Treg development occurs. More specifically we aimed to identify the antigen presenting cells that coordinate the presentation of tissue-specific, Aire-dependent antigens alongside the proper co-stimulatory signals to enable the selection of organ-specific Tregs in the thymus. We generated a variety of mixed BMCs in which a low frequency of MJ23tg bone marrow was engrafted alongside bone marrow cells from mice either lacking the ability to present antigen, *MHC-II*^{-/-}, or deficient for co-stimulatory ligands critical for Treg development, *CD80/CD86*^{-/-}, into

lethally irradiated wild type or *CD80/CD86*^{-/-} hosts. These experiments enabled us to determine that both antigen presentation and co-stimulatory signals by bone marrow derived APCs, and not the radio-resistant mTECs which express the tissue-specific antigens, are required for MJ23 Treg development. Furthermore, utilizing the intrathymic injection of MJ23tg thymocytes into *CD11c*^{Cre}*MHC-II*^{flox/flox} or *μMT/μMT* mice, we determined that MJ23tg Treg development is dependent on antigen presentation by thymic CD11c-expressing DCs and not B cells, respectively.

CD8α⁺ cDCs do not play a specialized role in thymic Treg development

To further delineate which CD11c⁺ APC population was responsible for the uptake and presentation of mTEC derived Aire-dependent antigens in the thymus we performed additional MJ23 thymocyte intrathymic injections into DT treated *BDCA2*^{DTR} mice, which lack pDCs, and *Batf3*^{-/-} mice, which lack CD8α⁺ cDCs. These experiments demonstrate that both pDCs and CD8α⁺ cDCs are independently dispensable for MJ23 Treg development. These findings were supported by complimentary MJ23tg BMC experiments in which all CD11c⁺ DCs, B cells, pDCs and CD8α⁺ cDCs were depleted or constitutively lost, which yielded similar results. Additionally, via intrathymic injection and BMC experiments, pDCs and CD8α⁺ cDCs were found to be dispensable for a second Aire-dependent Treg specificity, RT83. Finally, to significantly expand upon these findings we evaluated the impact and unique contribution of CD8α⁺ cDCs on the overall Treg TCR repertoire by performing high-throughput sequencing of all TCRα chains of thymic Tregs isolated from TCRβtg *Foxp3*^{GFP} mice either on a *Batf3*^{+/+} or

Batf3^{-/-} background. Sequencing studies determined that *Batf3*-deficiency has minimal impact on the thymic Treg repertoire, and thus argues that CD8 α ⁺ cDCs are dispensable for the development of a complete polyclonal thymic Treg repertoire and thus do not play a specialized role in the development of Aire-dependent Tregs.

***MJ23 enrichment and activation in the pLNs is dependent on prostate-derived antigen and lost in Ccr7*^{-/-} mice lacking mDCs**

Finally, seeing the utility of the MJ23tg model, as a well characterized and naturally derived Treg model system, we sought to better understand the mechanisms that regulate organ-specific Treg activation and homeostasis following development in the thymus. More specifically we aimed to determine the contribution of antigen presentation and APCs towards the anatomical localization and activation of prostate-specific MJ23 Tregs. Following observations that MJ23tg Tregs upregulate the TCR activation markers CD69 and Egr-2 specifically in the prostate-draining pLNs, we hypothesized that the anatomical enrichment of MJ23 Tregs in the pLN is due to continuous antigen presentation and TCR mediated activation. To directly test this hypothesis and determine the impact of antigen on MJ23tg Tregs, we castrated MJ23tg BMCs to induce prostate involution and hence significantly decrease prostate-antigen abundance in the pLNs. Additionally, prostate involution was rescued in half of the castrated mice via subcutaneous implantation of a testosterone pellet. Castration resulted in loss of MJ23tg Treg enrichment and activation in the pLN and in some mice the redistribution of MJ23tg Tregs to higher frequencies at other anatomical sites.

Testosterone supplementation resulted in the rapid regeneration of the prostate and rescued MJ23tg Treg enrichment and activation in the pLN.

Finding that continuous antigen presentation is critical for proper localization and activation of MJ23 Tregs, we next sought to identify the antigen presenting cells responsible for prostate-tissue presentation and thereby coordination of organ-specific Treg cell homeostasis. First, we selectively depleted CD11c⁺MHC-II⁺ DCs by generating low frequency MJ23tg BMCs containing a mixture of CD11c^{DTR} / MHC-II^{-/-} bone marrow and treating mice with DT. In complimentary experiments we also evaluated the impact of DC expansion on MJ23tg Treg anatomical enrichment by challenging MJ23 BMCs with a tumor cell line expressing Flt3L, B16-Flt3L. While DC depletion resulted in loss of a fraction of polyclonal Tregs in the spleen and lymph nodes and reduction in the frequency of MJ23 Tregs in the pLN, expansion of DCs did not further increase enrichment of MJ23 Treg cells at this anatomical site. These data suggest that DCs play a critical role in coordinating the enrichment of MJ23 Tregs in the pLN, however antigen abundance is likely limited as DC expansion failed to increase this enrichment. Finally, in order to evaluate the contribution of CCR7-dependent migratory DCs towards the enrichment of MJ23 Tregs, we performed intrathymic injections of MJ23tg thymocytes into wild type or *CCR7*^{-/-} mice. While MJ23tg Tregs developed in the thymus and could be recovered from the spleen and skin draining lymph nodes of both mice, MJ23tg Tregs failed to enrich or become activated in the pLNs of *CCR7*^{-/-} mice, suggesting that migratory DCs play a critical role in the presentation of organ-specific antigens to organ-specific Tregs in the draining lymph nodes.

Summary

Our findings suggest that Aire-dependent, organ-specific Tregs likely represent a significant proportion of Tregs found infiltrating prostate tumor lesions. These Tregs require the transfer of tissue-specific antigens from mTECs to DCs in the thymus to orchestrate their development, and upon exiting the thymus they require continuous cognate antigen presentation, likely by migratory DCs, to ensure proper anatomical localization and activation. These findings have wide reaching implications for our understanding of the mechanisms which enforce immune tolerance to tumors as well as various organs and specialized tissues at steady state. Additionally, the novel models and approaches created throughout this study, and the conclusions reached thus far, lead to clear future paths of inquiry which were not previously possible.

Developmental origins of tumor-associated Tregs and why targeting pTreg conversion may fail to provide clinical benefit

Clinical studies have demonstrated a negative correlation between the density of Treg infiltrates and disease outcomes for a variety of solid human tumors (36). In light of the role Tregs play in modulating immune responses to self, foreign and tumor-associated antigens, this may suggest that Tregs play a functional role in modulating tumor progression and/or dampening the efficacy of various immunotherapeutic approaches. Treg-depleting agents and various experimental approaches utilized to disrupt or deplete Tregs in mouse models of cancer have demonstrated improved efficacy for immunotherapeutic regimes and radiotherapies in the absence of Tregs (42, 46). In one such study, transient Treg depletion alone via DT treatment of *Foxp3^{DTR}*

mice was shown to slow tumor growth for a polyoma middle-T antigen-driven breast cancer model, and improved the efficacy of ionizing radiation when treating orthotopically transplanted cancer cells (46). Such studies have sparked significant interest in the manipulation of Tregs in cancer patients, however progress has been hindered by a limited understanding for the basic biology of tumor-associated Tregs and hence an inability to selectively target these cells without destabilizing Tregs systemically and triggering wide-spread, off-target autoimmunity.

Evidence for the conversion of tumor-reactive CD4⁺ Tconv cells into pTregs

We sought to better understand the developmental origins for Tregs found infiltrating tumor lesions, as it is largely unknown whether these cells primarily consist of thymic-derived tTregs, specific for self antigens, peripherally induced pTregs, generated de novo within the tumor environment, or a mixture of both. It had been previously hypothesized that due to the immune suppressive environment of some tumors, containing increased levels of TGF- β , immune suppressive cells and other factors, these lesions may drive the differentiation of CD4⁺ Tconv cells reactive to tumor-associated antigens into pTregs. If well supported, this paradigm would suggest that blockade of mechanisms leading to the induction of pTregs from tumor-reactive Tconvs would be a valuable means of disrupting the development of tumor-associated Tregs and potentially boosting efficacy of cytotoxic and immunotherapeutic treatments. However, findings supporting this model primarily come from highly artificial *in vitro* studies (63, 64), studies utilizing the expression of model antigens coupled with the adoptive transfer of model-antigen specific TCRtg T cells (32, 66), or TCR sequencing

studies utilizing TCR^{mini} mice which exhibit a prohibitively limited TCR repertoire of only several hundred unique TCRs (126).

Endogenous prostate-tumor-associated Tregs are primarily thymic derived

To address the question of tumor-associated Treg developmental origin in a spontaneous prostate cancer model system for naturally derived T cell specificities, we performed deep sequencing of Foxp3⁺CD4⁺ Tregs and Foxp3^{neg}CD4⁺ Tconvs taken from prostate tumors of male TCRβtg Foxp3^{GFP} TRAMP mice. By only fixing the TCRβ-chain and allowing the pairing of a full range of TCRα-chains we were able to maintain a high degree of TCR repertoire diversity. When focusing sequencing on the CDR3-region of one of the most commonly utilized TCRα-chains (Vα2/TRAV14) we were able to achieve 1,000-2,000 unique reads per sample, orders of magnitude higher than previous studies utilizing TCR^{mini} mice (126). From our studies utilizing the Morisita-Horn (MH) similarity index, we demonstrated that within a spontaneous murine prostate tumor the Treg and Tconv Vα2⁺ TCR repertoires are largely distinct and non-overlapping (Fig. 3). In similar TCR sequencing studies evaluating the TCR repertoire of carcinogen, MCA, induced sarcoma T cell infiltrates also found that Treg and CD4⁺ Tconv cell repertoires are distinct and non-overlapping (127). If Tconv clones specific for tumor-associated antigens differentiated into pTregs within the tumor microenvironment, then it is likely that these TCRs would be found in both Tconv and Treg subsets. Thus, these data demonstrate that for two separate tumor models, one genetically-driven and one carcinogen-induced, tumor infiltrating Treg and Tconv TCR sequences are non-overlapping and would suggest that the conversion of Tconv to

pTregs is not a high-frequency event for endogenous T cell specificities found in tumors. In support of these findings, we transgenically expressed two independent TCRs representing highly prevalent and recurrently enriched Treg specificities found in TRAMP prostate tumors (MJ23 and RT83), and found that T cells bearing these TCRs develop into Tregs in the thymus with high efficiency (Fig. 10) but fail to develop in the prostate-draining lymph nodes even in tumor-bearing mice (Fig. 15). Combined, these data support a model in which thymic derived tTregs are actively recruited and/or expanded into prostate tumor lesions and represent the majority of Tregs present at this site.

Expanding our understanding for the developmental origins of endogenous Treg specificities in autochthonous murine models of cancer

Since these analyzes were focused on the sequencing of one TCR α -chain (V α 2/TRAV14), due to the technical limitations of murine TCR sequencing at that time, in future analyzes we plan to expand sequencing of the TCR repertoire of Tregs and Tconv from TRAMP prostate tumors to a complete analysis of all TCR α -chains using the iRepertoire platform. Sequencing results from this expanded approach could be coupled with the generation of TCR retrogenics in order to evaluate the developmental origin of 10s to 100s of identified TCRs. These findings do not exclude a potential contribution of pTregs to any neoplastic lesion, and thus it will be critical to perform similar sequencing studies for T cells infiltrating genetically-driven, autochthonous tumors from other anatomical sites, such as breast, the gut or the lung, or those induced by a variety of oncogenic insults. Since pTregs have been shown to play critical roles in

modulating immune responses at mucosal sites that interface with the external environment (33), such as the lung and the colon, the tumor microenvironments or established immunomodulatory mechanisms at these sites may be permissive for the generation of new, or recruitment of pre-existing, pTregs. Alongside the anatomical context in which the neoplasm develops, the stage of tumor development, oncogenic context in which they develop (e.g. carcinogen, genetic or virally induced) and the oncogenes expressed by a tumor may all impact the contribution of tTregs versus pTregs, and thus warrant further inquiry.

Antigenic specificities of tumor-associated Tregs

Treg developmental origin and antigenic specificity are highly interrelated

Antigen recognition via the TCR influences numerous critical aspects of Treg cell biology, including their development, anatomical distribution, co-localization with cellular interaction partners and ultimately their function. Thus, by understanding the nature of the antigens recognized by Tregs and tumor-associated Tregs, we can gain valuable insights into the fundamental biology of these cells. Mechanistically, one could infer insights about antigenic specificity from the developmental origin of a Treg. TCR recognition of cognate antigen by developing thymocytes in the presence of IL-2 is a critical determining factor in the development of thymic derived tTregs (19, 29). Since tTregs are thought to primarily recognize self antigens (19, 26, 128), then one could infer that antigen recognized by tTregs must therefore be presented in the thymus for recognition during T cell development. On the other hand, pTregs develop from Tconv

cell precursors at extrathymic sites in a process that is augmented by exposure to TGF- β and retinoic acid (32). Mechanistically pTregs could recognize a similar array of self antigens as tTregs, however their extrathymic induction would also infer the possibility that they could also recognize foreign antigens such as those found on viruses, bacteria (pathogenic or commensal) and even tumor-associated antigens (including aberrantly expressed self antigens or unique tumor neoantigens). However, since no definitive markers are currently available to delineate nTreg from pTreg, the developmental origins of endogenous tumor-associated Tregs have been difficult to assess. Thus, in the absence of such information, elucidating the nature of the antigens recognized by tumor-associated Tregs could be helpful for understanding various fundamental aspects of the biology of these cells. If tumor-associated Tregs are found to recognize tumor-associated or tumor-specific antigens, these antigens are unlikely to be presented in the thymus to drive tTreg development, and therefore such Tregs would likely be of extrathymic origin (pTregs). Additionally, understanding the antigenic specificities of tumor-associated Tregs would be extremely useful when rationally designing therapeutic cancer vaccines in order to better avoid expanding tumor-associated Treg populations.

Tumor infiltrating Tregs and Tconv cells likely recognize distinct sets of antigens

As discussed above, in order to better delineate the developmental origins of endogenous tumor-associated Treg populations we performed TCR sequencing on Tregs and Tconvs taken from TRAMP murine prostate tumors. TCR repertoires from Tregs and Tconv were found to be largely distinct (Fig. 3), supporting the idea that

pTreg development was not likely to be a high frequency event in prostate tumors and also suggesting that tumor-infiltrating Tregs and Tconvs recognize distinct sets of antigens. Two previous studies support these findings as they also found the TCRs expressed by Tregs and Tconvs isolated from transplantable (129) and chemically-induced murine tumors (127) to be distinct and non-overlapping.

MJ23 Tregs are reactive to a prostate-specific, tumor-independent antigen

From our sequencing studies we identified two recurrently enriched Treg specificities, MJ23 and RT83, and found that they were primarily thymic derived. Insights into the antigenic specificity of MJ23 Tregs were first gained by evaluating the activation status and infiltration of T cells within MJ23tg *Rag1*^{-/-} male or female mice (Fig. 6). We observed that MJ23tg T cells upregulate CD44 in the pLN of male mice and infiltrate the prostate of tumor-free male mice. In MJ23 BMC experiments, we also observed that MJ23tg Tregs specifically enrich in the pLNs of male mice (regardless of tumor status) (Fig. 10) and upregulate TCR activation markers CD69 and Egr2 (Fig. 28). Furthermore, enrichment and activation of MJ23tg Tregs is lost in BMC mice following castration (Fig. 28). Combined these data strongly support the conclusion that MJ23 Tregs are reactive to a prostate-associated, tumor-independent self antigen. We go further to show MJ23tg Treg development is dependent on the transcription factor Aire, thereby providing a mechanism by which the prostate-specific antigen is expressed in the thymus to enable development of the organ-specific Treg specificity.

Identification of the MJ23 antigen could provide valuable tools for future inquiry

While the MJ23 Treg antigen has been narrowed down to a prostate-specific and Aire-dependent antigen, it will be important in future experiments to identify the protein containing the antigen and the exact peptide sequence. To date, no naturally derived Treg antigen has been identified and thus identification of the MJ23 antigen would allow us to better understand the precise nature of the antigens recognized by tTregs in general and more specifically tumor-associated Tregs. Additionally, elucidating the cognate MJ23 Treg antigen would allow for the creation of peptide/MHC multimers and subsequently the identification of endogenous T cells bearing the MJ23 Treg specificity. It would also open avenues of further inquiry utilizing various biochemical, *in vitro* and *in vivo* approaches to evaluate Treg TCR-antigen-MHC-II interactions to determine the affinity of such interactions, and, for the first time, the biochemical structure of a natural derived Treg TCR in complex with MHC-II bearing its cognate antigen.

Finally, the affinity selection model for Treg development in the thymus (28) has been a long standing paradigm and stipulates that a relatively tight range of affinities towards self antigens, that fall somewhere between the highest affinities that would lead to negative selection and lower affinities that lead to positive selection, are primarily responsible for the selection of Tregs. Data providing indirect evidence for the TCR affinity model of thymic Treg selection primarily come from experiments that either genetically manipulated TCR signal strength via a variety of downstream signaling factors (130, 131) or utilized non-Treg derived TCR transgenics with varying affinities for a foreign model antigen (132). However, by identifying the exact peptide sequence responsible for MJ23 Treg development we would be able to manipulate TCR affinity via

mutation of the MJ23 TCR and its cognate peptide antigen in order to directly test the affinity selection hypothesis utilizing a naturally derived thymic Treg specificity.

Identifying the antigenic specificities of other tumor-associated Treg clonotypes in mice and humans

To expand upon our findings, it will be critical to determine the antigenic specificity of additional tumor-associated Treg populations. As discussed above, deep sequencing of Tregs and Tconvs taken from a variety of tumor microenvironmental contexts will be important to gain insights towards the developmental origins of these cells. Such studies would also provide a catalog of additional naturally derived Treg TCRs to be retrogenically expressed in order to evaluate their antigenic specificities utilizing *in vitro* and *in vivo* approaches.

It will also be important to evaluate the TCR overlap of Tregs and Tconvs taken from human cancer patients and to delineate their antigenic specificities. It would be useful to evaluate overlap between T cell subsets in cells taken from primary human tumors and to assess the overlap of sequences between the same T cell subsets in comparison to cells recovered from metastatic lesions. Do metastases recruit similar Treg and Tconv specificities as the parental primary tumor, or are they distinct, recognizing distinct sets of antigens? Several studies in human cancer patients have been conducted in an attempt to address such questions. Two previous studies utilized *in vitro* culture-based assays to detect tumor-associated antigen reactive Tregs in the peripheral blood of melanoma patients (133, 134). While a proportion of circulating Tregs were found to be reactive to isolated tumor-associated antigens, it was unclear from these studies whether the Tregs evaluated were derived from endogenous Tregs

or merely originated from the preliminary *in vitro* expansion required for such analyzes. In future studies it will be critical to utilize tumor-associated peptide antigens bound to MHC multimers in order to detect tumor-reactive Tregs *ex vivo* from patient blood and tumor samples. Additionally, by performing single cell sequencing of individual Treg clones and retrovirally transducing Treg derived TCRs into immortalized cell lines, reactivity to panels of tumor-associated antigens could be evaluated.

The contribution of Aire to organ specific immune tolerance

Mirroring peripheral self through the presentation of TRA's in the thymus

During T cell development and the establishment of central tolerance in the thymus, the immune system faces a substantial logistical problem. How can thymic processes expose developing thymocytes to self antigens that are not normally expressed by the cellular subsets present in the thymus, such as tissue restricted antigens (TRAs) that are selectively expressed in the peripheral organs? One potential solution to this dilemma would be to facilitate the transportation of TRAs from the periphery into the thymus. In support of this, studies in parabiotic mice have demonstrated that a proportion of thymic DCs originate extrathymically and migrate to the thymus (135), while other studies demonstrated that antigen-bearing circulating DCs can be recruited to the thymus and mediate the deletion of antigen-specific thymocytes (136). A second potential solution would be to express such TRAs *in situ* via specialized transcriptional mechanisms within the thymus. Aire (96), and the recently identified Fezf2 (137), are transcriptional regulators expressed by mTECs that promote the

expression of a variety of transcripts, including TRAs and various antigen processing and presentation machinery. Loss-of-function mutations in AIRE are associated with an autoimmune disease referred to as APECED/APS-1 in humans (138) and results in T cell autoimmune infiltrates into a variety of organs, depending on background, in mice (96). Similar to Aire, loss of Fezf2 in mTECs leads to autoimmune infiltration of T cells to a variety of organs, however the organs affected are distinct from those of *Aire*^{-/-} mice on the same B6 background (137). While conceptually Aire could contribute the establishment of immune tolerance by driving the deletion of thymocytes reactive to TRAs and/or promoting the differentiation of such thymocytes into the Treg lineage, conclusions drawn by the authors of previous studies had favored an exclusive role for Aire in negative selection (139).

The impact of Aire on T cell development in the thymus

In an effort to determine whether Aire enforces immune tolerance via deletional tolerance or Treg development, one study assessed development of autoimmunity following the grafting of thymic from *Aire*^{+/+} and *Aire*^{-/-} mice into athymic hosts (95). These data revealed that thymic grafts from *Aire*^{-/-} mice induced organ-specific autoimmunity to a similar extent as that observed in *Aire*^{-/-} mice, and when both *Aire*^{+/+} and *Aire*^{-/-} thymi were co-grafted at equal ratios into the same host they still developed autoimmunity. The authors reasoned that if the primary defect of an *Aire*^{-/-} thymus is the failure to select TRA reactive Treg specificities, then the provision of Tregs selected on an *Aire*^{+/+} thymic stroma should rescue autoimmunity in a dominant fashion. Since co-engraftment of *Aire*^{+/+} thymi failed to rescue autoimmunity, the authors concluded that

Aire must function primarily to impart recessive, deletional tolerance. However, in the same set of experiments when four *Aire*^{+/+} thymi were co-grafted with one *Aire*^{-/-} thymus autoimmunity was rescued, suggesting that the autoimmune effects of an *Aire*^{-/-} thymi can be overcome by “outnumbering” the thymic output of an *Aire*^{-/-} thymus. The idea that Aire enforces immune tolerance primarily through negative selection was further propagated by the observation that compared to *Aire*^{+/+} mice, *Aire*^{-/-} mice only exhibit a partial loss of Treg frequency in the thymus and have comparable Treg frequencies in the spleen and lymph nodes (95). Additionally, in TCR sequencing studies utilizing TCR^{mini} mice the authors concluded that the Treg repertoires of *Aire*^{-/-} or *Aire*^{+/+} mice have a high degree of similarity and that “the global Treg repertoire are not controlled by Aire-dependent TSAs” (140). Despite the extremely limited TCR repertoire diversity exhibited by the TCR^{mini} Tregs analyzed in this study, with fewer than 500 CDR3 sequence reads per experimental group, the data clearly show a loss of several TCR sequences, 11 out of 29 recurrent sequences, in the Treg repertoire of *Aire*^{-/-} mice. Thus a variety of caveats warranted further investigation into the relevance of Aire in the selection of TRA-reactive, thymic-derived Tregs.

Aire-dependent development of naturally derived Treg specificities

Intrigued by our results demonstrating that in BMC experiments prostate-specific MJ23tg Tregs developed in the thymus of both male and female mice, we sought to test the hypothesis that Aire drives the expression of the prostate-tissue restricted MJ23 antigen by mTECs in the thymus, thereby promoting the development of MJ23 Tregs regardless of sex. Indeed, in BMC mice (Fig. 16) and intra thymic injection experiments

(Fig. 21) where MJ23tg precursors are seeded at low clonal frequencies, MJ23 Treg development was dependent on Aire. Importantly, the same effect was observed for a second naturally occurring and tumor-associated Treg specificity, RT83 (Fig. 16 and Fig. 25). Additionally, similar to previous studies (95) we consistently observed a partial loss of Treg frequency among polyclonal cells in the thymi of *Aire*^{-/-} mice (Fig. 16 and Fig. 21). Thus for the first time, we provided a functional demonstration that Aire is essential for the thymic development of some but not all Treg specificities and in particular Aire was required for the development of two specificities that are highly relevant to prostate tumors. In support of our findings, recent TCR sequencing studies by Perry et al demonstrate the Aire-deficiency results in the loss of a significant proportion of the thymic Treg repertoire (141). These data suggest that Aire enforces immune tolerance in part by promoting Treg development, and since Aire-dependent transcripts encode for a variety of TRAs (96), it would imply that Aire promotes the development of TRA- and organ-specific Tregs that may function to prevent organ-specific autoimmunity in the periphery. In agreement with the idea that Aire plays a critical role in the development of non-redundant Treg specificities, recent findings demonstrate that on the NOD background Aire is required for the development of a distinct set of Tregs within the perinatal period that play a critical role in the suppression of the multi-organ autoimmune manifestations associated with Aire deficiency (141).

Is there a role for Aire-dependent, organ-specific Tregs in modulating tumor progression and antitumor immunity?

Since both of the prostate-tumor-associated Tregs analyzed in our studies were found to be Aire-dependent, it is tempting to speculate that Aire-dependent, organ-specific tTregs constitute a large proportion of tumor-infiltrating Tregs. However, as discussed above, in future studies we will expand sequencing efforts to include a complete analysis of the CDR3-region of all TCR- α chains and evaluate the developmental origins and Aire-dependence of newly identified Treg specificities found recurrently enriched in TRAMP prostate tumors via the retrogenic expression of such TCRs. By performing such experiments we can functionally determine the relative contribution of Aire-dependent Tregs to the tumor-associated Treg pool. These analyzes could then be complemented by T cell reconstitution experiments in which Tregs taken from either *Aire*^{-/-} mice, lacking Aire-dependent Tregs, or *Aire*^{+/+} mice, containing both Aire-dependent and Aire-independent specificities, are co-transferred along with CD4⁺ and CD8⁺ Tconv into T cell deficient hosts. Reconstituted mice could then be challenged with various transplantable tumor models or reconstitution could be performed into genetically-driven mouse models of cancer.

A surprising conclusion: Tregs go “rogue” in the absence of Aire

In light of our findings and the studies discussed above, it is likely that Aire-dependent processes can promote both clonal deletion and Treg development for thymocytes reactive to TRAs. It would also suggest that the autoimmunity associated with Aire deficiency may be a result of either autoimmune attack by TRA-reactive T cells

which escape negative selection or failed Treg development for distinct TRA-reactive specificities resulting in a lack of critical organ-specific Tregs within the Treg repertoire, or both. In unpublished work by our group (142), we sought to delineate the functional contributions of both mechanisms towards Aire-dependent immune tolerance. By utilizing a variety transfer experiments in which Tregs from *Aire*^{-/-} or *Aire*^{+/+} mice were transferred alongside CD4⁺ Tconv cells from *Aire*^{-/-} or *Aire*^{+/+} mice we aimed to address whether Aire-dependent Tregs serve non-redundant roles in comparison to their Aire-independent Treg counterparts. In summary, we determined that Tregs taken from *Aire*^{-/-} mice, lacking Aire-dependent Treg specificities, were equally capable of suppressing autoimmune infiltration of the prostate as Tregs taken from *Aire*^{+/+} mice. Additionally, we found that regardless of Treg donor origin, Tregs failed to suppress prostate auto-infiltration upon co-transfer with Tconv cells from *Aire*^{-/-} mice. These data suggested that the autoimmune manifestation observed in the absence of Aire functionally map to the Tconv cell compartment, raising the question of whether these cells arose due to failed negative selection. To address this critical question we then performed TCR repertoire analyzes, as described above, in which the CDR3-region of all TCR- α chains were sequenced for Tregs and CD4⁺ Tconv cells taken from pooled spleen and lymph nodes or the prostate of either *Aire*^{-/-} or *Aire*^{+/+} mice. Upon comparison of TCR sequences found in each TCR catalog, we uncovered an unexpected third possibility to explain the emergence of multi-organ autoimmunity in *Aire*^{-/-} mice. If Aire mediated immune tolerance was primarily enforced by the negative selection of TRA-specific Tconv cells, one would anticipate the emergence of new TCR sequences in the absence of Aire and that Tconv cells expressing said TCRs would make up the bulk of the specificities found

infiltrating prostate lesions. While we do find the emergence of new Tconv cells specificities in the spleen and lymph nodes in the absence of Aire, we also find that the majority of the newly arising Tconv TCR sequences are found enriched in the Treg compartment of *Aire*^{+/+} mice. Furthermore, we find that the predominant Tconv cell clonotypes found infiltrating the prostate of *Aire*^{-/-} mice are also preferentially expressed by Tregs in *Aire*^{+/+} mice. These data support a novel model for our understanding of how Aire enforces immune tolerance in which self-reactive thymocytes, likely representing specificities with the highest pathogenic potential, are selectively purged from the Tconv cell repertoire by diverting them into the Treg lineage. Failure to select such autoreactive specificities into the Treg lineage results in highly pathogenic Tconv, or “Trogues”, which can no longer be suppressed by the Tregs present in *Aire*^{-/-} or *Aire*^{+/+} mice, at least at the physiological frequencies utilized in our experiments. These findings bring clarity to the ambiguous findings of thymic co-grafting experiments by Anderson et al, discussed above, in which the autoimmune effects of an *Aire*^{-/-} thymus can be overcome by addition of a larger proportion of *Aire*^{-/-} thymi (95). Thus, the predominance of Aire-dependent, organ specific Tregs in comparison to their Trogue counterparts may be enough to overcome their pathogenic potential and suppress multi-organ autoimmune infiltrations.

While these data demonstrate that Trogue specificities make up the majority of the Tconv cell auto-infiltrates in *Aire*^{-/-} prostate lesions, a minority of Tconv cell specificities were also shown to be newly arising TCRs, not detected in *Aire*^{+/+} mice, that were likely a result of failed negative selection in *Aire*^{-/-} mice. Thus, in future experiments it will first be important to confirm the developmental fate of individual

Troque and deletional escapee specificities via retrogenic expression of identified TCRs followed by intra thymic transfer into *Aire*^{-/-} or *Aire*^{+/+} mice. Next to directly evaluate the pathogenic potential of Trogues versus deletional escapees it will be important to provide functional evidence demonstrating the ability of retrogenically expressed Troque and deletional escapee TCRs to induce autoimmunity *in vivo*. Additionally, can we find evidence for the emergence of Trogues in Aire-deficient humans (APECED patients)? While challenging, it may be possible to perform TCR sequencing of Tregs and Tconv cells taken from APECED patients versus healthy HLA-matched donor controls.

Interesting, we also found newly arising Treg specificities in pooled spleen and lymph nodes of *Aire*^{-/-} mice which were not detected in *Aire*^{+/+} mice. Do these represent newly arising tTregs, Tregs expanded in the periphery that compensate for the lack of Aire-dependent specificities or are they induced pTregs generated in response to the multi-organ autoimmunity occurring in the absence of Aire?

Fezf2: a new player in the presentation of “peripheral self” in the thymus

What are the primary immune tolerance mechanisms at play for the newly identified autoimmune regulator *Fezf2* (137)? While *Fezf2*-deficient thymi exhibit a decrease in Treg frequency (137), it will be critical to perform similar adoptive transfer as those described above for *Aire*^{-/-} mice, in order to delineate which T cell population autoimmunity functionally maps to. Do the aforementioned “Troque” specificities also emerge from *Fezf2* deficient thymi? Do they represent a significant portion of the autoimmune infiltrates observed in these mice? TCR sequencing studies would be useful to address such questions, to determine the extent to which *Fezf2* deficiency

impacts the CD4⁺ Treg, CD4⁺ Tconv and CD8⁺ Tconv repertoires, and to elucidate the nature of the T cells infiltrating the organs impacted by loss of Fezf2 in the thymus.

Antigen presentation and Treg development in the thymus

A variety of environmental signals have been attributed to the selection of Treg in the thymus. First, Treg development is dependent on self antigen presentation in the context of MHC-II and occurs in a TCR-instructive process in which distinct TCR specificities facilitate efficient differentiation into the Treg lineage (93). In addition, proper co-stimulatory signaling via CD80/86 (B7-1/B7-2) on thymic APCs has also been shown to play a critical role in tTreg development (28). Following TCR-mediated signals and the upregulation of the IL-2 high affinity receptor, CD25, the availability IL-2, as well as other cytokines, have been shown to act as a secondary signal to facilitate the selection of tTregs (29). While these mechanisms have been well documented as broad critical steps required for thymic Treg development, it is still unclear why and how some auto-reactive thymocytes become Tregs while others are negatively selected. The affinity selection model (28) provides one potential explanation for why one autoreactive specificity would be deleted versus selected into the Treg lineage, however the precise microenvironmental context in which a self-reactive specificity receives stimulatory signals may also play a distinct role in this critical immune tolerance mechanism. Perhaps the micro-anatomical location within the thymus where a developing thymocyte receives antigenic signals is important, such as the cortex versus the medulla, or by whom they receive such signals, such as an mTEC versus a thymic DC.

Various APC subsets play distinct roles in the generation of a complete Treg repertoire

In regards to the contribution of APCs towards the development of tTregs, the thymus contains a diverse array of MHC-II-expressing APCs, including TECs, B cells, macrophages, and multiple DC subsets (77, 117). Both mTECs and CD11c⁺ DCs have been shown to be required to establish a complete Treg pool, suggesting that these presentation pathways collaborate to form a complete Treg repertoire (69, 70, 141). While macrophages and B cells express intermediate levels of MHC-II in the thymus, they express low levels of CD80 and CD86 (72) and have not been shown to appreciably impact Treg development. In a reaggregate thymic organ culture system supplemented with exogenous OVA peptide, thymic DCs were shown to facilitate Treg development of OT-II^{tg} thymocytes with high efficiency, while thymic B cells and macrophages did not (72). In agreement with these findings, while thymic B cells have been implicated in the negative selection of some self-reactive specificities, μ MT/ μ MT mice, which lack B cells systemically, do not exhibit a paucity of Tregs in the thymus or periphery (116) and (Fig. 21).

Presentation of Aire-dependent antigens in the thymus

In regards to the development of Aire-dependent Tregs, two models had been proposed to describe the presentation of TRAs encoded by Aire-dependent transcripts (69). In the first model, Aire-expressing mTECs function autonomously, directly presenting Aire-dependent antigens to thymocytes. In the second model, antigens expressed by mTECs are transferred to neighboring DCs, which then present acquired

antigen to developing thymocytes. Here we demonstrate that Aire-dependent MJ23 Treg development requires both MHC-II and CD80/86 on bone marrow derived cells, while CD80/86 are dispensable on the radioresistant TEC compartment (Fig. 19 and Fig. 20). Thus our data support the second model in which mTEC derived antigens must be transferred to a bone marrow derived APC in order to provide the proper stimulatory signals to orchestrate MJ23 Treg development. Additionally, in support of this model, by performing intrathymic injections of MJ23 thymocytes into $CD11c^{cre}MHC-II^{flox/flox}$ mice we demonstrate the MJ23 Treg development is dependent on antigen presentation by $CD11c^+$ DCs (Fig. 21 and Fig. 22). While multiple DC subsets are present in the thymus, including pDCs, $CD8\alpha^+$ cDCs and $Sirp\alpha^+$ cDCs, we go on to demonstrate that both pDCs and $CD8\alpha^+$ cDCs are dispensable for MJ23 Treg development (Fig. 23 and Fig. 24). Furthermore, pDCs and $CD8\alpha^+$ cDCs were shown to be dispensable for the development of a second Aire-dependent Treg specificity, RT83 (Fig. 25). Finally, we show that *in vitro*, both $Sirp\alpha^+$ and $CD8\alpha^+$ cDCs are capable of inducing Foxp3 and CD69 upregulation by MJ23tg thymocytes (Fig. 27), suggesting that both subsets are capable of acquiring antigen from Aire-expressing mTECs, presenting the antigen via MHC-II, and promoting the differentiation of MJ23tg thymocytes into the Treg lineage.

Cumulatively, our results are consistent with the idea that there is considerable functional redundancy amongst thymic DC subsets in the capacity to promote the thymic development of Treg cells reactive to Aire-dependent antigens. These findings are consistent with previous work demonstrating that both $Sirp\alpha^+$ and $CD8\alpha^+$ cDCs are capable of acquiring antigen from mTECs *in vivo* (71, 113), paired with *in vitro* studies

showing that both Sirp α^+ and CD8 α^+ cDC subsets are capable of supporting Treg development of non-Treg TCR transgenics upon provision of exogenous model antigens (72, 143).

Specialized or redundant: conflicting results for the role of CD8 α^+ cDCs in thymic Treg development

Our findings that Batf3-dependent CD8 α^+ cDCs are largely dispensable for Aire-dependent Treg development are incongruous with the conclusions of Perry and colleagues, who suggested that CD8 α^+ cDCs play a specialized role in coordinating the development of Aire-dependent Tregs (141). In that study, the authors demonstrated that the thymic development of four Aire-dependent Treg clones was abolished in *Batf3*^{-/-} hosts. However, these four clones differ by a single amino acid substitution, suggesting that they may be reactive to a single antigen. In contrast, we present data demonstrating that Batf3-dependent CD8 α^+ cDCs are dispensable for the development of two well-characterized Aire-dependent Treg clones.

In addition, to bring further clarity to this discrepancy, we performed deep TCR sequence analysis of polyclonal Tregs in the thymus of *Batf3*^{+/+} versus *Batf3*^{-/-} mice. We found that Batf3 deficiency had negligible impact on the >8,000 recurrent Treg TCR clonotypes identified in the analysis (Fig. 26), indicating that CD8 α^+ cDCs are dispensable for the formation of a complete Treg repertoire. Additionally, utilizing currently unpublished data sets (142) of Treg TCR sequence catalogs taken from pooled spleen and lymph nodes of wild type, *Batf3*^{-/-} and *Aire*^{-/-} mice, we were able to detect substantial alterations in the Treg repertoires of *Batf3*^{-/-} and *Aire*^{-/-} mice as

compared to wild type (Fig. 33, A and B). These included the identification of Treg TCR sequences significantly underrepresented in either *Batf3*^{-/-} and *Aire*^{-/-} mice, suggesting that these Treg specificities may be Batf3-dependent and Aire-dependent, respectively. In support of our conclusion that CD8 α ⁺ cDCs do not play a specialized role in Aire-dependent Treg development, we find that the vast majority of putative Batf3-dependent Treg specificities are equally represented in the catalogs of wild type and *Aire*^{-/-} mice (Fig. 33C). Reciprocally, we find that the vast majority of putative Aire-dependent specificities are equally represented in wild type and *Batf3*^{-/-} catalogs (Fig. 33D). Additionally, if CD8 α ⁺ cDCs did play a specialized role in Aire-dependent Treg development, one would predict that the Treg repertoire's of *Batf3*^{-/-} and *Aire*^{-/-} mice would exhibit a high degree of similarity. However, upon comparison of Treg TCRs from *Batf3*^{-/-} and *Aire*^{-/-} catalogs, we find a high degree of dissimilarity (Fig. 33E). Finally, our results are consistent with recent findings of Yang et al., who observed a paucity of thymic CD8 α ⁺ cDCs in the perinatal period, an age that is thought to be critical for the development of Aire-dependent Treg cells (144).

In sum, and in the absence of an experimental means to selectively manipulate Sirp α ⁺ cDCs, our results are consistent with the idea that there is likely considerable functional redundancy amongst thymic DC subsets in their capacity to promote the thymic development of Treg cells reactive to Aire-dependent antigens.

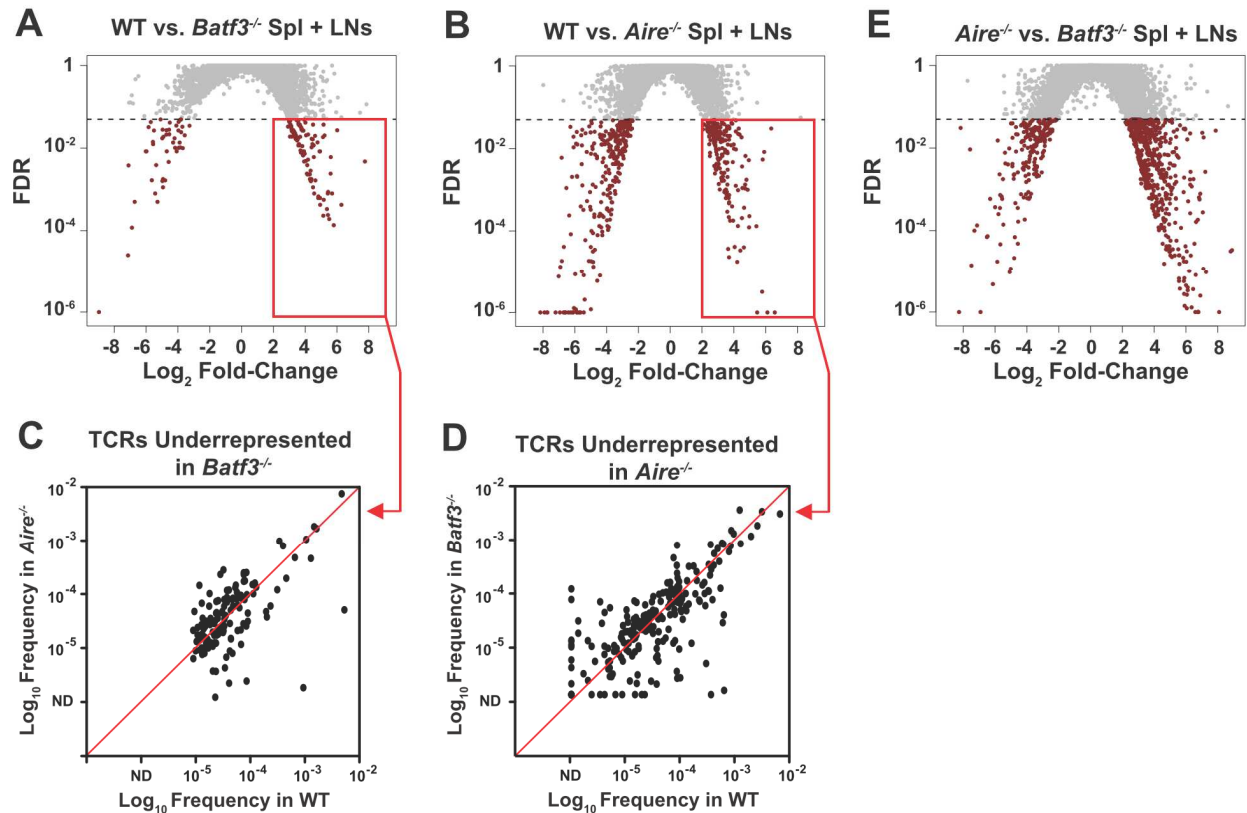


Figure 33: *Batf3*-deficiency has a minimal impact on the Aire-dependent Treg repertoire. CD4⁺CD8^{neg}Foxp3⁺ Treg cells were purified by fluorescence-activated cell sorting (FACS) from 9-week-old TCRβtg *Foxp3*^{GFP} males on a wild-type (WT), *Batf3*^{-/-} or *Aire*^{-/-} background, and subjected to complete TCRα sequencing and analysis. The impact of *Batf3*- and *Aire*-deficiency on the Treg TCR repertoire was analyzed via complete TCRα sequencing using the iRepertoire platform. (**A**, **B**, and **E**) For the TCRα chain sequences, volcano plots of false discovery rate (FDR) versus differential TCR representation (log₂ fold-change) for the indicated comparisons are shown. Comparisons were made using EdgeR and were adjusted for multiple comparisons. Red dots denote TCRs with fold-change > 4 and FDR < 0.05. Data points with FDR < 10⁻⁶ are plotted at 10⁻⁶. Horizontal dashed lines indicate FDR cutoff. *N* = 9 for WT Spl+LNs, *N* = 5 for *Batf3*^{-/-} Spl+LNs, and *N* = 5 for *Aire*^{-/-} Spl+LNs. (**C** and **D**) For Treg TCR clonotypes that are recurrently underrepresented in *Batf3*^{-/-} mice, **C**, or underrepresented in *Aire*^{-/-} mice, **D**, relative to WT (denoted in red in right arms of **A** and **B**, respectively), the mean frequencies of these TCRs within the indicated catalogs are plotted. The red diagonal represents equal representation within the compared catalogs.

The rationale for a specialized role for Sirp α ⁺ cDCs in thymic Treg development

While the results discussed here suggest that there may be functional redundancy in the capacity of thymic DC subsets to coordinate the development of Aire-dependent Treg specificities, it remains formally possible that Sirp α ⁺ cDCs play a unique role in this process. In this regard, during the course of our studies we noted three observations regarding *Batf3*^{-/-} mice. First, *Batf3*^{-/-} mice harbored increased numbers of thymic Sirp α ⁺ cDCs (Fig. 23), perhaps due to compensatory expansion in the absence of CD8 α ⁺ cDCs or lineage diversion in the absence of *Batf3* (145). Second, the thymi of *Batf3*^{-/-} mice also harbored increased percentages and absolute numbers of polyclonal Treg cells (Fig. 24 and Fig. 23). Third, our TCR profiling revealed that the polyclonal thymic Treg repertoire is largely unaltered in *Batf3*^{-/-} mice (Fig. 26), indicating that the increase in Treg cell numbers is not due to the emergence of distinct Treg specificities that are spared from clonal deletion in the absence of CD8 α ⁺ cDCs. Instead, we hypothesize that the expanded population of Sirp α ⁺ cDCs in *Batf3*^{-/-} thymi leads to an expanded "niche" capable of supporting the development of Treg cells. Thus, while both Sirp α ⁺ and CD8 α ⁺ cDCs may be capable of acquiring antigen from Aire-expressing mTECs, it is possible that Sirp α ⁺ cDCs have an enhanced capacity to support Treg cell development or survival, perhaps through the provision of additional antigen-independent accessory signals.

Moving forward, it will be critical to develop approaches that enable the inducible or constitutive ablation of Sirp α ⁺ cDCs, in an effort to elucidate the role of these cells in T cell selection. Moreover, it will be important to elucidate the impact of Sirp α ⁺ and

CD8 α^+ cDCs subsets on the negative selection of distinct autoreactive specificities. Such studies may help to elucidate the mechanisms and pathways that are ultimately responsible for dictating whether an autoreactive thymocyte undergoes clonal deletion or differentiation into the Treg lineage. In order to find new avenues for the selective manipulation of Sirp α^+ cDCs in the thymus it will first be important to analyze the gene expression profiles of thymic Sirp α^+ cDCs and CD8 α^+ cDCs in the hopes of identifying differentiating factors. If a gene is found to be uniquely upregulated in Sirp α^+ cDCs versus CD8 α^+ cDCs, the promoter elements of said gene could be utilized to drive the selective expression of the human diphtheria toxin receptor (DTR), enabling inducible depletion of the DC subset upon administration with DT. Alternatively, if a factor is determined to be selectively required for the development or function of Sirp α^+ cDCs it could be ablated by flanking the gene for said factor with loxp sites and driving the expression of Cre under the CD11c promoter.

Self antigen presentation in the function and homeostasis of Tregs

While it is well accepted that reactivity to self antigens in the thymus plays a pivotal role in Treg development (28), the contribution of cognate antigen presentation and TCR signaling for the survival, anatomical distribution, and function of Treg cells post thymic selection is only now starting to emerge. In the secondary lymphoid organs a substantial proportion of Tregs exhibit phenotypic markers associated with active TCR signaling and divide at steady state (25, 146). Conditional and selective ablation of the TCR on Tregs does not result in loss of Foxp3 or cell death, but does disrupt Treg cell

function and results in systemic autoimmunity (68, 147). These data provide evidence that TCR signaling, likely via interaction with cognate antigen, plays a critical role in the function of Tregs, however direct evidence demonstrating disruption of a naturally derived Treg in the absence of its cognate self antigen had not been provided.

Prostate-organ-specific Tregs require continuous antigen presentation for their activation and proper anatomical distribution

We provided, for the first time, direct evidence that the enrichment and activation of organ-specific Tregs in the draining lymph nodes requires continuous antigen presentation. Interestingly, castration-induced prostatic involution was associated with the loss of MJ23 TCR signaling in the pLNs (as assessed by CD69 expression), but did not lead to a global loss of MJ23 Tregs (Fig. 28). These experiments suggest that continued antigen recognition is required for the enrichment of organ-specific Treg cells in regional organ-draining lymph nodes, but is not required for the survival of these cells, at least within the time scales analyzed in this study. These findings are consistent with work involving the study of “disease-specific” polyclonal Treg cells by Tung and colleagues (103-105). In a representative study, it was shown that the local enrichment of Treg cells that possess the capacity to suppress experimental autoimmune prostatitis was eliminated by neonatal orchiectomy and restored by subsequent 5 α -dihydrotestosterone treatment, suggesting the existence of prostate-specific Treg cells that are dependent on antigen availability (105). Our current study extends these findings by providing direct evidence that TCR signaling and anatomical enrichment of a naturally occurring organ-specific Treg population requires sustained antigen

presentation and is reversible. Moreover, these findings suggest that the distribution and activation of organ-specific Treg specificities may be quite dynamic, with a regional Treg repertoire changing and adapting throughout life in response to varying physiological or inflammatory settings.

Identifying the APC interaction partners that orchestrate organ-specific Treg homeostasis and function

If TCR activation plays a critical role in the function of Tregs, then it would also imply that the APC interaction partners presenting a Treg's cognate antigen would ultimately orchestrate many aspects of that cell's biology, including anatomical distribution, spatial position within lymphoid and non-lymphoid organs, proximity to other immune cell subsets and access to distinct environmental cues. Despite the critical role APCs likely play in orchestrating Treg biology and ultimately enforcing immune tolerance, little is known about the cell types that present antigens for recognition by Tregs. In the spleen it was demonstrated that depletion or expansion of CD11c-expressing DCs results in a subsequent decrease or increase in splenic Tregs, respectively (75). In separate studies, the expansion of Flt3L-dependent DCs or administration of anti-ICOSL antibody induced the expansion or reduction of CD44^{high}CD62L^{low} splenic Treg cells, respectively (148). These studies suggest that in the spleen, DCs likely play a role in the modulation of Treg homeostasis and activation. However, since the spleen contains multiple subsets of CD11c-expressing cells, including pDCs, Sirp α^+ cDCs and CD8 α^+ cDCs (77), it is unknown whether a distinct DC subset supports Treg homeostasis at this site. Additionally, since lymph nodes contain a

variety of APC populations not found in the spleen, including several migratory DC subsets and langerhans cells (77), it was unclear whether a similar dependency would be exhibited at these sites.

CD11c-expressing DCs play a critical role in the homeostasis of MJ23 and some polyclonal Tregs in the pLNs

We thereby expand upon analyzes in the spleen by demonstrating that in the skin-draining (inguinal and brachial, i/bLNs) and prostate-draining (periaortic, pLNs) lymph nodes, CD11c⁺ DC depletion and FLT3L-dependent DC expansion leads to a decrease and increase of polyclonal Treg populations, respectively (Fig. 29). Additionally we find a positive correlation between DC and Treg frequency at these anatomical sites (Fig. 30). However, we also demonstrate that while CD11c⁺ DC depletion leads to a loss of MJ23 Treg enrichment in the pLNs, expansion of FLT3L-dependent DCs does not lead to an increase in MJ23 Tregs (Fig. 29). Taken together, these data suggest that within the lymph nodes DCs modulate the homeostasis and anatomical enrichment of some Treg specificities, including organ-specific MJ23 Tregs, however the abundance of cognate antigen may ultimately dictate the size of a Treg's "niche" since DC expansion alone did not increase the enrichment of MJ23 Tregs in the prostate-draining lymph nodes.

Organ-specific Tregs and their APC interaction partners

Several lines of evidence demonstrate that organ-specific Tregs likely play a specialized role in modulating both immunological and non-immunological processes.

First, in transfer experiments Tregs isolated from the organ-draining lymph nodes were more efficient at suppressing autoimmunity against a draining organ than Tregs taken from non-draining lymph nodes (103-105). In previous studies we also provided direct evidence for the existence of organ-specific Tregs by identifying the MJ23 Treg clonotype that selectively enriches in the prostate-draining lymph nodes of male mice (79). Second, Tregs have been found within a variety of non-lymphoid tissues, including tumors, adipose tissue and injured muscles, where they have been suggested to modulate adaptive and innate immune responses, as well as biological processes independent of immunoregulation (149). Visceral adipose tissue-associated Tregs have been shown to modulate several aspects of metabolism, insulin resistance and glucose intolerance (150), while Tregs found infiltrating injured skeletal muscle have been shown to dramatically impact tissue regeneration at this site (151). In tumors, studies have suggested that Tregs may impact tumor growth via the expression of VEGFA (152), stimulating angiogenesis, and RANKL (153), promoting tumor progression and metastasis. Finally, our studies identifying Aire-dependent, TRA-specific Tregs (79), and hence the existence of an evolutionarily evolved mechanism responsible for the generation of organ-specific Tregs, may suggest a specialized role and function for these cells. Thus, following the logic outlined above, if antigen presentation plays a critical role in the function of Tregs in general, then it will also be important to identify the APC subsets responsible for presenting antigens to organ-specific Tregs in particular.

Identifying the APC interaction partners that orchestrate organ-specific Treg homeostasis and function

DCs exhibit considerable phenotypic, developmental, and functional diversity, suggesting that distinct DC subsets may play unique roles in regulating tolerance, immunity, and inflammation. Based on our finding that CCR7-dependent mDCs are required for the enrichment of MJ23 Tregs in the pLNs (Fig. 31), we hypothesize that mDCs bearing organ-derived antigen are specialized to interface with organ-specific Treg cells in lymph nodes throughout the body. In recent work, Idoyaga and colleagues demonstrated that the experimental targeting of antigen to mDCs, delivered by anti-DEC-205 or anti-Langerin antibodies, induced the peripheral differentiation of antigen-specific T cells into Foxp3⁺ cells (73). While the extrathymic Treg cell induction observed by Idoyaga et al. is inherently different from the enrichment of thymic-derived organ-specific Treg cells demonstrated in our study, together these findings suggest that mDCs are endowed with the capacity to support the activation, enrichment, and differentiation of Treg cells within the lymph nodes. This illustrates that the rules governing Treg biology in the spleen, which lacks mDCs, are likely to be different from those dictating Treg biology in the lymph nodes.

Given the heterogeneity of mDCs in the lymph nodes (125), it will be important to determine whether antigen presentation to organ-specific Treg cells is a general property of all mDC subsets, or whether a distinct mDC subset is specialized to interface with these Tregs. For example, the findings of Gerner et al. suggest that different mDC subsets are localized to distinct regions within the lymph node microenvironment, with CD11b⁺ mDC primarily found in the interfollicular zone and

CD103⁺ mDCs residing in the T cell zones (108). mDC localization may be critical for the proper positioning of organ-specific Treg cells in order to place them in direct proximity to conventional T cells or other environmental niches. Interestingly, very recently published work by the same group found that in the skin draining lymph nodes Tregs exhibiting increased levels of pSTAT5, a signaling molecule directly downstream of CD25 and IL-2 signaling, are asymmetrically localized throughout the lymph node microenvironment (154). They find that pSTAT5⁺ Tregs can be found clustered in direct proximity to mDCs and IL-2 producing CD4⁺ Tconv cells, that are likely autoreactive. SPF colonized and germ free mice exhibited similar levels of pSTAT5⁺ Treg clustering and thus clustering was not microbiota dependent, suggesting that Tregs are reacting to self antigens. Furthermore, selective ablation of the TCR on Tregs led to a loss of Treg clustering, arguing that interaction with mDC-Tconv cell clusters is TCR, and likely antigen, dependent. Thus, new insights provided by Liu et al combined with our data demonstrating the functional loss of organ-specific MJ23 Treg localization and activation in the absence of mDCs (Fig. 31), in sum, would suggest that mDCs orchestrate the enrichment, activation and micro-localization of organ-specific Tregs in the lymph nodes to bring Treg cells in direct proximity to potentially pathogenic autoreactive Tconv cells, thereby orchestrating Treg function and immune tolerance to peripheral organs. While these data suggest that mDCs may present self antigens to autoreactive Tconv cells it will be important to also determine whether the mDCs that present antigen to organ-specific Treg cells in the lymph nodes are the same DCs that are poised to prime T cell responses to infections or neoplasms originating in the peripheral organs.

Evaluating the contributions of distinct mDC subsets towards organ-specific Treg homeostasis and immune tolerance

Our findings, as well as those discussed above, suggest that mDCs may play critical roles in the coordination of organ-specific Treg function and the enforcement of immune tolerance to a variety of tissues. In future experiments it will be important to elucidate the individual contributions of the CD103⁺ and CD11b⁺ mDC subsets towards the enrichment and activation of organ-specific Tregs and the enforcement of immune tolerance. While our data demonstrating a loss of MJ23 Treg enrichment in the pLN of *Ccr7*^{-/-} mice (Fig. 31) suggest that mDC take up prostate-derived antigens and traffic to the pLN where to present to MJ23 Tregs, it will be important to directly demonstrate antigenic uptake from the prostate and trafficking in the pLN. One means to provide direct evidence for uptake and trafficking of distinct mDC subsets would be via the injection of fluorescently labeled beads directly into the prostate followed by characterization of the DC subsets in the prostate and pLN.

By generating MJ23 TCR tetramers, it could provide a secondary means to identify the APCs in the prostate and pLN that are actively presenting the MJ23 prostate-derived antigenic peptide in the context of MHC-II. Additionally, similar to the immunofluorescence analyzes by Liu et al. (154) discussed above, the interaction of MJ23tg Tregs and various DCs subsets in the pLN of low-frequency MJ23 BMCs could be evaluated to determine if these organ-specific Tregs cluster with a distinct APC subset and exhibit signs of TCR and CD25 activation. It will also be important to evaluate the phenotype of identified mDC subsets at steady state in wild type mice,

during autoimmune attack of the prostate in *Aire*^{-/-} mice and in the context of a prostate tumor in TRAMP mice.

Finally, it will be critical for the field to develop new methods to selectively target mDCs via depletion or inhibition of migration. Current approaches include the analysis of *Ccr7*^{-/-} mice and the administration of anti-CCR7 blocking antibody, both of which have systemic effects on other immune cells subsets, including the disruption of developing thymocyte and T cell migration. One way this could be accomplished would be via the selective ablation of *Ccr7* in CD11c-expressing DCs via a Cre-lox system. The selective manipulation of mDCs will be a critical step for the elucidation their overall function and impact on the enforcement of tolerance to peripheral tissues.

Conclusions

Despite the fact that the seminal studies performed by Shimon Sakaguchi characterizing the existence of a CD4⁺CD25⁺ suppressor T cell subset were carried out over 20 years ago (20), we are only now beginning to understand fundamental aspects of the biology of this cell subset in the context of health and disease. At the onset of our work, we set out to better define the developmental origins and antigenic specificities of endogenous tumor-associated Tregs found in murine TRAMP prostate tumors. We found that the TCR repertoires of prostate-tumor-infiltrating Tregs and Tconv cells are largely distinct, suggesting that pTreg induction of Tconv cells in the tumor microenvironment is likely not a common event. Additionally, we expressed the TCRs of highly abundant and recurrently enriched Treg specificities found in prostate tumors, MJ23 and RT83, and determined that these cells are selected into the Treg lineage in

the thymus in an Aire-dependent manner. We also determined that MJ23 Tregs are reactive to a prostate-associated, tumor-independent antigen. These findings led to clear paths of additional inquiry where we sought to identify the antigen presenting cells which facilitate the development of MJ23 Tregs in the thymus and orchestrate their activation and anatomical enrichment in the periphery. We demonstrate that, while not required for their survival, MJ23 Tregs were dependent on continuous presentation of prostate-derived antigens by CCR7-dependent mDCs for their activation and anatomical enrichment in the pLN.

In summary, our results support a model in which tumors recruit and/or expand thymic derived, organ-specific Tregs. In the thymus these Aire-dependent Tregs receive critical developmental signals from DCs that take up mTEC derived antigens, and upon exiting the thymus the activation and localization of organ-specific Tregs is dependent on antigen presentation by mDCs in the organ-draining lymph nodes.

REFERENCES

1. C. A. Janeway, Jr., The immune system evolved to discriminate infectious nonself from noninfectious self. *Immunity Today* **13**, 11 (Jan, 1992).
2. P. Matzinger, Tolerance, danger, and the extended family. *Annu Rev Immunol* **12**, 991 (1994).
3. J. W. Kappler, N. Roehm, P. Marrack, T cell tolerance by clonal elimination in the thymus. *Cell* **49**, 273 (Apr 24, 1987).
4. M. J. Bevan, Minor H antigens introduced on H-2 different stimulating cells cross-react at the cytotoxic T cell level during in vivo priming. *J Immunol* **117**, 2233 (Dec, 1976).
5. M. J. Bevan, Cross-priming for a secondary cytotoxic response to minor H antigens with H-2 congenic cells which do not cross-react in the cytotoxic assay. *J Exp Med* **143**, 1283 (May 1, 1976).
6. L. R. Zacharski, V. P. Sukhatme, Coley's toxin revisited: immunotherapy or plasminogen activator therapy of cancer? *Journal of thrombosis and haemostasis : JTH* **3**, 424 (Mar, 2005).
7. G. Klein, H. O. Sjogren, E. Klein, K. E. Hellstrom, Demonstration of resistance against methylcholanthrene-induced sarcomas in the primary autochthonous host. *Cancer Res* **20**, 1561 (Dec, 1960).
8. R. T. Prehn, J. M. Main, Immunity to methylcholanthrene-induced sarcomas. *J Natl Cancer Inst* **18**, 769 (Jun, 1957).
9. E. J. Foley, Antigenic properties of methylcholanthrene-induced tumors in mice of the strain of origin. *Cancer Res* **13**, 835 (Dec, 1953).
10. S. I. Grivennikov, F. R. Greten, M. Karin, Immunity, inflammation, and cancer. *Cell* **140**, 883 (Mar 19, 2010).
11. D. Hanahan, R. A. Weinberg, Hallmarks of cancer: the next generation. *Cell* **144**, 646 (Mar 4, 2011).
12. F. S. Hodi *et al.*, Improved survival with ipilimumab in patients with metastatic melanoma. *N Engl J Med* **363**, 711 (Aug 19, 2010).
13. S. L. Topalian *et al.*, Safety, activity, and immune correlates of anti-PD-1 antibody in cancer. *N Engl J Med* **366**, 2443 (Jun 28, 2012).

14. D. S. Chen, I. Mellman, Oncology meets immunology: the cancer-immunity cycle. *Immunity* **39**, 1 (Jul 25, 2013).
15. G. L. Stritesky *et al.*, Murine thymic selection quantified using a unique method to capture deleted T cells. *Proc Natl Acad Sci U S A* **110**, 4679 (Mar 19, 2013).
16. J. W. Lee *et al.*, Peripheral antigen display by lymph node stroma promotes T cell tolerance to intestinal self. *Nat Immunol* **8**, 181 (Feb, 2007).
17. S. Z. Josefowicz, L. F. Lu, A. Y. Rudensky, Regulatory T cells: mechanisms of differentiation and function. *Annu Rev Immunol* **30**, 531 (2012).
18. P. Sharma, J. P. Allison, The future of immune checkpoint therapy. *Science* **348**, 56 (Apr 3, 2015).
19. M. S. Jordan *et al.*, Thymic selection of CD4+CD25+ regulatory T cells induced by an agonist self-peptide. *Nat Immunol* **2**, 301 (Apr, 2001).
20. S. Sakaguchi, N. Sakaguchi, M. Asano, M. Itoh, M. Toda, Immunologic self-tolerance maintained by activated T cells expressing IL-2 receptor alpha-chains (CD25). Breakdown of a single mechanism of self-tolerance causes various autoimmune diseases. *J Immunol* **155**, 1151 (Aug 1, 1995).
21. L. B. Clark *et al.*, Cellular and molecular characterization of the scurfy mouse mutant. *J Immunol* **162**, 2546 (Mar 1, 1999).
22. M. E. Brunkow *et al.*, Disruption of a new forkhead/winged-helix protein, scurf, results in the fatal lymphoproliferative disorder of the scurfy mouse. *Nat Genet* **27**, 68 (Jan, 2001).
23. R. S. Wildin *et al.*, X-linked neonatal diabetes mellitus, enteropathy and endocrinopathy syndrome is the human equivalent of mouse scurfy. *Nat Genet* **27**, 18 (Jan, 2001).
24. J. D. Fontenot, M. A. Gavin, A. Y. Rudensky, Foxp3 programs the development and function of CD4+CD25+ regulatory T cells. *Nat Immunol* **4**, 330 (Apr, 2003).
25. S. Fisson *et al.*, Continuous activation of autoreactive CD4+ CD25+ regulatory T cells in the steady state. *J Exp Med* **198**, 737 (Sep 1, 2003).
26. C. S. Hsieh *et al.*, Recognition of the peripheral self by naturally arising CD25+ CD4+ T cell receptors. *Immunity* **21**, 267 (Aug, 2004).
27. A. K. Abbas *et al.*, Regulatory T cells: recommendations to simplify the nomenclature. *Nat Immunol* **14**, 307 (Apr, 2013).

28. C. S. Hsieh, H. M. Lee, C. W. Lio, Selection of regulatory T cells in the thymus. *Nat Rev Immunol* **12**, 157 (Mar, 2012).
29. C. W. Lio, C. S. Hsieh, A two-step process for thymic regulatory T cell development. *Immunity* **28**, 100 (Jan, 2008).
30. A. Toker *et al.*, Active Demethylation of the Foxp3 Locus Leads to the Generation of Stable Regulatory T Cells within the Thymus. *J Immunol*, (Feb 18, 2013).
31. Y. Zheng *et al.*, Role of conserved non-coding DNA elements in the Foxp3 gene in regulatory T-cell fate. *Nature* **463**, 808 (Feb 11, 2010).
32. A. M. Bilate, J. J. Lafaille, Induced CD4+Foxp3+ regulatory T cells in immune tolerance. *Annu Rev Immunol* **30**, 733 (2012).
33. S. Z. Josefowicz *et al.*, Extrathymically generated regulatory T cells control mucosal T(H)2 inflammation. *Nature*, (Feb 8, 2012).
34. R. M. Samstein, S. Z. Josefowicz, A. Arvey, P. M. Treuting, A. Y. Rudensky, Extrathymic generation of regulatory T cells in placental mammals mitigates maternal-fetal conflict. *Cell* **150**, 29 (Jul 6, 2012).
35. S. K. Lathrop *et al.*, Peripheral education of the immune system by colonic commensal microbiota. *Nature* **478**, 250 (Oct 13, 2011).
36. R. J. deLeeuw, S. E. Kost, J. A. Kakal, B. H. Nelson, The prognostic value of FoxP3+ tumor-infiltrating lymphocytes in cancer: a critical review of the literature. *Clin Cancer Res* **18**, 3022 (Jun 1, 2012).
37. T. J. Curiel *et al.*, Specific recruitment of regulatory T cells in ovarian carcinoma fosters immune privilege and predicts reduced survival. *Nat Med* **10**, 942 (Sep, 2004).
38. G. J. Bates *et al.*, Quantification of regulatory T cells enables the identification of high-risk breast cancer patients and those at risk of late relapse. *J Clin Oncol* **24**, 5373 (Dec 1, 2006).
39. A. M. Miller *et al.*, CD4+CD25high T cells are enriched in the tumor and peripheral blood of prostate cancer patients. *J Immunol* **177**, 7398 (Nov 15, 2006).
40. A. Flammiger *et al.*, High tissue density of FOXP3+ T cells is associated with clinical outcome in prostate cancer. *Eur J Cancer*, (Dec 21, 2012).
41. S. Ladoire, F. Martin, F. Ghiringhelli, Prognostic role of FOXP3+ regulatory T cells infiltrating human carcinomas: the paradox of colorectal cancer. *Cancer Immunol Immunother* **60**, 909 (Jul, 2011).

42. J. Shimizu, S. Yamazaki, S. Sakaguchi, Induction of tumor immunity by removing CD25+CD4+ T cells: a common basis between tumor immunity and autoimmunity. *J Immunol* **163**, 5211 (Nov 15, 1999).
43. J. M. Kim, J. P. Rasmussen, A. Y. Rudensky, Regulatory T cells prevent catastrophic autoimmunity throughout the lifespan of mice. *Nat Immunol* **8**, 191 (Feb, 2007).
44. J. Kim *et al.*, Cutting edge: depletion of Foxp3+ cells leads to induction of autoimmunity by specific ablation of regulatory T cells in genetically targeted mice. *J Immunol* **183**, 7631 (Dec 15, 2009).
45. M. W. Teng *et al.*, Conditional regulatory T-cell depletion releases adaptive immunity preventing carcinogenesis and suppressing established tumor growth. *Cancer Res* **70**, 7800 (Oct 15, 2010).
46. P. D. Bos, G. Plitas, D. Rudra, S. Y. Lee, A. Y. Rudensky, Transient regulatory T cell ablation deters oncogene-driven breast cancer and enhances radiotherapy. *J Exp Med* **210**, 2435 (Oct 21, 2013).
47. N. S. Joshi *et al.*, Regulatory T Cells in Tumor-Associated Tertiary Lymphoid Structures Suppress Anti-tumor T Cell Responses. *Immunity* **43**, 579 (Sep 15, 2015).
48. D. G. DeNardo *et al.*, CD4(+) T cells regulate pulmonary metastasis of mammary carcinomas by enhancing protumor properties of macrophages. *Cancer Cell* **16**, 91 (Aug 4, 2009).
49. Y. He *et al.*, Tissue damage-associated "danger signals" influence T-cell responses that promote the progression of preneoplasia to cancer. *Cancer Res* **73**, 629 (Jan 15, 2013).
50. G. K. Alderton, Tumour immunology: suppressing tumorigenic inflammation. *Nat Rev Cancer* **12**, 228 (Apr, 2012).
51. K. Nakamura, A. Kitani, W. Strober, Cell contact-dependent immunosuppression by CD4(+)CD25(+) regulatory T cells is mediated by cell surface-bound transforming growth factor beta. *J Exp Med* **194**, 629 (Sep 3, 2001).
52. L. Fahlen *et al.*, T cells that cannot respond to TGF-beta escape control by CD4(+)CD25(+) regulatory T cells. *J Exp Med* **201**, 737 (Mar 7, 2005).
53. T. Takahashi *et al.*, Immunologic self-tolerance maintained by CD25(+)CD4(+) regulatory T cells constitutively expressing cytotoxic T lymphocyte-associated antigen 4. *J Exp Med* **192**, 303 (Jul 17, 2000).

54. K. S. Peggs, S. A. Quezada, C. A. Chambers, A. J. Korman, J. P. Allison, Blockade of CTLA-4 on both effector and regulatory T cell compartments contributes to the antitumor activity of anti-CTLA-4 antibodies. *J Exp Med* **206**, 1717 (Aug 3, 2009).
55. X. Cao *et al.*, Granzyme B and perforin are important for regulatory T cell-mediated suppression of tumor clearance. *Immunity* **27**, 635 (Oct, 2007).
56. L. W. Collison *et al.*, The inhibitory cytokine IL-35 contributes to regulatory T-cell function. *Nature* **450**, 566 (Nov 22, 2007).
57. A. M. Thornton *et al.*, Expression of Helios, an Ikaros transcription factor family member, differentiates thymic-derived from peripherally induced Foxp3+ T regulatory cells. *J Immunol* **184**, 3433 (Apr 1, 2010).
58. J. Verhagen, D. C. Wraith, Comment on "Expression of Helios, an Ikaros transcription factor family member, differentiates thymic-derived from peripherally induced Foxp3+ T regulatory cells". *J Immunol* **185**, 7129; author reply 7130 (Dec 15, 2010).
59. D. J. Zabransky *et al.*, Phenotypic and functional properties of Helios+ regulatory T cells. *PLoS One* **7**, e34547 (2012).
60. T. Akimova, U. H. Beier, L. Wang, M. H. Levine, W. W. Hancock, Helios expression is a marker of T cell activation and proliferation. *PLoS One* **6**, e24226 (2011).
61. M. Yadav *et al.*, Neuropilin-1 distinguishes natural and inducible regulatory T cells among regulatory T cell subsets in vivo. *J Exp Med* **209**, 1713 (Sep 24, 2012).
62. J. M. Weiss *et al.*, Neuropilin 1 is expressed on thymus-derived natural regulatory T cells, but not mucosa-generated induced Foxp3+ T reg cells. *J Exp Med* **209**, 1723 (Sep 24, 2012).
63. V. C. Liu *et al.*, Tumor evasion of the immune system by converting CD4+CD25- T cells into CD4+CD25+ T regulatory cells: role of tumor-derived TGF-beta. *J Immunol* **178**, 2883 (Mar 1, 2007).
64. W. Z. Ai *et al.*, Follicular lymphoma B cells induce the conversion of conventional CD4+ T cells to T-regulatory cells. *Int J Cancer* **124**, 239 (Jan 1, 2009).
65. D. Getnet *et al.*, Tumor recognition and self-recognition induce distinct transcriptional profiles in antigen-specific CD4 T cells. *J Immunol* **182**, 4675 (Apr 15, 2009).

66. G. Zhou, H. I. Levitsky, Natural regulatory T cells and de novo-induced regulatory T cells contribute independently to tumor-specific tolerance. *J Immunol* **178**, 2155 (Feb 15, 2007).
67. A. G. Levine, A. Arvey, W. Jin, A. Y. Rudensky, Continuous requirement for the TCR in regulatory T cell function. *Nat Immunol* **15**, 1070 (Nov, 2014).
68. J. C. Vahl *et al.*, Continuous T cell receptor signals maintain a functional regulatory T cell pool. *Immunity* **41**, 722 (Nov 20, 2014).
69. L. Klein, M. Hinterberger, G. Wirnsberger, B. Kyewski, Antigen presentation in the thymus for positive selection and central tolerance induction. *Nat Rev Immunol* **9**, 833 (Dec, 2009).
70. A. I. Proietto *et al.*, Dendritic cells in the thymus contribute to T-regulatory cell induction. *Proc Natl Acad Sci U S A* **105**, 19869 (Dec 16, 2008).
71. J. S. Perry *et al.*, Distinct contributions of Aire and antigen-presenting-cell subsets to the generation of self-tolerance in the thymus. *Immunity* **41**, 414 (Sep 18, 2014).
72. L. Guerri *et al.*, Analysis of APC types involved in CD4 tolerance and regulatory T cell generation using reaggregated thymic organ cultures. *J Immunol* **190**, 2102 (Mar 1, 2013).
73. J. Idoyaga *et al.*, Specialized role of migratory dendritic cells in peripheral tolerance induction. *J Clin Invest* **123**, 844 (Feb 1, 2013).
74. M. Merad, P. Sathe, J. Helft, J. Miller, A. Mortha, The dendritic cell lineage: ontogeny and function of dendritic cells and their subsets in the steady state and the inflamed setting. *Annu Rev Immunol* **31**, 563 (2013).
75. G. Darrasse-Jeze *et al.*, Feedback control of regulatory T cell homeostasis by dendritic cells in vivo. *J Exp Med* **206**, 1853 (Aug 31, 2009).
76. K. S. Smigiel *et al.*, CCR7 provides localized access to IL-2 and defines homeostatically distinct regulatory T cell subsets. *J Exp Med* **211**, 121 (Jan 13, 2014).
77. A. Mildner, S. Jung, Development and Function of Dendritic Cell Subsets. *Immunity* **40**, 642 (May 15, 2014).
78. D. S. Leventhal *et al.*, Dendritic cells coordinate the development and homeostasis of organ-specific regulatory T cells. *Immunity*, (In Press).
79. S. Malchow *et al.*, Aire-Dependent Thymic Development of Tumor-Associated Regulatory T Cells. *Science* **339**, 1219 (March 8, 2013, 2013).

80. V. Kouskoff, K. Signorelli, C. Benoist, D. Mathis, Cassette vectors directing expression of T cell receptor genes in transgenic mice. *J Immunol Methods* **180**, 273 (Mar 27, 1995).
81. Magurran, *Ecological Diversity and Its Measurement*. (Princeton University Press, Princeton, NJ, 1988).
82. K. Aschenbrenner *et al.*, Selection of Foxp3+ regulatory T cells specific for self antigen expressed and presented by Aire+ medullary thymic epithelial cells. *Nat Immunol* **8**, 351 (Apr, 2007).
83. M. D. Vesely, M. H. Kershaw, R. D. Schreiber, M. J. Smyth, Natural innate and adaptive immunity to cancer. *Annu Rev Immunol* **29**, 235 (2011).
84. N. M. Greenberg *et al.*, Prostate cancer in a transgenic mouse. *Proc Natl Acad Sci U S A* **92**, 3439 (Apr 11, 1995).
85. J. R. Gingrich, R. J. Barrios, B. A. Foster, N. M. Greenberg, Pathologic progression of autochthonous prostate cancer in the TRAMP model. *Prostate Cancer Prostatic Dis* **2**, 70 (Mar, 1999).
86. J. D. Fontenot *et al.*, Regulatory T cell lineage specification by the forkhead transcription factor foxp3. *Immunity* **22**, 329 (Mar, 2005).
87. Materials and methods are available as supplementary materials in Science Online.
88. J. Wong, D. Mathis, C. Benoist, TCR-based lineage tracing: no evidence for conversion of conventional into regulatory T cells in response to a natural self-antigen in pancreatic islets. *J Exp Med* **204**, 2039 (Sep 3, 2007).
89. J. Wong *et al.*, Adaptation of TCR repertoires to self-peptides in regulatory and nonregulatory CD4+ T cells. *J Immunol* **178**, 7032 (Jun 1, 2007).
90. C. S. Hsieh, Y. Zheng, Y. Liang, J. D. Fontenot, A. Y. Rudensky, An intersection between the self-reactive regulatory and nonregulatory T cell receptor repertoires. *Nat Immunol* **7**, 401 (Apr, 2006).
91. S. K. Lathrop, N. A. Santacruz, D. Pham, J. Luo, C. S. Hsieh, Antigen-specific peripheral shaping of the natural regulatory T cell population. *J Exp Med* **205**, 3105 (Dec 22, 2008).
92. M. J. Barnden, J. Allison, W. R. Heath, F. R. Carbone, Defective TCR expression in transgenic mice constructed using cDNA-based alpha- and beta-chain genes under the control of heterologous regulatory elements. *Immunol Cell Biol* **76**, 34 (Feb, 1998).

93. J. L. Bautista *et al.*, Intraclonal competition limits the fate determination of regulatory T cells in the thymus. *Nat Immunol* **10**, 610 (Jun, 2009).
94. M. W. Leung, S. Shen, J. J. Lafaille, TCR-dependent differentiation of thymic Foxp3+ cells is limited to small clonal sizes. *J Exp Med* **206**, 2121 (Sep 28, 2009).
95. M. S. Anderson *et al.*, The cellular mechanism of Aire control of T cell tolerance. *Immunity* **23**, 227 (Aug, 2005).
96. M. S. Anderson *et al.*, Projection of an immunological self shadow within the thymus by the aire protein. *Science* **298**, 1395 (Nov 15, 2002).
97. D. Mathis, C. Benoist, Aire. *Annu Rev Immunol* **27**, 287 (2009).
98. Y. Lei *et al.*, Aire-dependent production of XCL1 mediates medullary accumulation of thymic dendritic cells and contributes to regulatory T cell development. *J Exp Med* **208**, 383 (Feb 14, 2011).
99. A. Liston, S. Lesage, J. Wilson, L. Peltonen, C. C. Goodnow, Aire regulates negative selection of organ-specific T cells. *Nat Immunol* **4**, 350 (Apr, 2003).
100. R. T. Taniguchi *et al.*, Detection of an autoreactive T-cell population within the polyclonal repertoire that undergoes distinct autoimmune regulator (Aire)-mediated selection. *Proc Natl Acad Sci U S A* **109**, 7847 (May 15, 2012).
101. J. DeVoss *et al.*, Spontaneous autoimmunity prevented by thymic expression of a single self-antigen. *J Exp Med* **203**, 2727 (Nov 27, 2006).
102. S. Sakaguchi, T. Yamaguchi, T. Nomura, M. Ono, Regulatory T cells and immune tolerance. *Cell* **133**, 775 (May 30, 2008).
103. K. M. Wheeler, E. T. Samy, K. S. Tung, Cutting edge: normal regional lymph node enrichment of antigen-specific regulatory T cells with autoimmune disease-suppressive capacity. *J Immunol* **183**, 7635 (Dec 15, 2009).
104. E. T. Samy, L. A. Parker, C. P. Sharp, K. S. Tung, Continuous control of autoimmune disease by antigen-dependent polyclonal CD4+CD25+ regulatory T cells in the regional lymph node. *J Exp Med* **202**, 771 (Sep 19, 2005).
105. Y. Y. Setiady *et al.*, Physiologic self antigens rapidly capacitate autoimmune disease-specific polyclonal CD4+ CD25+ regulatory T cells. *Blood* **107**, 1056 (Feb 1, 2006).
106. S. Malchow *et al.*, Aire-dependent thymic development of tumor-associated regulatory T cells. *Science* **339**, 1219 (Mar 8, 2013).

107. J. Derbinski *et al.*, Promiscuous gene expression in thymic epithelial cells is regulated at multiple levels. *J Exp Med* **202**, 33 (Jul 4, 2005).
108. M. Y. Gerner, W. Kastenmuller, I. Ifrim, J. Kabat, R. N. Germain, Histo-cytometry: a method for highly multiplex quantitative tissue imaging analysis applied to dendritic cell subset microanatomy in lymph nodes. *Immunity* **37**, 364 (Aug 24, 2012).
109. A. A. Itano *et al.*, Distinct dendritic cell populations sequentially present antigen to CD4 T cells and stimulate different aspects of cell-mediated immunity. *Immunity* **19**, 47 (Jul, 2003).
110. C. Scheinecker, R. McHugh, E. M. Shevach, R. N. Germain, Constitutive presentation of a natural tissue autoantigen exclusively by dendritic cells in the draining lymph node. *J Exp Med* **196**, 1079 (Oct 21, 2002).
111. J. S. Markowitz, H. Auchincloss, Jr., M. J. Grusby, L. H. Glimcher, Class II-positive hematopoietic cells cannot mediate positive selection of CD4+ T lymphocytes in class II-deficient mice. *Proc Natl Acad Sci U S A* **90**, 2779 (Apr 1, 1993).
112. B. Salomon *et al.*, B7/CD28 costimulation is essential for the homeostasis of the CD4+CD25+ immunoregulatory T cells that control autoimmune diabetes. *Immunity* **12**, 431 (Apr, 2000).
113. C. Koble, B. Kyewski, The thymic medulla: a unique microenvironment for intercellular self-antigen transfer. *J Exp Med* **206**, 1505 (Jul 6, 2009).
114. S. Jung *et al.*, In vivo depletion of CD11c+ dendritic cells abrogates priming of CD8+ T cells by exogenous cell-associated antigens. *Immunity* **17**, 211 (Aug, 2002).
115. T. Yamano *et al.*, Thymic B Cells Are Licensed to Present Self Antigens for Central T Cell Tolerance Induction. *Immunity* **42**, 1048 (Jun 16, 2015).
116. J. Perera, L. Meng, F. Meng, H. Huang, Autoreactive thymic B cells are efficient antigen-presenting cells of cognate self-antigens for T cell negative selection. *Proc Natl Acad Sci U S A* **110**, 17011 (Oct 15, 2013).
117. L. Klein, B. Kyewski, P. M. Allen, K. A. Hogquist, Positive and negative selection of the T cell repertoire: what thymocytes see (and don't see). *Nat Rev Immunol* **14**, 377 (Jun, 2014).
118. M. Swiecki, S. Gilfillan, W. Vermi, Y. Wang, M. Colonna, Plasmacytoid dendritic cell ablation impacts early interferon responses and antiviral NK and CD8(+) T cell accrual. *Immunity* **33**, 955 (Dec 14, 2010).

119. K. Hildner *et al.*, Batf3 deficiency reveals a critical role for CD8alpha+ dendritic cells in cytotoxic T cell immunity. *Science* **322**, 1097 (Nov 14, 2008).
120. N. Kyprianou, J. T. Isaacs, Activation of programmed cell death in the rat ventral prostate after castration. *Endocrinology* **122**, 552 (Feb, 1988).
121. J. T. Isaacs, *Control of cell proliferation and cell death in the normal and neoplastic prostate: A stem cell model.*, (U.S. Dept. of Health and Human Services, Bethesda, MD, 1987).
122. M. A. Curran, J. P. Allison, Tumor vaccines expressing flt3 ligand synergize with ctla-4 blockade to reject preimplanted tumors. *Cancer Res* **69**, 7747 (Oct 1, 2009).
123. D. Hashimoto, J. Miller, M. Merad, Dendritic cell and macrophage heterogeneity in vivo. *Immunity* **35**, 323 (Sep 23, 2011).
124. M. Haniffa, M. Collin, F. Ginhoux, Ontogeny and functional specialization of dendritic cells in human and mouse. *Adv Immunol* **120**, 1 (2013).
125. G. J. Randolph, J. Ochando, S. Partida-Sanchez, Migration of dendritic cell subsets and their precursors. *Annu Rev Immunol* **26**, 293 (2008).
126. M. Kuczma *et al.*, Intratumoral convergence of the TCR repertoires of effector and Foxp3+ CD4+ T cells. *PLoS One* **5**, e13623 (2010).
127. J. P. Hindley *et al.*, Analysis of the T-cell receptor repertoires of tumor-infiltrating conventional and regulatory T cells reveals no evidence for conversion in carcinogen-induced tumors. *Cancer Res* **71**, 736 (Feb 1, 2011).
128. I. Apostolou, A. Sarukhan, L. Klein, H. von Boehmer, Origin of regulatory T cells with known specificity for antigen. *Nat Immunol* **3**, 756 (Aug, 2002).
129. A. Sainz-Perez, A. Lim, B. Lemercier, C. Leclerc, The T-cell receptor repertoire of tumor-infiltrating regulatory T lymphocytes is skewed toward public sequences. *Cancer Res* **72**, 3557 (Jul 15, 2012).
130. A. J. Caton *et al.*, Strength of TCR signal from self-peptide modulates autoreactive thymocyte deletion and Foxp3(+) Treg-cell formation. *Eur J Immunol* **44**, 785 (Mar, 2014).
131. S. Hwang *et al.*, Reduced TCR signaling potential impairs negative selection but does not result in autoimmune disease. *J Exp Med*, (Sep 3, 2012).
132. H.-M. Lee, Jhoanne L. Bautista, J. Scott-Browne, James F. Mohan, C.-S. Hsieh, A Broad Range of Self-Reactivity Drives Thymic Regulatory T Cell Selection to Limit Responses to Self. *Immunity*, (2012).

133. L. M. Ebert, S. E. MacRaid, I. D. Davis, J. Cebon, W. Chen, A novel method for detecting antigen-specific human regulatory T cells. *J Immunol Methods* **377**, 56 (Mar 30, 2012).
134. L. Vence *et al.*, Circulating tumor antigen-specific regulatory T cells in patients with metastatic melanoma. *Proc Natl Acad Sci U S A* **104**, 20884 (Dec 26, 2007).
135. J. Li, J. Park, D. Foss, I. Goldschneider, Thymus-homing peripheral dendritic cells constitute two of the three major subsets of dendritic cells in the steady-state thymus. *J Exp Med* **206**, 607 (Mar 16, 2009).
136. R. Bonasio *et al.*, Clonal deletion of thymocytes by circulating dendritic cells homing to the thymus. *Nat Immunol* **7**, 1092 (Oct, 2006).
137. H. Takaba *et al.*, Fezf2 Orchestrates a Thymic Program of Self-Antigen Expression for Immune Tolerance. *Cell* **163**, 975 (Nov 5, 2015).
138. A. C. Finnish-German, An autoimmune disease, APECED, caused by mutations in a novel gene featuring two PHD-type zinc-finger domains. *Nat Genet* **17**, 399 (Dec, 1997).
139. P. A. Savage, D. S. Leventhal, S. Malchow, Shaping the repertoire of tumor-infiltrating effector and regulatory T cells. *Immunol Rev* **259**, 245 (May, 2014).
140. D. Daniely, J. Kern, A. Cebula, L. Ignatowicz, Diversity of TCRs on natural Foxp3+ T cells in mice lacking Aire expression. *J Immunol* **184**, 6865 (Jun 15, 2010).
141. J. S. Perry *et al.*, Distinct Contributions of Aire and Antigen-Presenting-Cell Subsets to the Generation of Self-Tolerance in the Thymus. *Immunity*, (Sep 9, 2014).
142. S. malchow *et al.*, Aire enforces immune tolerance by directing autoreactive T cells into the regulatory T cell lineage. *Immunity*, (Accepted).
143. G. Wirnsberger, F. Mair, L. Klein, Regulatory T cell differentiation of thymocytes does not require a dedicated antigen-presenting cell but is under T cell-intrinsic developmental control. *Proc Natl Acad Sci U S A* **106**, 10278 (Jun 23, 2009).
144. S. Yang, N. Fujikado, D. Kolodin, C. Benoist, D. Mathis, Immune tolerance. Regulatory T cells generated early in life play a distinct role in maintaining self-tolerance. *Science* **348**, 589 (May 1, 2015).
145. G. E. Grajales-Reyes *et al.*, Batf3 maintains autoactivation of Irf8 for commitment of a CD8alpha(+) conventional DC clonogenic progenitor. *Nat Immunol* **16**, 708 (Jul, 2015).

146. K. S. Smigiel, S. Srivastava, J. M. Stolley, D. J. Campbell, Regulatory T-cell homeostasis: steady-state maintenance and modulation during inflammation. *Immunol Rev* **259**, 40 (May, 2014).
147. A. G. Levine, A. Arvey, W. Jin, A. Y. Rudensky, Continuous requirement for the TCR in regulatory T cell function. *Nat Immunol*, (Sep 28, 2014).
148. K. S. Smigiel *et al.*, CCR7 provides localized access to IL-2 and defines homeostatically distinct regulatory T cell subsets. *J Exp Med*, (Dec 30, 2013).
149. D. Burzyn, C. Benoist, D. Mathis, Regulatory T cells in nonlymphoid tissues. *Nat Immunol* **14**, 1007 (Oct, 2013).
150. M. Feuerer *et al.*, Lean, but not obese, fat is enriched for a unique population of regulatory T cells that affect metabolic parameters. *Nat Med* **15**, 930 (Aug, 2009).
151. D. Burzyn *et al.*, A special population of regulatory T cells potentiates muscle repair. *Cell* **155**, 1282 (Dec 5, 2013).
152. A. Facciabene *et al.*, Tumour hypoxia promotes tolerance and angiogenesis via CCL28 and T(reg) cells. *Nature* **475**, 226 (Jul 14, 2011).
153. W. Tan *et al.*, Tumour-infiltrating regulatory T cells stimulate mammary cancer metastasis through RANKL-RANK signalling. *Nature* **470**, 548 (Feb 24, 2011).
154. Z. Liu *et al.*, Immune homeostasis enforced by co-localized effector and regulatory T cells. *Nature*, (Nov 25, 2015).